UNIVERSITA' DEGLI STUDI DI PADOVA

Sede Amministrativa: Università degli Studi di Padova

Dipartimento di Pediatria

SCUOLA DI DOTTORATO DI RICERCA IN MEDICINA DELLO SVILUPPO
E SCIENZE DELLA PROGRAMMAZIONE
INDIRIZZO: EMATOONCOLOGIA ED IMMUNOLOGIA
XXI CICLO

CARDIOMYOGENIC POTENTIAL OF AMNIOTIC FLUID STEM CELLS AS A NEW TOOL FOR CELL BASED CARDIAC TISSUE ENGINEERING

Direttore della Scuola: Ch.mo Prof. Giuseppe Basso
Supervisore: Ch.ma Prof.ssa Chiara Messina

Dottoranda: Sveva Bollini

"Considerate la vostra semenza:

fatti non foste a viver come bruti,

ma per seguir virtute e canoscenza."

Dante, Inf. XXVI, 118-120.

SOMMARIO

Introduzione.

In questi ultimi anni l'area di ricerca dell'ingegneria tissutale e della terapia cellulare sono state ampiamente sviluppate e studiate al fine di curare o rigenerare il tessuto cardiaco leso o affetto da patologie.

Gli approcci piu' innovativi nel campo dell'ingegneria tissutale cardiaca si basano sulla stretta interazione di diverse discipline, quali, ad esempio, la terapia cellulare e la chirurgia, attraverso l'impiego di matrici biocompatibili e cellule staminali.

Recentemente, sono state ampiamente analizzate diverse tipologie di cellule staminali ed il loro relativo potenziale differenziativo in senso cardiaco.

Considerando poi in particolar modo il contesto clinico pediatrico, in cui spesso le malformazioni cardiache richiedono un intervento tempestivo alla nascita, all'interno del vasto scenario delle cellule staminali, le cellule progenitrici fetali potrebbero rappresentare una fonte cellulare alternativa molto vantaggiosa.

Il nostro gruppo di ricerca ha precedentemente individuato, isolato e caratterizzato una linea di cellule staminali presenti nel liquido amniotico (AFS cells, *Amniotic Fluid Stem Cells*), dimostrando inoltre come tali fossero in grado di esprimere un fenotipo "cardiomiocita-simile", se co-coltivate *in vitro* con cellule cardiomiocitarie neonatali di ratto.

Obbiettivo dello Studio.

L'obbiettivo di questo studio è stato caratterizzare il potenziale cardiomiogenico di tali cellule, sia *in vitro* che *in vivo*. Nella parte di studio *in vitro* si è cercato di migliorare l'organizzazione spaziale delle colture, per incrementare il differenziamento cardiomiocitario delle cellule AFS, tramite un approccio di ingegneria tissutale, introducendo culture bidimensionali su matrici microstrutturate biocompatibili; *in vivo* si è proceduto caratterizzando il loro potenziale terapeutico attraverso l'iniezione in due modelli sperimentali animali (ratto) di ischemia cardiaca attraverso lesione da freddo e infarto del miocardico.

II

Materiali e Metodi.

Le cellule cardiomiocitarie neonatali di ratto (rCM) sono state isolate tramite digestione enzimatica di cuori di ratto neonato di 2-3 giorni. Le cellule staminali GFP-positive del liquido amniotico di ratto (gfp^+rAFS) sono state ottenute da liquido amniotico di ratte gravide transgeniche per l'espressione della GFP. Le cellule staminali del liquido amniotico umane (hAFS) sono state isolate a partire da i campioni residuati della diagnosi prenatale prelevati tramite amniocentesi previo consenso informato. In entrambi i casi, le cellule AFS sono state isolate dalla popolazione cellulare totale del liquido amniotico attraverso immunoselezione per l'espresione del marcatore staminale ckit, recettore per lo Stem Cell Factor. L'analisi *in vitro* del potenziale differenziativo cardiomiocitario delle cellule AFS, tramite cocoltura, era già stato precedentemente dimostrato dalla dottoranda in lavori precedenti (*Chiavegato A., Bollini S. et al. 2007*); prima di procedere con lo studio del differenziamento *in vitro* attraverso cocolture su matrici biocompatibili, si è voluto approfondire la caratterizzazione del fenotipo "cardiomiocita-simile" mostrato da tali cellule, mediante un approccio funzionale con tecnica di patch-clamp, per definire il loro potenziale di azione.

Successivamente, si è proceduto a testare con colture primarie di cellule cardiomiocitarie di ratto, due differenti tipi di supporti biocompatibili, film di polimeri bidimensionali microstrutturati in hydrogel e membrane in silicone (PDMS, *Polydimethylsiloxane,* silicone). Le matrici polimeriche sono state ottenute tramite tecnica di micro-contact printing e impiegando stampi su cui era stata impressa la microtrama della struttura polimerica. Una volta dimostrato come il supporto migliore per una prolungata coltura *in vitro* fosse la matrice a trama microstrutturata in PDMS, si è proceduto a coltivare assieme le due tipologie cellulari (AFS e rCM) su tali membrane, con successiva analisi dell'espressione della troponina T dopo 6 e 10 giorni di coltura, attraverso immunostaining.

Nello studio *in vivo* si è fatto inizialmente uso di un modello ischemico di lesione da freddo (*cryoinjury*), attuata sulla superficie cardiaca del ventricolo sinistro di ratti immunocompromessi. Successivamente sull'area lesa è stata applicata una matrice polimerica tridimensionale di collagene; dopo 15 giorni dall'applicazione della matrice, si è proceduto con iniezione locale (intramiocardica) e sistemica (intravenosa) di $5x10^6$ cellule hAFS/animale, marcate col colorante fluorescente intracellulare rosso CMTMR.

Il tessuto cardiaco è stato quindi analizzato dopo 1, 15 e 30 giorni dall'iniezione cellulare, tramite immunostaining per marcatori cardiaci e infiammatori.

Il potenziale delle cellule gfp^+rAFS e hAFS è stato inoltre anche studiato in un modello sperimentale di infarto miocardico acuto in ratti Wistar. In questa parte dello studio gli animali sono stati sottoposti a legatura del ramo discendente anteriore dell'arteria coronaria, al fine di provocare un insulto ischemico della durata di 30 minuti, con successiva iniezione per via sistemica attraverso la vena giugulare esterna di 10^7 o 10^6 cellule gfp^+rAFS/animale e di 10^7 o $5x10^6$ cellule hAFS/animale, durante un periodo di riperfusione di 2 ore.

Gli animali sono stati poi sacrificati, i tessuti prelevati e i cuori processati per determinare l'estensione area infartuata attraverso colorazione con soluzione di colorante Evans blue (per individuare l'area ischemica non perfusa dal miocardio normalmente ossigenato) e successivamente con la soluzione di 2,3,5-trifenoll tetrazolio cloruro (*TTC staining*, per individuare l'area ischemica e all'interno di questa, più specificatamente, l'area infartuata). La misura dell'estensione dell'area infartuata è stata quindi ricavata analizzando le sezioni di tessuto cardiaco trattato con TTC staining con il software ImageJ, attraverso planimetria.

Si è poi proceduto ad indagare la presenza di cellule AFS all'interno di organi quali cuore, polmoni, fegato, milza dopo le 2 ore di riperfusione, tramite immunostaining utilizzando un marcatore specifico umano, l'anticorpo anti-mitocondri umani. Le cellule AFS sono state poi ulteriormente analizzate *in vitro* sia per studiare la presenza o meno al loro interno di una sottopopolazione di progenitori cardiaci, tramite RT-PCR, per i geni di differenziamento precoce cardiaco Isl1 e Kdr, sia per valutarne la capacità di secernere la proteina timosina β4, fattore paracrino con attività cardioprotettrice e angiogenica.

Risultati e Conclusioni.

I risultati *in vitro* hanno evidenziato come le cellule AFS, co-coltivate con le cellule cardiomiocitarie neonatali di ratto, siano in grado di acquisire un potenziale di azione simile alle cellule cardiache del tessuto di conduzione.

Riguardo l'impiego delle matrici polimeriche biocompatibili, le membrane microstrutturate di PDMS hanno dimostrato di influenzare l'orientamento spaziale della cocoltura a livello di singola cellula, garantendo così una organizzazione

bidimensionale ben definita e un incremento del contatto e delle interazioni dirette tra le due diverse tipologie cellulari. Le cellule hAFS, cocoltivate su tali polimeri, hanno dimostrato in alcuni casi attivita' contrattile ed espressione di marker cardiomiocitari come la proteina troponina T. Nelle cocolture di controllo circa il 5,06±2,8% delle cellule AFS seminate a 1000 cellule/cm^2 e il 2,1±0,08% di quelle a 4000 cellule/cm^2 were expressing the cardiac marker troponinsono risultate positive per l'espressione di troponina T dopo 6 giorni di coltura; dopo 10 nelle cocolture seminate con cellule AFS a 1000 cellule/cm^2 non sono state riscontrate cellule differenziate, mentre negli esperimenti con cellule AFS seminate in cocoltura a 4000 cellule/cm^2 le cellule umane positive per la troponina T erano il 4.97±2,5%. Nelle cocolture allestite sulla matrice di silicone microstrutturata, circa il 2,5 ± 2,4% delle cellule hAFS cells seminate a 1000 cells/cm^2 e nel 6,73 ± 2% delle stesse seminate a 4000 cells/cm^2 esprimevano troponina T, dopo 6 giorni di coltura. A 10 giorni di coltura questi valori sono incrementati all'11 ± 4,7%, con cellule hAFS seminate a 1000 cells/cm^2 e al 13 ± 4,2% di quelle seminate a 4000 cells/cm^2.

In vivo, le cellule umane iniettate nel modello sperimentale di cryoinjury cardiaca sono state ritrovate dopo 30 giorni sia a livello sia dell'area lesa che del miocardio. A differenza delle cellule cardiomiocitarie, impiegate come controllo e presenti a cluster solo a livello del sito di iniezione, le cellule hAFS sono state trovate in stretta vicinanza a cellule endoteliali e muscolari lisce dell'ospite, in alcuni casi partecipando anche alla formazione di vasi chimerici quali capillari nella misura, rispettivamente, dell 20,83 ± 8,0%, (iniezione locale) e 19,30±8,1% (iniezione i.v.) dei vasi presenti nell'area del patch e della cryoinjury. Nel modello sperimentale di infarto acuto del miocardio, le hAFS si sono dimostrate capaci di esercitare un effetto paracrino *in vivo* riducendo in maniera significativa l'estensione dell'area infartuata (calcolata quale rapporto tra la zona infartuata e la zona ischemica a rischio), da un valore del 53,9 ± 2,3% della superficie ischemica, ottenuto negli animali di controllo con iniezione di PBS, a un valore del 40,0 ± 3,0% della superficie ischemica, ottenuto negli animali trattati con iniezione sistemica di $5x10^6$ cellule hAFS. A supporto di tale ipotesi si è, inoltre, dimostrato come le cellule hAFS siano in grado di secernere timosina β4, fattore paracrino recentemente dimostrato avere funzione cardioprotettiva e angiogenica e di

contenere al loro interno una sottopopolazione di cellule progenitrici cardiache, positive per l'espressione di geni di differenziamento precoce quali Isl1 e Kdr.

In conclusione, i risultati ottenuti fin'ora hanno evidenziato come le cellule staminali del liquido amniotico possiedano un interessante potenziale differenziativo cardiomiogenico e cardioprotettore, che potrebbe essere sfruttato nel campo dell'ingegneria tissutale e della terapia cellulare cardiaca.

SUMMARY

Background.

In the last years tissue engineering for cardiac pathologies has been broadly developed with the aim to restore or improve the diseased or damaged heart.

Novel cardiac tissue engineering approaches combine the use of biocompatible scaffolds with stem cells to conjugate material science, surgery and cell therapy techniques. So far, different kinds of stem cells have been described and their potential for cardiac regeneration broadly investigated.

Considering the paediatric scenario, in which congenital heart malformations often require treatments shortly after birth, progenitors derived from the foetus during gestation could represent a great clinical advantage in these settings.

We have previously described that it is possible to derive lines of broadly multipotent cells from the amniotic fluid (*Amniotic Fluid Stem* cells; AFS cells); it has also been previously demonstrated that these cells, co-cultured *in vitro* with rat neonatal cardiomyocytes (rCM), can acquire a "cardiomyocyte-like" phenotype.

Aim of the Study.

The aim of this study was to characterize more in detail the AFS cells cardiomyogenic potential both *in vitro* and *in vivo*.

The *in vitro* study was mainly focused on creating a suitable environment for the AFS-rat neonatal cardiomyocyte cell co-culture in order to promote the *in vitro* AFS cells differentiation performing bidimensional culture on micro-patterned scaffolds; whereas in the *in vivo* study we analyzed the AFS cells therapeutic potential by the injection into a rat model of cardiac cryoinjury and acute myocardial infarct.

Methods.

Neonatal rat cardiomyocyte (rCM) cells were obtained by enzymatic digestion of 2-3-days old rat hearts. GFP-positive rat AFS (gfp^+rAFS) cells were obtained from amniotic fluid samples from GFP-positive transgenic pregnant rats. Human AFS (hAFS) cells were obtained from healthy amniotic fluid back up samples from prenatal diagnosis, following informed consent. AFS cells were isolated by immunosorting for the stem marker c-kit. The cardiomyocyte differentiation potential of AFS cells, *in vitro* cocultured with rat neonatal cardiomyocytes, had been already demonstrated by the PhD candidate in a previous work (*Chiavegato A., Bollini S. et al. 2007*); considering that,

before applying a tissue engineering approach, using biocompatible scaffolds, to the AFS and rCM cells coculture, the AFS cells "cardiomyocyte-like" phenotype, acquired in cocolture, had been functionally evaluated by patch-clamp analysis.

In this work two different kinds of bidimensional micropatterned scaffolds were used: hydrogel films and PDMS (silicon) membranes. The scaffolds were obtained by microcontact printing technique and using a mold scratched with the desidered micropattern and their viability was tested using, at first, the rat neonatal primary culture. Once that the the PDMS scaffold was identified as the most suitable support, AFS and rCM cells were seeded together on the micropatterned PDMS membranes and analyzed for the expression of troponin T by immunostaining after 6 and 10 days of culture.

For the *in vivo* study, immunodeficient nude male rats underwent a *cryoinjury* on the heart left ventricle with a 3D collagen scaffold implantation and $5x10^6$ hAFS cells/animal local or systemic injection after 15 days. hAFS cells were previously labelled with the red intracellular fluorescent dye CMTMR. Animals were sacrificed at 24 hours, 15 and 30 days after cells injection and hearts stained for cardiac and inflammatory markers. For the acute myocardial infarct model, male Wistar rats underwent an ischemic injury by left anterior descendent coronary artery ligation for 30 minutes and then they were reperfused injecting via the external jugular vein 10^7 or 10^6 gfp^+rAFS and 10^7 or $5x10^6$ hAFS cells/animal for 2 hours; rats were sacrificed afterwards and hearts analyzed for infarct size measurement by Evans blue staining, by 2,3,5-triphenolltetrazolium chloride (TTC) staining and planimetry with the software Image J. Heart, lungs, spleen and liver were analyzed as well by immunostaining for evaluating hAFS cells content.

hAFS cells were also analyzed for the presence of a subpopulation of cardiac progenitors, by RT-PCR analysis, for the expression of early cardiac commitment genes as Isl1 and Kdr. The cells were then studied by ELISA essay to speculate if they can secrete in the culture medium the protein thymosin β4, paracrine and cardioprotector factor.

Results and Conclusions.

Regarding the *in vitro* results, AFS cells were demonstrated to express a "pace maker cell-like" action potential, when cocultured with rat neonatal cardiomyocyte cells.

Moreover, when cultured on the bidimensional scaffold, AFS cells showed to follow the longitudinal orientation of the microstruttured membrane, expressing beating activity and the cardiac protein troponin T. The coculture seeded as control showed that after 6 days about 5,06±2,8% of AFS cells seeded at 1000 cells/cm^2 and 2,1±0,08% of the AFS cells seeded at 4000 cells/cm^2 were expressing the cardiac marker troponin T; after 10 days none of hAFS cells expressing TnT was found in the control coculture at 1000 cells/cm^2, whereas in the one with hAFS cells at 4000 cells/cm^2 were 4.97±2,5%. In the coculture on the micropatterned membrane 2,5 ± 2,4% of hAFS cells seeded at 1000 cells/cm^2 and 6,73 ± 2% of the ones seeded at 4000 cells/cm^2. After 10 days these values increased to 11 ± 4,7% of hAFS cells seeded at 1000 cells/cm^2 and 13 ± 4,2% of the ones seeded at 4000 cells/cm^2.

Our *in vivo* data revealed that hAFS cells, injected into the cryoinjured rat heart, survived in the host up to 30 days, moved from the injection site to the lesioned area in the heart and gave rise to new chimeric capillaries as, respectively, the 20,83 ± 8,0%, (local injection) and 19,30 ± 8,1% (i.v. injection) of the whole vessels amount in the patch and cryoinjury area.

In the acute myocardial infarct model the results obtained suggested that hAFS cells could exert a paracrine effect *in vivo,* decreasing the infarct size (measured as the ratio between the infarct area and the ischemic area at risk of necrosis) from a 53,9 ± 2,3% (obtained in control animals receiving PBS injection) to 40,0 ± 3,0% of the ischemic area.

Furthermore, hAFS cells were also demonstrated to have a subpopulation of cardiac progenitors, positive for the expression of the early cardiac commitment genes Isl1 and Kdr and to to secrete in the culture medium thymosin β4, a paracrine factor previously shown to act as cardioprotector and angiogenic agent.

In conclusions, our results are very encouraging and challenging, suggesting that AFS cells can show cardiomyogenic potential and cardioprotective therapeutic application in cell based therapy tissue engineering.

X

TABLE OF CONTENTS

ABBREVIATION

ES	Embryonic Stem Cells
BM-MSC	Bone Marrow Mesenchymal Stem Cells
MSC	Mesenchymal Stem Cells
Sca-1	Stem Cell Antigen-1
VSELs	Very Small Embryonic-like Stem Cells
LV	Left Ventricle
maGSCs	Multipotent Adult Germline Stem Cells
iPS	Induced Pluripotent Stem Cells
EPC	Endothelial Progenitor Cells
AFS	Amniotic Fluid Stem Cells
SSEA4	Stage Specific Embryonic Antigen 4
3D	Three-dimensional
PLA	Poly Lactic Acid
PLGA	Poly Lactic Glycolic Acid
GMP	Good Manifacturing Practice
αMEM	α Modified Essential Medium
DMEM	Dulbecco's Modified Essential Medium
EDTA	EthyleneDiamineTetraacetic Acid
FBS	Foetal Bovine Serum
hAFS	Human Amniotic Fluid Stem Cells
CMTMR	5-and-6-(4-chloromethyl)benzoyl)amino)tetramethylrhodamine
$cmtmr^+$ hAFS	CMTMR-positive Human Amniotic Fluid Stem Cells
GFP	Green Fluorescent Protein
gfp^+ hAFS	GFP-positive Human Amniotic Fluid Stem Cells
gfp^+ rAFS	GFP-positive Rat Amniotic Fluid Stem Cells
rCM	Neonatal Rat Cardiomyocyte Cells
gfp^+ rCM	GFP-positive Neonatal Rat Cardiomyocyte Cells
PDMS	Poly (dimethylsiloxane), Silicon
PFA	Paraformaldeide
PBS	Phosphate Buffer Solution

BSA	Bovine Serum Albumin
TnI	Troponin I
cTnT	cardiac Troponin T
CD	Cluster of Differentiation
Stro-1	Stromal factor-1
NGFr	Receptor for Neural Growth Factor
MHC	Major Histocompatibility Complex
APD50	Action Potential Duration at 50% Repolarization
APD90	Action Potential Duration at 90% Repolarization
Em	Membrane Potential
Δ	Membrane Depolarisation during Action Potential
µCP	Micro Contact Printing
rNU	Nude Immunodeficient Rats
s.c.	Sub Cutaneous
i.p.	Intra-Peritoneum
i.m.	Intra-Muscular
ANI	Acute Necrotizing Injury
LAD	Left Anterior Descending Coronary Artery
MI	Myocardial Infarct
SMA	α Smooth Muscle Actin
vW	von Willebrand's Factor
AAR	Area At Risk of necrosis
IS	Infarct Size
In	Infarct Area
TTC	Triphenyl Tetrazolium Chloride
OCT	Optimal Cutting Temperature solution
mRNA	Messenger Ribonucleic Acid
RT-PCR	Reverse Transcription Polymerase Chain Reaction
dNTP's	Nucleotides
ELISA	Enzyme-Linked ImmunoSorbent Assay
Hum Mit	Human Mitochondria Antigen

Mϕ	Macrophage cell

Chapter 1 Introduction.

In the last years cell therapy and tissue engineering for cardiac pathologies has been broadly developed with the aim to restore or improve the diseased or damaged heart through the use of cell transplantation, living graft, cardiac patch, vascular and valve constructs.

Novel cardiac tissue engineering approaches combine the use of biocompatible scaffolds seeded with stem cells to conjugate material science, surgery and cell therapy.

Different kinds of stem cells have been described and their potential for cardiac regeneration broadly investigated. Despite embryonic stem (ES) cells possess the greatest differentiation potential among all stem sources, concerns are still present regards their immunogenic and teratogenic effects. On the contrary, adult stem cells are beneficial as not being tumourogenic and can be used in an autologous setting, but they can be found only in small numbers and have a smaller differentiation potential. To avoid these problems, different strategies have been evaluated. Therapeutic cloning has been suggested to avoid rejection with ES cells, while reprogramming of adult stem cells, towards the embryonic stages, has also been more recently explored.

Considering the paediatric scenario, in which congenital heart malformations often require treatments shortly after birth, it is also particular interesting to discuss about progenitors derived from the foetus during gestation that could represent a great clinical advantage in this particular setting.

1. Cardiac Tissue Engineering.

Tissue engineering represents "*the restoration of function through the delivery of living elements which become integrated into the patient"* as reported by Vacanti in 1999 [(1)].

The development of biological substitutes is accomplished by the combination of various interdisciplinary aspects, such as cell biology, surgery and transplantation, materials science and engineering [(2)].

Patients with diseases or congenital malformations, affecting critical organs, are ultimately treated with transplantation. Unfortunately, there is an ever increasing patient need that does not correspond to an increase in donor organs. Tissue engineering could have the potential to face this crisis.

In particular in the heart, that has been always considered an organ with very little, or null, regeneration properties, cardiac tissue engineering has been proposed as a promising approach to repair congenital cardiovascular defects and large scar areas due to ischemia [3]. The aim of cardiac tissue engineering is, therefore, to repair or regenerate a damaged section of the heart and it has been suggested to create valves [4], small diameter blood vessels as well as for myocardial muscle [5,6].

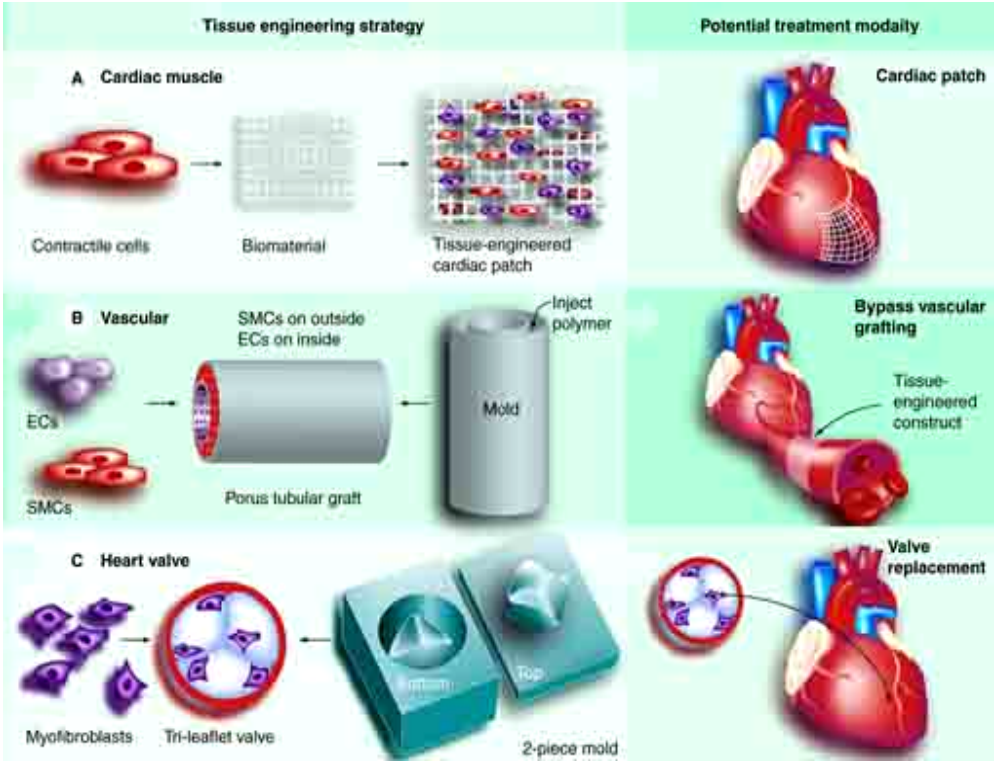

Figure 1. Cardiac tissue engineering strategies and targets, from *www.med.umich.edu*

Many cardiac defects can require tissue reconstruction with particular care to systemic connections often using non autologous inert synthetic constructs that can be associated with tromboembolic complications, hemolysis and infective endocarditis [7, 8]. Considering all these aspects, the best approach for cardiac tissue engineering should be combining an homogeneous mixture of biopolymers and cells able to engraft in a

fashion that would not distort the geometry of the heart nor evoke an immune reaction. According to Zimmermann, myocardial engineered grafts should be contractile, electrophysiologically stable, mechanically robust yet flexible and vascularised after implantation [9]. This ambitious program is very challenging as the graft must be flexible and integrated structurally and functionally with the host counterpart and even if tissue engineering has rapidly evolved, there are various obstacles that need to be overcome yet to proceed towards clinical applications.

Table 1. Advantages and disadvantages of myocardial tissue engineering approaches [6].

Approach	Advantages	Disadavantages
Cellular cardiomyoplasty (injection of cells only either directly or intravenously)	Minimally invasive surgery if injection is intravenous.	Lack of knowledge about cell contribution to myocardial regeneration or repair. Concerns about cell loss.
***In situ* engineering** (injection of cells and an injectable biomaterial)	Biomaterial acts as supporting matrix while cells will simultaneously regenerate infarction.	Involves open chest surgery and this suggestion is at infancy.
Injection of biomaterial alone	Matrix for homing autologous progenitor cells.	Immunogenicity, as only natural polymers have been suggested.
Left ventricular restraints	Does not involve cell injections.	No repair or regeneration.
Tissue engineering	Ensures cells are delivered to desired area with minimal cell loss.	Involves open chest surgery and more work is required to determine suitable cell type and material.

The first attempts of introducing biomaterials in culturing cells for improving *in vitro* efficiency and organization were in the late 80's, when Vandenburgh HH et al. embedded contractile primary avian myotubes in a collagen gel matrix (*collagel*) to avoid detachment from dishes [10].

In 1997 Eschenhagen et al. demonstrated how to culture functional beating embryonic-derived cardiomyocytes in a collagen matrix, between two Velcro-coated glass tubes, to produce a 3-dimensional model for measurement of isometric contractile force: in that work cells formed spontaneously contracting biconcave structures anchored on the glass tubes and attached to mechanical force transducer to record contractile force [11].

In order to improve strength of the engineered myocardium, solid matrices, that could have be easily shaped in any three-dimensional geometric form on a microscopic but also on a macroscopic level, have been developed. This new approach gave the opportunity to computer design the ideal polymer and to seed that with cardiomyocytes, or even other cell types, to generate tissue similar to the native heart. Li et al. in 1999 reported a fetal rat ventricular cardiomyocyte cell inoculum embedded into Gelfoam, a biodegradable gelatin mesh, to form 3D viable cardiac graft that contracts spontaneously once implanted onto myocardial scar tissue, forming junctions with the recipient heart cells [12].

Moreover, Zimmermann and colleagues, in 2002, demonstrated how to produce engineered heart tissue by mixing cardiomyocytes from neonatal rats with liquid collagen type I, matrigel and culture medium, casting them in circular molds subjected to mechanical stretch. The introduction of circular casting molds was particular significant for large scale production, with minimal handling and better tissue formation, as the circular geometry caused homogeneous force distribution [13]. Further attempt to engineer 3D cardiac graft was also suggested in 2002 by Shimuzu et al. with the application of a thermo-sensitive surface coated with poly(N-isopropylacrylamide) (PIPAAm). The cell engineered sheets were attached to the culture dishes at 37°C and detached as an intact sheet under controlled conditions at room temperature. Using this procedure, beating monolayers could be stacked on one another to form interconnected three-dimensional tissue of up to 50 to 70 um thickness [14]. This approach as scaffoldless tissue engineering has opened up in these years to other applications, such as experimental therapeutic angiogenesis in ischemic rat limbs, using human smooth

muscle cell sheets with the resulting increase in blood perfusion [15]. In 2004 electrical stimulation has also been introduced with generation of cardiac muscle constructs, to improve tissue morphology, contractile function and molecular marker expression [16].

Recently much attention has been focused in improving culture conditions with particular consideration to medium perfusion and metabolite production in three-dimensional cell systems. Bioreactors have been developed to provide the cells the suitable environmental conditions that can be closely monitored and controlled to permit or induce the desired biologic or biochemical process [17].

One of the biggest problems, indeed, involved in generating *in vitro* functional three dimensional cardiac tissues is assessing nutrient delivery to cells in the graft. Bearing in mind that diffusion can only supply nutrients to a depth of 150 um, we have to consider the thickness of human heart left ventricle which is 1- to 1.5 centimetres [18]. So far, bioreactor conditioning has been widely used in cardiac tissue engineering for heart valves, vascular grafts and cardiac patches. Dynamic bioreactor systems were used, for example, by Cebotari et al. for cultivating and differentiating autologous endothelial progenitor cells on the surface of human pulmonary heart valves scaffolds for 21 days *in vitro* [19]; Flanagan and colleagues showed that conditioning fibrin-based tissue-engineered heart valves, seeded with ovine carotid artery cells, for 12 days in a bioreactor system, enhanced cell adhesion and alignment within the scaffold [20]; Hahn et al. analysed the influence of biomechanical stimuli on vascular graft cells cultured in a pulsatile flow bioreactor resulting in significantly higher collagen production [21]; Gonen-Wadmany and colleagues in 2004 used a bioreactor system to improve cell organization in a bioartificial cardiac muscle by strain preconditioning [22]; Yang et al. developed a pulsatile flow system bioreactor for regulating human patch-tissue development in vitro with pediatric aortic cells [23]. Finally, recently bioreactor have been also used to better understand how scaffold architecture affects cell behavior, as showed by Fromstein and colleagues with ES-derived cardiomyocytes on porous, 3-dimensional scaffolds [24].

2. Cell Sources for Cardiac Tissue Engineering.

The "best cells" choice for cell based cardiac tissue engineering remain a matter of discussion that requires careful consideration for several aspects as isolation, expansion, delivery, integration, immunogenicity, survival, proliferation and functional integration in the host tissue for obtaining a viable graft [17] . Different cellular sources have been evaluated, as follows.

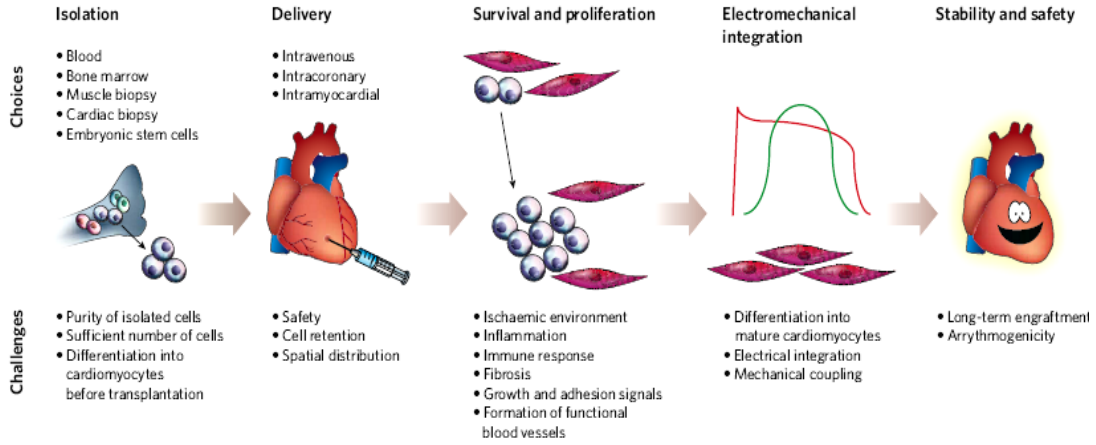

Figure 2. Cardiac regeneration requires careful consideration at each step, from isolation of the cell candidate to its safe and long-term integration in the host [31].

2.1. Primary Culture of Cardiomyocyte Cells.

Initially cardiomyocytes represented the ideal cell source since they possess the specialized characteristics of the aimed tissue. At that time, neonatal and adult cardiomyocytes had been widely used as *in vitro* model for studying cardiac biology and physiology, for analysis of cardiac development and for pharmacological drugs screening [6].

Cardiomyocytes have been extremely helpful in the development of contractile heart muscle grafts: culturing cardiac myocytes on synthetic or biologic matrices, supporting cardiac myocytes to form beating clusters by entrapment in collagen and making cardiac myocyte monolayers to form multi-layered heart constructs [25] are only some of the studies resulted by applying those strategies .

In this scenario, as previously mentioned, Zimmermann et al. developed a method to engineer cardiomyocytes in heart tissue grafts into collagen gels under cyclic stretching stimulation to create myofibers able of force generation and surviving after transplantation into rat hearts [11]; Shimitzu et al. created sheets of cardiomyocytes on a temperature-sensitive polymer surface able to fuse and beat synchronously and, even more, to be vascularised when implanted *in vivo* [26]. Despite all the encouraging results obtained with these cells, strong evidences are missing that cardiac tissue grafts could be generated at a size and with complete functional properties that would give enough support to failing or diseased hearts [27] or to be clinically applied, in particular, to paediatric patients. First of all, it is important to consider that specialized cells naturally loose their ability to divide and the number of fully differentiated cardiomyocytes, able to engraft a large polymer, can only be obtained using high proliferating cells.

Moreover, several important issues remain in using cardiomyocytes: the inability to get human cells in the necessary amount and, of course, the immune rejection aspect related to transplantation in allogenic settings [28].

Furthermore it has been taken more and more in consideration the crucial role that non-myocytes cells (fibroblasts, endothelial and smooth muscle cells, macrophages, etc) play in the heart development and physiology [29]. As a consequence, more attention has been focused on stem cells as a pluripotent source for generating all the principal cardiac cellular population: cardiomyocytes, endothelial and smooth muscle cells.

2.2. Stem Cells.

As well known, stem cells are characterized by the following general properties: the capability of producing new cells with equal stem functionality (*self renew*) or with restricted more specialized potential, expressing a specific committed phenotype (*differentiation*) [30].

Stem and progenitors cells, both from autologous or allogenic donors, have been analyzed to find the right candidate for cardiac cell therapy: ES cells have been demonstrated to give rise to cardiomyocytes contributing to heart contractility and electrical properties; resident endogenous cardiac progenitors and stem cells have been shown to be able to differentiate in the three main cardiac cellular types with interesting

applications in infarct and extracellular matrix remodelling and angiogenesis; adult stem cells from blood, bone marrow and adipose tissue have been proved to differentiate to endothelial cells and exert paracrine effects, inducing activation of cardiac resident stem cells [31, 32].

Originally stem cell therapy was thought to mainly improve cardiac condition by cardiomyocyte differentiation. Although several studies reported the ability of stem cells to regenerate cardiomyocytes, some others failed in supporting these results, suggesting that the mechanistics of cardiac stem cell therapy seems to be far more complex. Recently different pathways of benefits have eventually been proposed in stem cell based cardiac therapy: differentiation into cardiac lineages, fusion of stem donor cells with the host cardiomyocytes and paracrine effect [33].

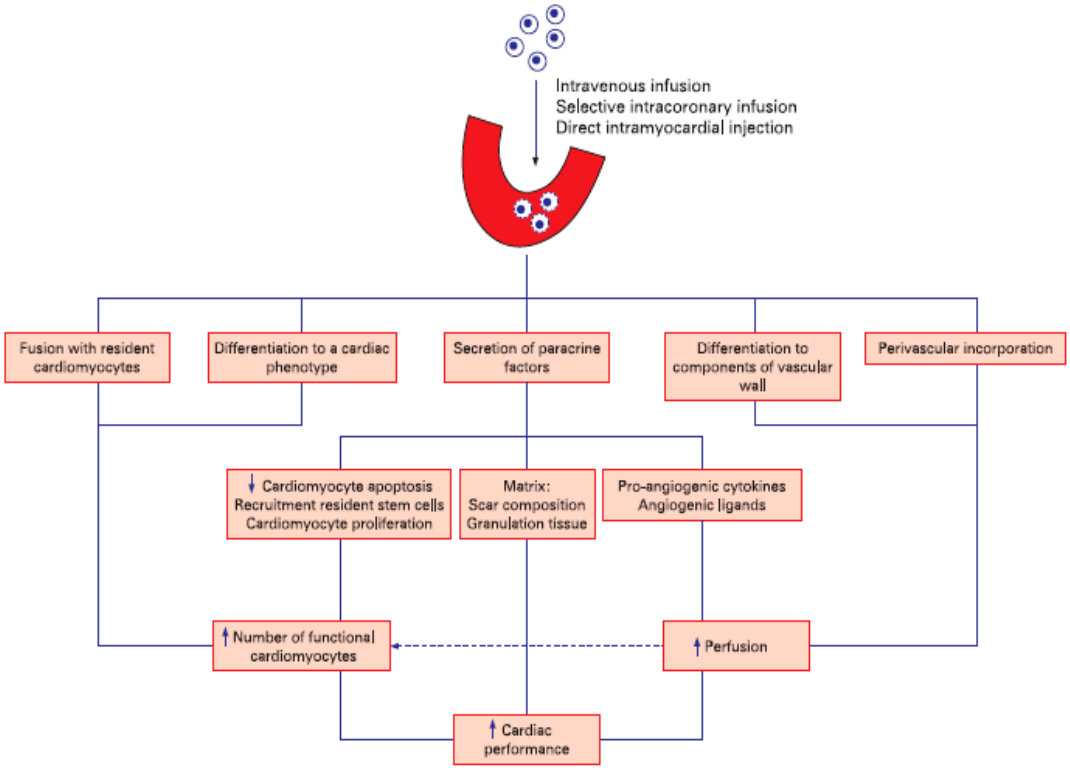

Figure 3. Potential mechanism through which stem cells may improve cardiac performance [33].

2.2.1. Embryonic Stem Cells.

ES cells, derived from the inner mass of the blastocyst, are pluripotent cells able to form tissue of all the three germ layers [34]. As a consequence, if rightly stimulated, they can

generate all different cardiac cell types, such as pacemaker, atrial, nodal, Purkinjie-like and ventricular cells [35].

In the last years different ES lines have been established and used with promising results in the cardiac field. Undifferentiated green fluorescent protein (GFP)-positive mouse ES cells, seeded on collagen type I scaffold and implanted in the infarcted area of athymic nude rats, formed stable integrated grafts without distorting myocardial geometry [36]. More recently, Caspi et al. reported the formation of synchronously contracting engineered human cardiac tissue derived from human ES cells containing endothelial vessel networks on porous sponges of poly-L-lactic acid and polylactic-glycolic acid [37]. Moreover, the use of stem cells in the field of gene therapy and tissue engineering for the treatment of cardiovascular disorders has also been explored by engrafting pace making cells derived from human ES cells or adult stem cells, into the myocardium [38].

Even if the results obtained with ES are really promising, there are many aspects and concerns to be worked out: derivation of hES requires embryos destruction, with all the ethical consequences and, more important, immunogenic and teratogenic problems have not completely solved. In conclusions, while they represent the best tool for investigating cardiac development, their clinical application has still not been explored.

2.2.2. Adult Stem Cells.

Adult stem cells have been isolated from different tissues, such as bone marrow, brain, liver, skin, skeletal muscle, gastrointestinal tract, pancreas, eye, blood, dental pulp, appendix [2, 39].

Their use avoid all the ethical problems associated with ES and so far they have been the only stem population to be employed in the clinical setting [31]. They can differentiate both *in vitro* and *in vivo* into cardiomyocytes, even though the heart's function is poorly improved [40]. Different *in vitro* methods have been evaluated, including the use of the metilating agent 5-azacytidine [41], the employment of cardiomyocyte conditioned media [42] or of growth, soluble factors and cytokines enriched media [43] and, finally, the direct interaction with cardiomyocytes by the use of co-culture systems [44,5,6,7, 8] .

Bone marrow- and skeletal muscle-derived stem cells have mostly been investigated both in research and clinical trials [49].

Bone marrow mesenchymal stem cells (BM-MSC) have high self renew properties, can be easily isolated and expanded in laboratory and have been demonstrated to differentiate *in vivo* and *in vitro* into cardiac cells. They have been widely studied both for engineering heart valves and for repairing damaged myocardium. In 2005 Knight et al. [50] demonstrated that human mesenchymal progenitor cells have the capacity to infiltrate an acellular porcine valve matrix, while, one year later, Bin et al. [51] showed that human BM-MSC, seeded onto aortic or pulmonary decellularized valve homografts, could differentiate *in vitro* into endothelial cells. Adult BM-MSC cells have also been successfully delivered into the rat heart infarcted region using collagen scaffolds [52] and more recently, in a lamb model, MSC were injected on a xenogenic decellularized scaffold, showing satisfactory hemodynamic improvement [53]. Up to this time, different studies reported the positive effects of MSC transplantation in infarcted heart, but the mechanism behind is still unclear: lately it has been suggested that these cells could mediate a paracrine effect on the ichemic area, stimulating resident stem cell or modulating inflammatory response [54]. Furthermore, a new sub population of bone marrow cells, defined as Sca-1+/Lin-/CD45- (VSELs), was demonstrated to express cardiac markers, to differentiate into cardiomyocytes *in vitro* and to improve LV function and alleviate myocyte hypertrophy after myocardial infarct *in vivo* [55]. Finally MSC have also been proposed as a new cell source to engineer blood vessel, as reported recently by Gong and Niklason, in a work demonstrating cell differentiation to smooth muscle cells using biodegradable scaffold and a biomimetic perfusion system [56].

Besides MSC, skeletal muscle-derived stem cells represent an easy accessible source for autologous regenerative therapy as they can be isolated from muscle biopsies, are able to contract, regenerate damaged muscle and have a high proliferative and myogenic potential, but, on the contrary, they seem not to establish electromechanical coupling with resident cardiomyocytes when implanted *in vivo*, with the subsequent risk of arrhythmic problems [57]. However, transplanted myoblast sheets were able to repair the infarcted rat myocardium and prevented remodelling in association with recruitment of hematopoietic stem cells releasing stromal-derived factor 1 and other growth factors [58]. Moreover, polyurethane scaffolds seeded with myoblasts prevented heart failure after

myocardial infarct in rats by paracrine effect [59, 60]. These cells, transfected with a therapeutic gene, have been also used in a rat heart model of acute myocardial infarction to mediate angiomyogenesis as reported by Ye et al. [61]. In these prospective, satellite cells has been also the advantage of being easily transfected making them an ideal vehicle for gene therapy [62].

So far, it has been shown that adult stem cell therapy can avoid all the concerns associated with ES, but, at the same times, these cells have been demonstrated to have some other limitations: they can be found in small numbers, express differentiation low rate, low self renewal and can be exposed to virus and toxic agents during life [63, 4]. Considering the paediatric scenario, a cell source with more immature properties would probably enhance the proper differentiation and integration in the young developing host tissue.

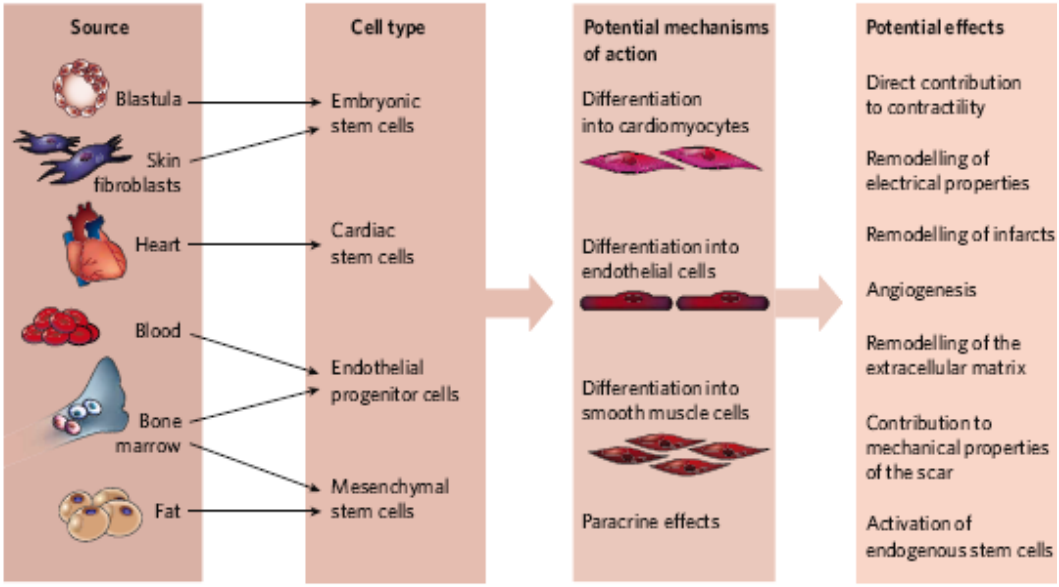

Figure 4. Different types of stem and progenitor cells have been demonstrated to be useful to improve cardiac function through different mechanisms [31].

2.2.3. Germline Stem Cells.

Multipotent adult germline stem cells (maGSCs) can be classified as cells standing between ES and adult cells. These cells have been recently decsribed by Guam et al. who reported, indeed, their successful isolation from mouse testis. These cells showed

characteristics similar to ES, including spontaneous differentiation into derivatives from all 3 germ layers. In that work maGSCs were also demonstrated to differentiate into functional cardiomyocytes, possibly useful for potential cardiac therapy [65]. As germline stem cells have been demonstrated to resemble ES on the cellular plasticity level, theoretically, they can satisfy both needs of having adult stem cells with the ES differentiating properties and the standard of care that needs an autologous cell line, suitable for the individual needs of the patient avoiding rejection if implanted. The perspective cell therapy application could, for example, rely on individual cell and gene-therapy via transdifferentiation of the maGSC into the desired somatic stem cells. On the contrary, as maGSC can be reprogrammed to ES-like cells and contribute to several tissues if implanted in an early blastocyst [66], they could have the same problem as ES regarding teratoma formation.

2.2.4. Induced Pluripotent Stem (iPS) cells.

Lately new approaches have been also developed to create pluripotent stem cells from adult somatic cells, by somatic nuclear transfert or genetic reprogramming. Recently Takahashi et al, and, independently, Okita et al. demonstrated, indeed, the generation of pluripotent embryonic-like stem (iPS) cells obtained by a novel protocol consisting in reprogramming somatic cells with retroviral transfection for the pluripotent genes as Oct4, Sox2, C-Myc, klf4 [67, 8]. These cells, firstly obtained using mouse fibroblasts, have been shown to be functionally identical to ES [69, 70] and the protocol has been then applied also to human somatic cells to obtain human iPS cells [71].

iPS differentiation properties have still to be fully elucidated, but some interesting works have already demonstrated their promising cardiovascular potential: Narazaki and colleagues have just showed that mouse iPS cells can be induced to cardiovascular lineages by applying ES culture conditions [72]; furthermore Mauritz et al. have recently demonstrated that functional murine cardiomyocytes can be derived from iPS cells for cellular cardiomyoplasty and myocardial tissue engineering purposes [73].

Considering the preliminary results obtained so far, iPS cells seem to be really promising for research and patient-specific therapy: this technology, indeed, represents a new method not only to obtain but even more to generate de novo pluripotent cells

from an adult somatic source. In particular, these cells can be achieved in a way completely independent of the need of embryos or ES, unlike some previous protocol as nuclear transfer and fusion of somatic with ES cells. Moreover, they can be derived from the patient's biopsy, so they could represent an autologous source for cell therapy and transplantation, bypassing problems related to immune rejection.
On the other hand, as these cells are "created" by genetic manipulations and their stability has not been fully understood yet, the possibility of their therapeutic clinical applications still needs to face several regulatory aspects. iPS have to be more fully investigated and analyzed for being used in clinical setting and, for the time being, they can be only used as models for development or for human diseases [(74)].

2.2.5. Foetal related Stem and Progenitors Cells.

Autologous cells are the most ideal cell source for tissue engineering in regenerative medicine. For long time in this scenario adult stem cells have been the preferred choice for transplantation purposes. Autologous adult stem cells can be isolated from biopsies (i.e. bone marrow, skeletal muscle, etc) and then *in vitro* cultured to engineer tissues grafts, but being adult cells they have limited turn over and *in vitro* differentiation. Furthermore, the possibility of doing autograft, with stem cells derived from an adult remains problematic, particularly for genetic diseases. Hence, recently, more attention has been focused on the isolation and use of foetal progenitors and stem cells, that, as they are more immature, seem to have wider proliferative and differentiation abilities and could offer a unique opportunity to correct genetic diseases. Foetal tissue is an attractive source of stem cells for autograft and allograft transplantation because of it's pluripotency, proliferative ability and lack of immunogenecity; foetal tissue could be obtained from a direct biopsy of the fetus during gestation or from cord blood, umbilical cord, term placenta, villi and amniotic fluid: as the first procedure is associated with a defined morbidity and mortality, the other ones are preferred.
More in detail, in the scenario of pediatric cardiology, congenital heart malformations may required shortly after birth surgical treatment: it would be really advantageous to find and employ an autologous source of progenitors from the foetus to engineer living heart tissues *in vitro* in parallel to pregnancy, ready to be implanted at birth.

Stem cells have been isolated from human umbilical cord blood [75, 6] and placenta [77, 78, 79], showing a fibroblast-like morphology and a mesenchymal phenotype similar to BM-MSC. In particular, both hematopoietic and mesenchymal stem cells have been isolated from human umbilical cord blood: the first are commonly used clinically for transplantation on paediatric patients suffering from leukaemia and cord blood banks have been established for the stem cell cryopreservation [80].

Lastly, different works on engineering cardiac tissues have been developed, using both foetal cells and progenitors: in 2002, Kadner et al. cultivated cells isolated from human umbilical cord on biocompatible patches *in vitro* for 14 days [81]; in 2004, Schmidt and colleagues used human umbilical cord blood-derived endothelial progenitors on biodegradable vascular scaffolds for the repair of congenital defects [82] and in 2005, they reported the generation of living tissue engineered patches from umbilical cord-derived myofibroblast and EPC [83]. More recently, Fang and colleagues in 2007 suggested how to overcome the limitations of heart valve replacements using human umbilical cord blood-derived endothelial progenitor cells and decellularized valve scaffolds [84].

Regarding placental tissue, foetal membranes were demonstrated to contain human mesenchymal stem cells that can be used in cardiac tissue engineering, according to their potential to express cardiac lineage markers *in vitro* under specific condition and to exert *in vivo* a positive effect on infarct size in a rat model [85]. Even more, cells from the chorionic plate in the foetal portion of human placenta were demonstrated to express cardiomyocyte specific genes and suggested as candidate for stem cell- based cardiac therapy [86].

Along foetal sources, amniotic fluid is another very important source of cells containing progenitors and stem cells, with suitable potential for cardiac tissue engineering applications.

Amniotic fluid is, indeed, known to contain multiple cell types derived from the developing fetus and it could represent an alternative, more accessible source: cells can be easily collected using amniocentesis, a well established technique for prenatal diagnosis, with low risk both for the foetus and the mother. Until very recently, cells present in the amniotic fluid have been only used for prenatal diagnosis; in these last few years, our and other groups have presented various studies demonstrating the

presence of different progenitors in the amniotic fluid, mainly with mesenchymal characteristics [87, 8, 9, 90]. Amniotic fluid derived mesenchymal stem cells have indeed been shown to acquire a smooth muscle cell-like phenotype *in vitro* and *in vivo* [91] and have the potential to differentiate into other various mesenchymal lineages, while keeping the proprieties of forming functional endothelial lineages. Moreover, we have recently described that it is possible to derive lines of broadly multipotent cells from the amniotic fluid (amniotic fluid stem -AFS cells) [92]. Using discarded back-up amniocentesis samples, we isolated AFS cells by selection for expression of the membrane stem cell factor receptor c-Kit. So far our group has analyzed the AFS cells differentiating potential demonstrating that clone AFS human lines, expressing stem markers SSEA4 and Oct 4, were induced to differentiate into cell types representing each embryonic germ layer, including cells of adipogenic, osteogenic, myogenic, endothelial, neuronal and hepatic lineages.

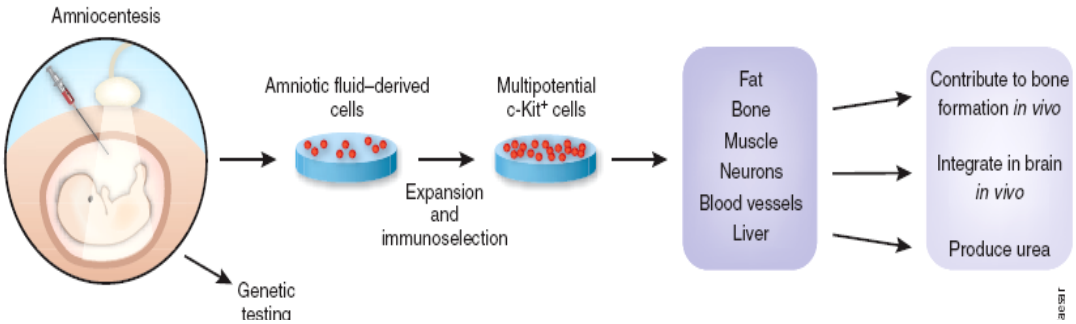

Figure 5. Under appropriate inducing conditions cKit$^+$AFS can be differentiated into cells of all three germ layers [93].

Furthermore, human AFS cells are able to express cardiomyocyte marker when co-cultured with rat neonatal cardiomyocytes [94]; these cells, similar to the amniotic fluid-derived mesenchymal stem cells demonstrated by Zhao and colleagues [95], seem to contain a cardiac progenitor population, since they express mRNA for cardiac early transcription factors as well as proteins in their undifferentiated state. These data suggest that undifferentiated AFS cells could posses cardiomyocyte plasticity *in fieri* and that this differentiation potential into cardiomyocyte cell lineages has to be trigged and enhanced by specific culture conditions.

Other groups have characterized amniotic fluid-derived mesenchymal stem and progenitor cell as well: in particular Schmidt et al. in 2007 reported a methodology to first isolate $CD133^+$ amniotic fluid progenitors cells, that were subsequently combined with the proportion $CD133^-$, enabling the prenatal fabrication of heart valves [96]. This is an interesting approach for the correction of congenital heart defect; however, Schmidt et al. did not investigate whether $CD133^+$ cells derived from the amniotic fluid had the ability to undergo to cardiomyogenic differentiation as previously showed for other fetal cell subpopulation [97].

As recently shown by several studies [98, 9,100,1,2], more interest is now addressed to amniotic fluid derived stem cells for clinical applications: considering their potential, these cells could be chosen among those cellular sources suggested for being cryopreserved and banked, to be used in novel cell based therapy [103]. Their peculiar properties, such as survival at lower oxygen tension and the ability of withstanding protracted cryopreservation, maintaining their phenotype and their self renewal potential, make them suitable for being used into clinical settings. In this scenario, their application in the tissue engineering field seems now close for some of congenital disease, such as the diaphragmatic hernia treatment [104].

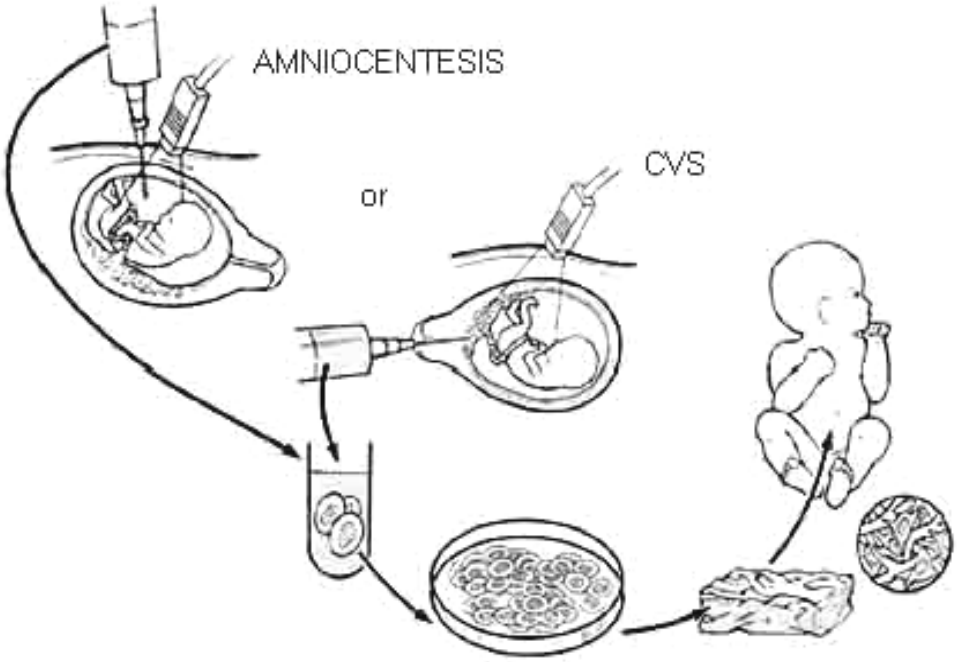

Figure 6. Paediatric tissue engineering with foetal stem cells collected by amniocentesis or chorionic villi sampling [105].

Considering all these aspects, amniotic fluid stem cells could represent a good cellular source for cardiac tissue engineering purposes applied to paediatric congenital cardiovascular malformation: large quantities of amniotic fluid are available during pregnancy and at the time of birth, so stem cells could be easily obtained from this source and expand *in vitro*; furthermore, these cells seem to be able to acquire a cardiomyocyte-like phenotype under specific conditions and to differentiate in smooth muscle and endothelial cells; finally c-kit selection could represent also a good reproducible strategy for obtaining cells prone to create possible substitutes for neonatal cardiac repair.

3. Biomaterials for Cardiac Tissue Engineering

The other crucial aspect related to cardiac tissue engineering is represented by the biomaterials used.

Matrices and polymers used in tissue engineering could be formed by naturally derived substances (i.e. collagen or alginate) or synthetic polymers (PLA, PLGA) [2]. Scaffold

can be in form of meshes, fibres, porous, solids or hydrogels. Ideally, a suitable biomaterial should be biocompatible, biodegradable, not immunogenic, highly permeable to nutrients, able to become vascularised and support tissue growth and, finally, clinically approved by GMP procedures [17].

In cell based tissue engineering the main function of the biomaterials is to mimic the biological function and mechanical support of extracellular matrix, providing a substrate for cell seeding and/or a way of delivering them into the host tissue.

Acellular matrices, obtained by removing cellular components from tissue, were the first to be studied, in particular in the field of heart valve and vessels engineering [2]. Different studies were reported, for example endothelial precursors cells from peripheral blood, seeded on decellularized porcine iliac vessels, were able to engraft for 130 days into a sheep carotid [106]; following this first study, many others investigated how to engineer valve replacements using acellular porcine aortic valve matrices seeded with mesenchymal progenitors cells or smooth muscle cells [107]. More recently, new synthetic biopolymeric materials have been introduced, as the modified PGA (poly glycolic lactic acid) that has been used in the work of Mol et al., where they analyzed the biocompatible and functional properties of this degrading synthetic scaffold, seeded with human saphenous vein cells [108]. Recently Ott et al. showed how to produce an acellular, perfusable vascular architecture of the mouse heart, by decellularization generating a bioartificial heart by reseeding the construct with endothelial and cardiomyocytes cells with functional properties up to a month in bioreactors [109].

Table 2. Scaffold materials and their use in myocardial constructs engineering applications [27].

Scaffold material	Cells	Conditioning	*In Vivo* Model	Results
Gelatin Mesh	Fetal rat ventricular cells.	Static	Rat myocardial cryoinjury	Long term survival of engineered constructs.
Porous alginate	Neonatal rat cardiomyocytes.	Static	Rat myocardial infarction.	Safety and vascularisation with host myocardium.
Laminin	Cardiomyocytes + fibroblast.	Static	Rat s.c. model.	Vascularization of constructs.
Collagen matrigel	Neonatal rat cardiomyocytes.	Static	Uninjured hearts.	Highly differentiated cardiac tissue construct obtained.
Urinary bladder-derived extracellular matrix	None	None	Pig myocardial infarct	Biodegradable and form a vascularised myocardial tissue
Polyglycolic acid	Rat ventricular cells/bone marrow stem cells	Spinner flask/static	None/ Myocardial infarct	Cardiac structural and electrophysiological properties
Polyurethane	Myoblasts/ embryonic stem cell-derived cardiomyocytes	Static	Rat myocardial infarct/ none	Feasibility of using stem cells in myocardial constructs engineering
Polytetrafluoroethylene + polylactide + collagen	Mesenchymal stem cells	Static	Rat myocardial infarct	Tissue engineering with MSCs was established

Considering more novel scaffolds, different studies demonstrated that hydrogels could potentially be very useful in the cardiac tissue engineering scenario: Landa and colleagues showed that a calcium-crosslinked alginate hydrogel implant colonized up to half the scar area into infarcted heart, preventing cardiac remodelling after injection [110]; besides, as reported by Fuchs et al. in 2006, collagen hydrogels, combined with lamb foetal myoblast, supported the engraftment in the heart after birth and cell differentiation into cardiomyocyte-like cells *in vivo* [111].
Furthermore, in recent years, collagen gels and scaffolds have become one of the most common biopolymers used in cardiac tissue engineering. Human bone marrow-derived MSC, combined with human umbilical cord vein endothelial cells in a collagen gel, implanted *in vivo* into immunodeficient mice, were able to sustain the engineering of long lasting functional vasculature [112]. Moreover, a three-dimensional porcine derm derived type I collagen sponge has been used *in vitro* to engineering functional bioartificial grafts for supporting neonatal cardiomyocytes in bioreactor under electrical stimulation [16]. The same biomaterial, applied *in vivo* onto intact and cryoinjured rat hearts, was demonstrated to induce a powerful neo-vascularization response in the host tissue with new vessels formation increasing up steadly to 60 days; besides the scaffold itself became highly vascularised, representing therefore a useful substrate for *in vivo* stem cell seeding [113].

So far, all the biomaterials used in cardiac tissue engineering have been mainly designed as matrices suitable for adult subjects and for recovering or regeneration of heart valve defects or ischemic myocardium. Since therapeutic options for myocardial repair remain limited in the neonatal patients, further improvements are needed in paediatric cardiology and surgery for the treatment of congenital malformations and biocompatible polymers would be able to sustain completely the integration and the growth of the graft, soon after birth.
In conclusions, different strategies could be used for cardiac regeneration and cardiac tissue engineering. In this scenario, stem cells represent a key element in cardiac regeneration and they can be derived from different tissues before/after birth: it's a very fast developing field that has to be studied carefully to be applied to clinical settings in the near future.

Aim of the Study.

The aim of this study was to evaluate more in detail the cardiomyogenic potential of rat and human amniotic fluid stem (AFS) cells performing both *in vitro* and *in vivo* studies.
For the *in vitro* part of this work we analyzed more in details the cardiomyocyte differentiating capacity of these cells, from the functional point of view, performing electrophysiological assays; moreover, we screened some biocompatible bidimensional scaffolds to identify the most suitable one in order to create a proper environment for improving the cardiac potential of the cells, by tissue engineering approaches.
In the *in vivo* studies we used chronic and acute cardiac ischemic rat models to understand the therapeutic effect of AFS cells in the heart environment, both as cells regenerating cardiac tissue and mediators of cardioprotection by paracrine effect.

Chapter 2 *In Vitro* Study.

METHODS

1. Cell isolation, expansion and characterization.

1.1. Human Amniotic Fluid Stem Cells.

The human Amniotic Fluid Stem (hAFS) cells were prepared according to De Coppi et al. [92]. Briefly, samples of amniotic fluid were collected by amniocentesis from women, mean gestational age 14 weeks, during routine prenatal diagnosis. A written consensus was obtained from each woman to use the remaining amniotic fluid experimentally. Amniotic fluid samples were spun at 1,200 rpm in a Heraeus Multifuge S-R (Milan, Italy). Pellets were re-suspended in the culture medium, named as Chang medium [αMEM (Gibco, Invitrogen Italy), 20% of Chang Medium (Chang B plus Chang C; Irvine Scientific, CA, USA), 15% of foetal bovine serum (FBS, Gibco, Invitrogen, Italy), 1% of streptomycin and penicillin and L-glutamine (all from Invitrogen, Italy)]. Cells were seeded in non-tissue culture petri dishes. After three days, non-adherent cells and debris were discarded and the adherent cells cultivated in pre-confluency. Adherent cells were then detached from the plastic plate using a 0,05-0,02 w/v trypsin sodium-EDTA solution (Biochrom AG, Germany), and then immuno-magnetically sorted for c-kit using a mouse monoclonal anti-c-kit (CD117) antibody (Santa Cruz, Santa Cruz, CA) and a goat IgG anti-mouse IgG CELLection Dynabeads M-450 (Miltenyi Biotech, Bergisch Gladbach, Germany). Control cell sorting was performed by non-immune IgG, followed by the secondary antibody. C-kit$^+$ cells were replated at a density of $2x10^3$ cells/cm^2, expanded, cultured in Chang medium in 5% CO_2 37°C incubator and maintained at subconfluency.

1.2. Human Amniotic Fluid Stem Cells Labelling.

1.2.1. Intracellular Fluorescent Labelling.

In some experiments hAFS cells were labelled with the red fluorescent intracellular dye (5-and-6-(4-chloromethyl)benzoyl)amino)tetramethylrhodamine) CMTMR (Molecular Probes, Invitrogen), by a 30 minutes incubation with a solution of 0,25 ul/ml CMTMR in MEMα Medium at 37°C.

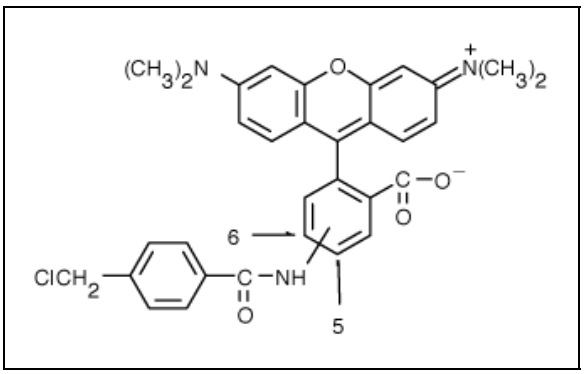

Figure 7: Chemical structure of CMTMR cell tracker.

1.2.2. GFP Lentiviral Transduction.

For some *in vitro* experiments hAFS cells underwent lentiviral vector transduction for GFP expression. Briefly self-inactivating (SIN) HIV-1 derived lentiviral vector with deleted U3 HIV LTR promoter activity and encoding a central polypurine tract (cPPT) element, for enhanced nuclear entry, was used. A strong murine retroviral promoter, derived from the Spleen Focus Forming Virus (SFFV) drives transgene (eGFP) expression (all courtesy of Dr. Waseem Qasim, ICH, UCL London). hAFS cells were transduced with vector pseudotyped with the vesicular stomatitis virus envelope at an MOI of ~10. After 72 hours and 15 days after transduction gfp^{+}hAFS cells were analyzed for evaluating the efficiency of the transduction by flow cytometry and in both cases it was about 70% of total cells.

1.3. GFP-positive Rat Amniotic Fluid Stem Cells.

Samples of rat amniotic fluid were collected by amniocentesis from transgenic GFP-positive pregnant Sprague-Dawley rats, mean gestational age 16 days p.c.
Amniotic fluid cells were processed according to De Coppi et al. 2007 [92]. Briefly, amniotic fluids were diluted with PBS and then spun at 1200 rpm; pellets were resuspended in Chang medium. Cells were seeded at a density of $2x10^3$ cells/cm^2. After a few days, non-adherent cells were discarded and the adherent cells cultivated until 80% preconfluency. Adherent cells were detached using a a 0,05-0,02 w/v trypsin sodium-EDTA solution, immunosorted with a rabbit anti-CD117 antibody (H-300 Santa Cruz Biotechnology, CA, USA-DBA Italia s.r.l., Italy) and mouse anti-rabbit IgG CELLection Dynabeads M-450 (Dynal Biotech, Invitrogen, Italy) and then replated at a density of $2x10^3$ cells/cm^2. GFP-positive rat AFS (gfp^+rAFS) cells were expanded and subsequently cloned by limiting dilution and kept growing in sub-confluent conditions.

1.4. Rat Neonatal Cardiomyocyte Cells.

Rat neonatal cardiomyocyte (rCM) cells were prepared according two different protocols by enzymatic digestion of newborn rat hearts. Wild type and GFP-positive neonatal (2-3 days-old) Sprague-Dawley rats were provided by the Department of Sperimental Surgery of the University of Padua.
The first protocol was used at the beginning and in the experiments regarding the use of biocompatible bidimensional scaffold, such as the hydrogel films.
Briefly, hearts were washed with ice-cold, sterile HBBS (Hank's Balanced Salt Solution, Worthington Biochemical Corporation), trimmed of auricles and excess of connective and adipose tissue and minced with sterile scissors. Myocardial tissue was then dissociated to release ventricular cardiomyocytes by an enzymatic isolation procedure first using a trypsin solution (50 μg/ml, Worthington Biochemical Corporation, USA), incubating overnight at 4°C,and then a collagenase solution (300 units/ml, Worthington Biochemical Corporation, USA) at 37°C for 45 minutes. rCM cells were then collected by centrifugation and non-myocytes cells were removed by preplating on culture dishes. Enriched CM were seeded in Plating Medium (Dulbecco's

Modified Eagle's Medium, Gibco Italy, enriched with 5% FBS, 10% Horse Serum, all from Biochrom Ag. Germany and 1% L-Glutamine 1% Penicillin and Streptomicin, Gibco, and medium M199 17%, Biochrom Ag.) and cultured in a 95% humidified incubator 5% CO2 at 37°C. At day one after seeding, cells were rinsed with culture medium to remove non adhering cells. The culture medium was replaced once a day.
The second protocol, used for all the other studies was followed according to Radisic et al. [28]. Briefly, ventricles were quartered, incubated overnight at 4ºC in a 0.06 % (w/v) solution of trypsin (Gibco, Invitrogen, Italy) in Hank's Balanced Salt Solution (HBSS, Gibco, Invitrogen, Italy), washed in culture medium Cardiac Growth Medium (CGM: Dulbecco's Modified Eagle's Medium,Gibco, containing 4.5 g/L glucose supplemented with 10% FBS, 1% HEPES, 1% L-Glutamine 1% Penicillin and Streptomicin, Gibco, Invitrogen, Italy), and subjected to a series of digestions (4 min, 37ºC) in 0.1 % solution (w/v) of collagenase type II (Wortinghton Biochemicals Corporation, USA) in HBSS. The cells were collected by centrifugation and then pre-plated for one hour period to enrich for cardiomyocytes. rCM cells were seeded on 1% gelatine-coated petri dishes (Falcon, BD Biosciences, Italy). At day one after seeding, cells were rinsed with culture medium to remove non adhering cells. The culture medium was replaced once a day.

1.5. Cell characterization.

For cellular membrane characterization flow cytometry was mainly used. Briefly, cells were detached by citrate buffer solution (diluted 10:1 from stock solution of 0.1M Citric Acid and 0.1 M Sodium Citrate, Sigma, Italy) from culture plate, resuspended in PBS at concentration of $5x10^5$ cells/100µl and then stained directly with FITC- or PE-labelled monoclonal antibodies.
Human AFS cells were stained directly with FITC-labeled monoclonal antibodies to several antigens: CD29, CD44, CD45, CD90, CD146 and HLA-ABC (Immunotech, Coulter Company, France). The following PE-conjugated monoclonal antibodies were also used to stain for CD34, CD73, CD105, CD117 and HLA-DR (Immunotech) and CD133 (Miltenyi Biotech), CD166 (PE Beckman Coulter CA, clone 3A6) and CD31 (FITC Immunotech, clone 5.6E).

For gfp^+ rAFS cells, the following antibodies were used: anti-CD45 (mouse monoclonal IgG Immunotech, MO, USA), anti-CD73 (mouse monoclonal IgG BD Pharmigen, BD Biosciences, Italy) and anti-MHC II (mouse monoclonal IgG Immunotech, MO, USA).
For rCM cells, the following antibodies were used: anti-CD29 (hamster monoclonal IgM, BD Biosciences, Italy), anti-CD 73 (mouse monoclonal IgG BD Biosciences, Italy), anti-CD90 (mouse monoclonal IgG BD Biosciences, Italy), anti-CD44 (mouse monoclonal IgG BD Biosciences, Italy), anti-CD45 (mouse monoclonal IgG, Immunotech, MO, USA), anti-CD54 (mouse IgG BD Biosciences, Italy, non conjugated: for this one was used as secondary antibody the rabbit anti-mouse Alexa Fluor. 488, Molecular Probes, Invitrogen, Italy), anti-CD31 (mouse monoclonal IgG BD Biosciences, Italy) and anti-MHC II (mouse monoclonal IgG, Immunotech, MO, USA). Analysis was performed by a COULTER Epics XL-MCL cytometer (Beckman Coulter, Fullerton, CA, USA) and data were elaborated by means of EXPO™ 32 ADC Software. Data are expressed as number of cells/10^6 cytometric events.
To monitor some cytoplasmic antigens in both populations, cells were also analysed by immunostaining on cytospun cellular spots as soon as they were isolated. For the immunostaining analysis, cells were collected using a Shandon Cytospin 4 centrifuge (Thermo Fisher Scientific, Inc., Waltham, MA, USA).
For characterizing human AFS cells phenotype, the following primary monoclonal antibodies were used: anti-SSEA4 (Chemicon, USA), anti-Oct 3/4 (rabbit polyclonal IgG, Santa Cruz Biotech, USA-DBA Italia s.r.l., Italy), anti-Nanog (rabbit polyclonal IgG, Abcam UK), anti-Flk-1 (mouse monoclonal IgG Santa Cruz Biotech,USA-DBA Italia s.r.l., Italy), anti von Willebrand factor (rabbit polyclonal IgG; Dako, Italy), anti-VE-cadherin (mouse monoclonal, Santa Cruz Biotech,USA-DBA Italia s.r.l., Italy), anti-NGF receptor (mouse monoclonal IgG Pharmigen BD Biosciences, Italy), anti-Stro-1 (mouse monoclonal IgG Iowa Hybridoma Bank, Iowa, USA), anti-α Smooth Muscle Actin (mouse monoclonal IgG Sigma, Italy), anti-pancytokeratin (mouse monoclonal IgG, Sigma, Italy) and anti-vimentin (mouse monoclonal IgG Dako, Italy).
For characterizing gfp^+rAFS cells phenotype, the following primary monoclonal antibodies were used: anti-SSEA4 (mouse monoclonal IgG Chemicon, Italy), anti-Oct 3-4 (rabbit polyclonal IgG, Santa Cruz Biotech, CA, USA DBA Italia s.r.l., Italy), anti-

CD34 (mouse monoclonal IgG, Sigma, Italy) anti-CD29 (mouse monoclonal IgG, Chemicon, Italy) anti-CD105 (mouse monoclonal IgG Cymbus Bioscience, UK), anti-CD90 (mouse monoclonal IgG Cymbus Bioscience, UK), anti-Stro 1 (mouse monoclonal IgG Iowa Hybridoma Bank, Iowa, USA), anti-Flk-1 (mouse monoclonal IgG Santa Cruz Biotech, CA, USA DBA Italia s.r.l., Italy), anti-α Smooth Muscle Actin (mouse monoclonal IgG Sigma, Italy), anti-NGF receptor (mouse monoclonal IgG Pharmigen BD Biosciences, Italy), anti-pancytokeratin (mouse monoclonal IgG, Sigma, Italy) and anti-vimentin (mouse monoclonal IgG Dako, Italy).

Fresh rCM cells were also analyzed by immunofluorescence means on cellular cytospun to fully characterize the cardiomyocyte primary culture as well. The following antibodies were used: FITC-conjugated anti-CD117 (mouse monoclonal IgG Dako, Italy), anti-cardiac troponin T (mouse monoclonal IgG, Abcam, UK), anti-4 prolil hydroxylase (mouse monoclonal IgG, Li StarFish, Italy), anti-α Smooth Muscle Actin (mouse monoclonal IgG, Sigma, Italy), anti-von Willebrand Factor (rabbit polyclonal IgG, Dako, Italy) and anti-vimentin (mouse monoclonal IgG Dako, Italy). Goat anti-mouse Alexa Fluorescence 594- or 488-coniugated, goat anti-rabbit Alexa Fluorescence488-coniugated IgG (Molecular Probes, Invitrogen, Italy) or the swine anti-rabbit TRITC-coniugated IgG (Dako, Italy) were used as secondary antibodies. Immunofluorescence observations were carried out using a Zeiss Axioplan epifluorescence microscope (Zeiss, Oberkochen, Germany) and acquired by Leica IM 1000 software.

2. *In Vitro* Differentiation.

2.1. AFS and rCM cells Co-Culture on plastic dishes.

gfp^+ rAFS and rCM cells co-cultures were established by admixing neonatal rCM and gfp^+rAFS cells at 10^5 and 10^3cells/cm^2 respectively and seeding the cell mixture in CGM on 1% gelatine-coated glass coverslips and plastic cell culture dishes (Falcon, BD Biosciences, Italy).

gfp^+hAFS and rCM cells co-cultures were established in the same way by admixing neonatal rCM and gfp^+hAFS cells at 10^4 and $2x10^3$ cells/cm^2 respectively and seeding

the cell mixture on 1% gelatine-coated glass coverslips and plastic cell culture dishes (Falcon, BD Biosciences, Italy).
Cells were cultured in CGM and the medium changes were carried out 3 times a week; co-cultured cells were analyzed by patch clamp technique after 4, 6 and 9 days. Experiments were done in triplicates.

2.2. Patch Clamp analysis on Co-Culture on plastic dishes.

Patch-clamp current recordings were performed with an Axopatch 200B amplifier (Axon Instruments, UK) using fire-polished pipettes with a resistance of 3-4 M□pulled from filamented borosilicated glass capillaries (Harvard Apparatus, 1.5 mm OD x 1.17 mm ID, USA). Data were acquired and analysed by using a Digidata 1322A interface (Axon Instruments, UK) and pCLAMP software (version 10, Axon Instruments, UK).
Action potential recordings of gfp^+rAFS, gfp^+hAFS and rCM cells were obtained by injecting current for 5 ms. For cells presenting a pacemaking activity, no current were injected. Cells were clamped at -80 mV in an extracellular solution containing (mM): NaCl 135, KCl 5.4, $CaCl_2$ 2, $MgCl_2$ 1, NaH_2PO_4 0.33, HEPES 5, Glucose 10 (all from Sigma). The intracellular solution was (mM): K gluconate 110, KCl 20, NaCl 10, $MgCl_2$ 1, MgATP 2, EGTA 2 GTP 0.3 (all from Sigma). Experiments were done in triplicates.

3. Biocompatible scaffolds.

3.1. Hydrogel Films.

Bidimensional hydrogel films were prepared according to Cimetta et al [114]. First of all glass slides surfaces were chemically modified creating a hydrophobic layer of methacrylate groups to ensure covalent binding of the hydrogel films. Briefly, slides were washed in ethanol and rinsed with distilled water, dried at 110°C and treated with air-plasma (Plasma Cleaner PDC-002, Harrick Plasma, USA) for 5 minutes at 0,5 mbar. A few drops of 3-(trimethoxysilyl)propyl methacrylate (Sigma-Aldrich, Italy) were

deposited on the glass slides, which were then stacked and after 1 hour dried in oven at 100°C for 10 minutes.

Hydrogels were prepared as follows. Acrylamide/bis-acrylamide 29:1 40% solution (Sigma-Aldrich) was diluted in phosphate-buffered saline (PBS, Sigma-Aldrich) to the final concentrations of 8, 10, 15 and 20%. The photoinitiator (Irgacure 2959; Ciba Specialty Chemicals, Italy), was initially dissolved in methanol at 200 mg/ml and then added to the acrylamide/bis-acrylamide solution in order to obtain a final concentration of 20 mg/ml, and mixed thoroughly.

Three individual 20µl volumes of the prepolymer solution were dropped over the functionalized glass surface and a glass coverslip was floated over each drop. Hydrogel polymerization occurred by exposing the prepolymer solution to UV light for 3 minutes. Irradiation was provided by a highpressure mercury vapor lamp (Philips HPR 125W) emitting at 365 nm. Selective photo-polymerization of acrylamide solutions on the glass surface was achieved by interposing a photomask with the desired geometry between the light source and the glass slide. Non-exposed regions were washed using distilled water to remove the non-polymerized solution. Such procedures resulted in homogeneous hydrogel films with an average thickness of 40 µm.

Hydrogel samples, shaped as 60mm diameter disks, were obtained photopolymerizing 20 ml of the prepolymer solution under UV light (λ=365 nm).

Hydrogel disks were placed between two parallel plates and compressed at the constant rate of 1 mm/min, until a final deformation of 120% was reached.

Glass slides with covalently bonded hydrogel films were immersed in ultra-pure distilled water for 48 hours to ensure complete removal of the un-reacted monomeric units or photoinitiator and then soaked in a 70% ethanol solution. After rinsing with ultra-pure distilled water, hydrogels were allowed to dry completely overnight; final sterilization occurred after 20 minutes exposure to UV light under a sterile hood. The desired array design was realized in digital form with Adobe Illustrator and consisted of 400 lanes 100 µm wide and 1 mm long, horizontally spaced by 100 µm and 300 µm vertically. This pattern was printed onto an overhead transparency and used as a photomask. A standard photolithographic technique was employed for the fabrication of the master using an SU-8 photoresist (MicroChem Corporation). Briefly, the SU-8 was spun over a silicon wafer, which was thermally treated, selectively polymerized by

interposing the patterned photomask, and exposed to UV light (λ=365 nm) for 50 seconds. It was finally developed with 1-methoxy-2-propanol acetate (Sigma-Aldrich). The PDMS (Poly DiMethylSiloxane) stamp was obtained via replica molding, curing Sylgard 184 (Dow Corning) on the patterned silicon master. Laminin lanes (100 μm wide) were printed on smooth hydrogel surfaces via μCP technique using the PDMS stamp just described. Specifically, the stamp was inked in the protein solution (mouse laminin 100 μg/ml in PBS, Sigma, Italy) for a few seconds, and then the excess solution was removed. Conformal contact between the dry hydrogel surface and the stamp was then achieved by applying a gentle pressure, thus transferring the desired protein micropattern on the substrate.

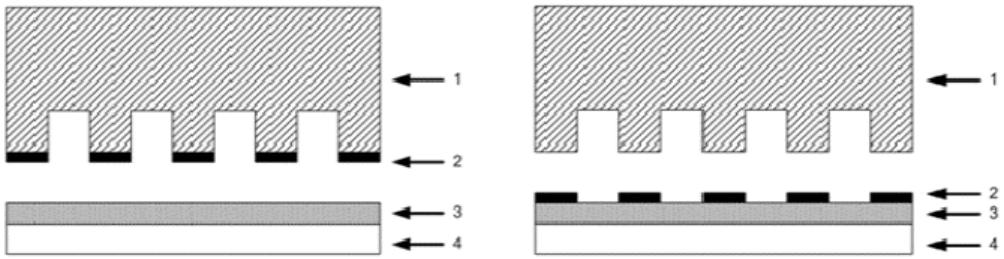

Figura 8. Schematic representation of the micro-contact printing (μCP) technique. On the left: the microstructured PDMS stamp (1) with a monolayer of laminin (2) adsorbed on its surface. A thin film of hydrogel (3) is covalently bonded to a glass slide (4). On the right: the result of the protein printing, the laminin (2) previously adsorbed on the PDMS stamp surface (1) has been transferred onto the hydrogel surface (3) adhered on the glass slide (4).

3.2. Poly (dimethylsiloxane, PDMS) microstructured membrane.

Bidimensional micro-grooved poly(dimethylsiloxane) (PDMS) membranes were prepared using polycarbonate cubes, 20mm high, abraded in one direction using lapping paper with abrasion grain sizes of 80μm. The mold, with the rough side down, was pressed in the centre of 35mm well, filled with 3ml of poly (dimethylsiloxane) (PDMS, Sylgard 184 Silicone Elastomer, Ellsworth Adhesives, WA). The mold was removed after silicone cross-linking and the frame/membrane device was sterilized in autoclave for 20min. In order to enhance cell attachment, the silicone surfaces were incubated at 37°C overnight with 25ug of fibronectin (Sigma Aldrich) in 2 mL of 0.2% gelatin

(Sigma Aldrich) in water. The observation of the membrane at the microscope allowed a rough measure of the groove width.

4. *In Vitro* Tissue Engineering.

4.1. rCM cells Culture on Hydrogel films.

For testing cell viability of the hydrogel films, primary rat neonatal cardiomyocyte cultures were performed according to the first protocol mentioned. Soon after isolation, rCM cells were seeded on the hydrogels at a density of 16×10^4 cells/cm^2 (final seeded area was about 2 cm^2) in about 600ul of Plating Medium. Hydrogel spots were distributed on the surface of a glass slide as 3 for each glass slide and put into a 100mm petri dish (Falcon BD). To avoid spots to dry up, medium was added in the plate surrounding the glass slide. Cells were cultured in a 95% humidified incubator 5% CO2 at 37°C. At day one after seeding, hydrogels were rinsed with culture medium to remove non adhering cells. The culture medium was replaced once a day. Experiments were done in triplicates.

4.2. AFS and rCM cell s Co-Culture on Hydrogel films.

cmtmr$^+$hAFS and rCM cells co-culture was established by admixing cells at 16×10^4 and 4×10^4 cells/cm^2 respectively and seeding them into Plating Medium on hydrogel spots as described previously.
In particular, cmtmr$^+$hAFS cells were added to the culture 48 hours later than rCM to allow rCM cells to settle down completely. Cells were cultured in a 95% humidified incubator 5% CO2 at 37°C. At day one after seeding, hydrogels were rinsed with culture medium to remove non adhering cells. The culture medium was replaced once a day. Experiments were done in triplicates.

4.3. rCM cells Culture on PDMS microstructured membrane.

For testing cell viability of the poly(dimethylsiloxane) (PDMS, silicon) membrane, primary rCM cell cultures were performed according to the second protocol mentioned. rCM and gfp^+ rCM cells obtained following Radisic et al. 2004 [28] were seeded at 10^5 cells/cm^2 in CGM medium on microtextured fibronectin and gelatin-coated silicon membrane in 6-well dishes. Cells were cultured in a 95% humidified incubator 5% CO2 at 37°C. At day one after seeding, membranes were rinsed with culture medium to remove non adhering cells. The culture medium was replaced once a day. Experiments were done in triplicates.

4.4. rCM and AFS cells Co-Culture on PDMS microstructured membrane.

rCm and gfp^+rAFS cells were seeded together on gelatin and fibronectin-coated micropatterned poly(dimethylsiloxane) (PDMS) membranes in 6-well dishes at respectively 10^5 and $5x10^2$ or 10^3 cells/cm^2 density in CGM. As control culture rCM and gfp^+rAFS cells were seeded together on gelatin and fibronectin-coated standard 6-well plastic dishes.

Both gfp^+rCM and hAFS cells coculture and rCm and hAFS cells cocultures were seeded on gelatin and fibronectin-coated micropatterned PDMS membranes in 6-well dishes at respectively 10^5 and 10^3 or $4x10^3$ cells/cm^2 density in CGM. As control rCM and hAFS cells cocultures were seeded on gelatin and fibronectin-coated standard 6-well plastic dishes. Experiments were done in triplicates.

4.5. Immunostaining analyses.

rCm cells cultured on hydrogel films and PDMS membranes were analyzed by immunostaining for the expression of the cardiomyocyte marker troponin I.

After 4 and 7 days of culture, cells on patterned hydrogel were fixed with 2% paraformaldeyde (PFA; Carlo Erba, Italy) for 20 minutes at 4°C and permeabilized with a 0.1% Triton X-100 solution (Sigma-Aldrich) at room temperature. rCM cells were then incubated for 25 minutes at 37°C with primary antibodies specific for cardiac

troponin I (mouse IgG 1:1000, Chemicon) and diluted in a 1% PBS/BSA solution. Alexa Fluor 594- or 488-conjugated goat anti-mouse IgG (Molecular Probes) was used as secondary antibody, diluted 1:150 in a 1% BSA/PBS and incubated for 25 minutes at 37°C. Cell nuclei were then stained for 5 minutes at room temperature with a 1:5000 Hoechst solution (Sigma-Aldrich) in PBS.

rCm and cmtmr^{+}AFS cell coculture on hydrogel films were analyzed after 4 and 7 days of culture as well, following the same protocol for the expression of troponin I.

rCm cells seeded on PDMS membranes were analyzed by immunofluorescence after 6 and 12 days for the expression of the structural sarcomeric protein troponin T, whereas rCm cocultured with AFS cells on PDMS scaffold were analyzed after 6, 12 and 15 days of culture for the expression of both troponin T and GFP.

Immunostaining analysis on rCM co-cultured with AFS was made both on cells seeded on silicone membrane and on cellular spots (*cytospins*) obtained from cells detached from silicone membranes by trypsinization and then centrifugated on glass coverslips in a Shandon cytocentrifuge at 400 rpm for 5 minutes.

Briefly, cells seeded on PDMS membranes and cellular spots were fixed in PFA 4% for 5 minute at room temperature, permeabilized with 0,1% Triton/PBS solution and incubated at 37°C for 25 minutes with the appropriate dilution of the primary antibody in PBS+1% bovine serum albumin (Gibco and Sigma).

To identify rCm, gfp^{+}rAFS and hAFS cells in co-culture the following primary monoclonal antibodies were used respectively: mouse monoclonal anti-Cardiac troponin T (Abcam, mouse IgG 1:500), rabbit polyclonal anti-GFP (Invitrogen, rabbit IgG 1:150), human specific anti platelet-derived non muscle myosin NMf6 (home made, mouse IgG, 1:50). Cells were then re-incubated at 37°C for 25 minutes with the appropriate dilution of the secondary antibody (goat anti-mouse IgG conjugated with Alexa Fluorescence 564 IgG 1:150, Molecular Probes; goat anti-rabbit conjugated with Alexa Fluorescence 488 IgG 1:150, Molecular Probes) PBS+1% bovine serum albumin with human and rat serum (1:100). Cell nuclei were stained with a Hoescht solution diluted 1:5000 in PBS 1X for 5 minutes at room temperature.

Observations were made using a Zeiss Axioplan epifluorescence microscope (Zeiss, Oberkochen, Germany), a Leica TCS SP5 confocal microscope and images were

obtained using a Leica DC300F digital videocamera. Optical images were acquired by a Leica DMR microscope connected to a Leica DC300 videocamera.

5. Statistical analyses.

All values were expressed as mean ± standard error. Statistical significance in comparing AFS cells differentiation in the different conditions described was evaluated with a Mann Whitney U-test by Graph Pad Instat (for assessing data normal distribution) and Graph Pad Prism4 softwares. A probability of <0.05 was considered significant.

RESULTS

1. Cell isolation, expansion and characterization.

1.1. Human Amniotic Fluid Stem Cells.

As previously shown [94], hAFS cells consistently expressed the "embryonic stem cell" markers SSEA4 (75%), Oct-4 (85%) and, partially, Nanog (1%).
They were also positive for CD105 (94.2%), CD29 (99.9%), CD73 (98.4%), CD44 (99.9%) and CD90 (87.4%), and negative for CD34, CD45 and CD133. In particular the early cardiomyogenic marker CD166 (85%) was also expressed by these cells.
As to HLA antigens, hAFS cells were positive for HLA-ABC (99.6%) and negative for HLA-DR. In cellular cytospun, preparation hAFS cells expressed the mesenchymal cell marker vimentin (100%) but not Stro-1. Endothelial markers as Flk-1 (70%), CD146 (78.4%) and von Willebrand factor (30%) were present but not CD31. Smooth muscle α actin was also present in 5-30% of hAFS cells. Cells were also positive for pancytokeratin (‹10%) and the receptor for the neural growth factor (30-60%).

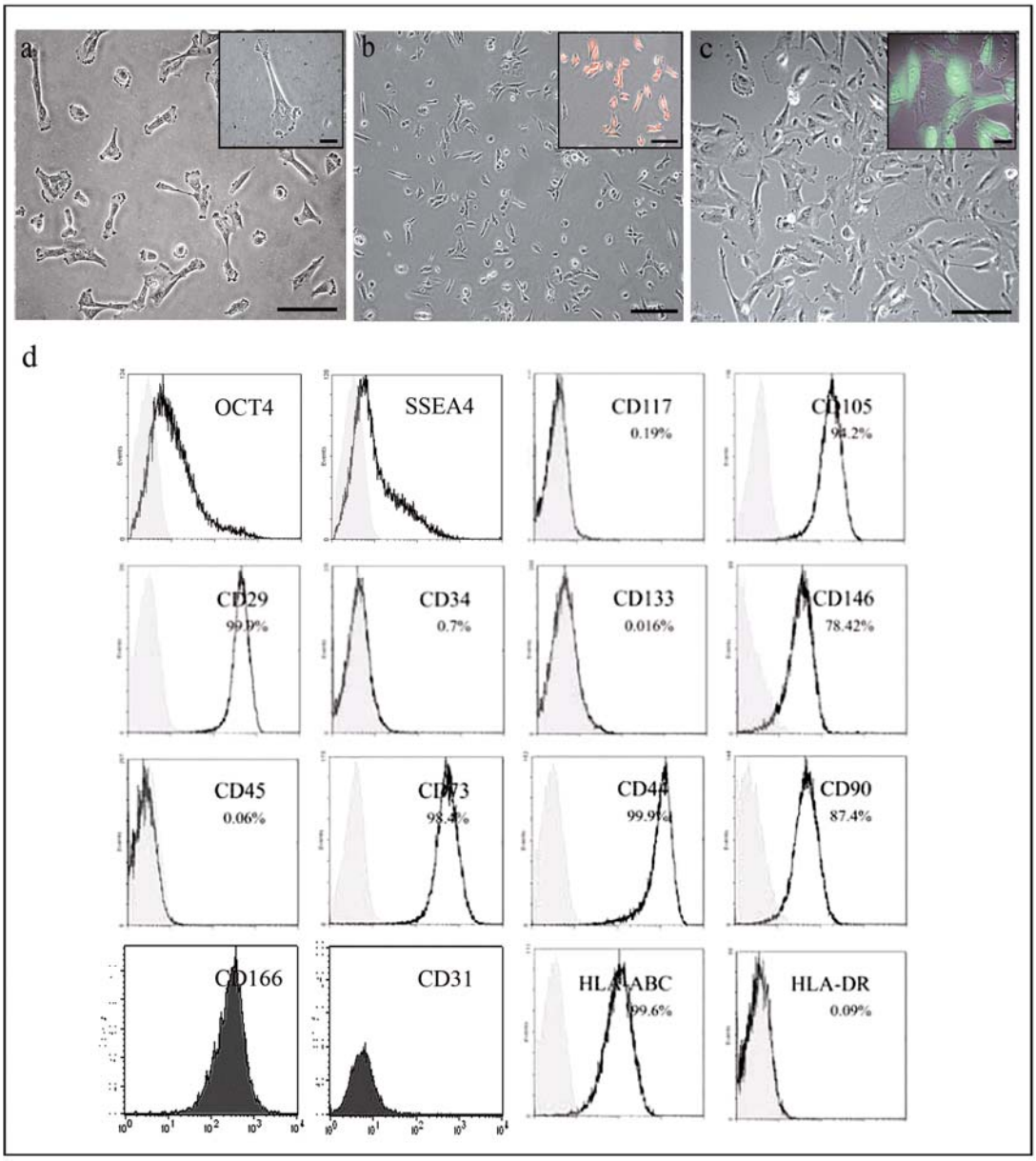

Figure 9. Human AFS phenotype. In **a**, **b** and **c**: wt, cmtmr^{+} and gfp^{+}cells morphology, magnification 20x and 10x, bar 100um and 250um respectively, inlets 40x and 20x, bar 75um and 100um respectively; in **d**: flow cytometry profile.

1.2. GFP-positive Rat Amniotic Fluid Stem Cells.

The gfp^{+}rAFS cells consistently expressed the "embryonic stem cell" marker SSEA4 (>90%) and were also positive, to a varying extent, for the expression of Oct 3-4 (10-30%), CD105 and CD29 (>90%), NGF receptor (60-90%), Flk-1 (>90%), SM-α-actin (60-90%), and CD90(<10%), CD73(<10%) and MHC II (<10%). They were negative for the hematopoietic antigens CD34 and CD45. All gfp^{+}rAFS cells expressed the mesenchymal cell marker vimentin but neither Stro-1 nor pancytokeratin.

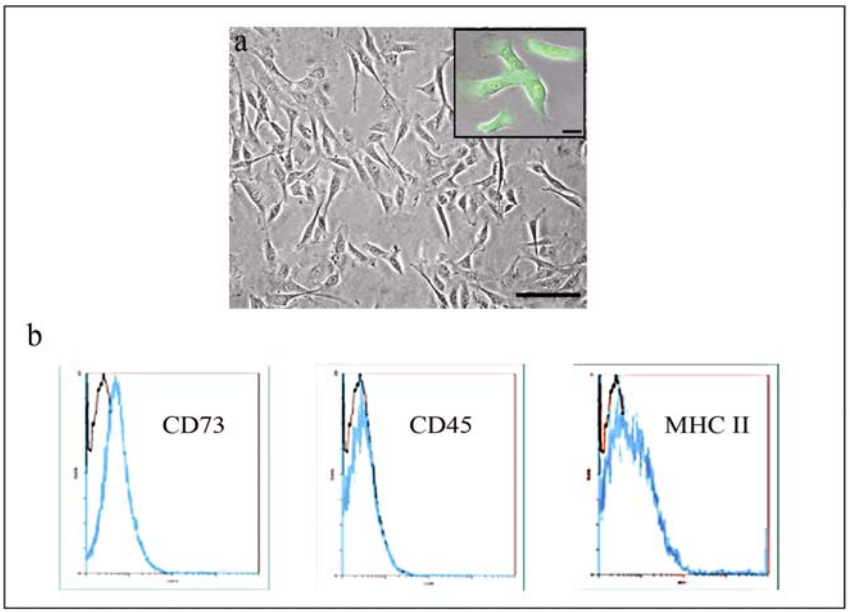

Figure 10. gfp^{+} rat AFS cells phenotype. In a: gfp^{+} cells morphology, magnification 20x, bar 100um, inlet 40x, bar 75um; in b: flow cytometry profile.

1.3. Rat Neonatal Cardiomyocyte Cells.

Freshly isolated rCM cells were positive for mesenchymal markers such as CD29 (87.5%), CD73 (70.6 %), CD90 (35.6 %), CD44 (42.7%) and vimentin (95%). rCM cells were also positive for the expression of CD54 (34.6 %) and MHC II (13.55%), probably because of lymphocytic contamination during cardiomyocyte isolation) and negative for CD117 and CD45. For some antigens (CD29, CD73, CD44), the cardiomyocyte primary culture was heterogeneous. This seems to be confirmed by the

positive expression of antigens of endothelial (about 10-30% CD31 and von Willebrand factor-positive cells) and smooth muscle (<10% α smooth muscle actin-positive cells) origin, revealing minor endothelia and smooth muscle cell contamination during cardiomyocyte isolation. Soon after isolation, the cardiac troponin T-positive rCM cells were about 65-70%, whereas after 16 days of culture they were less than 20%. This rCM cells reduction could be due to the 4-prolyl-hydroxilase-positive cardiac fibroblast cells, increasing from 10-30% initially, up to 48% after 16 days of culture.

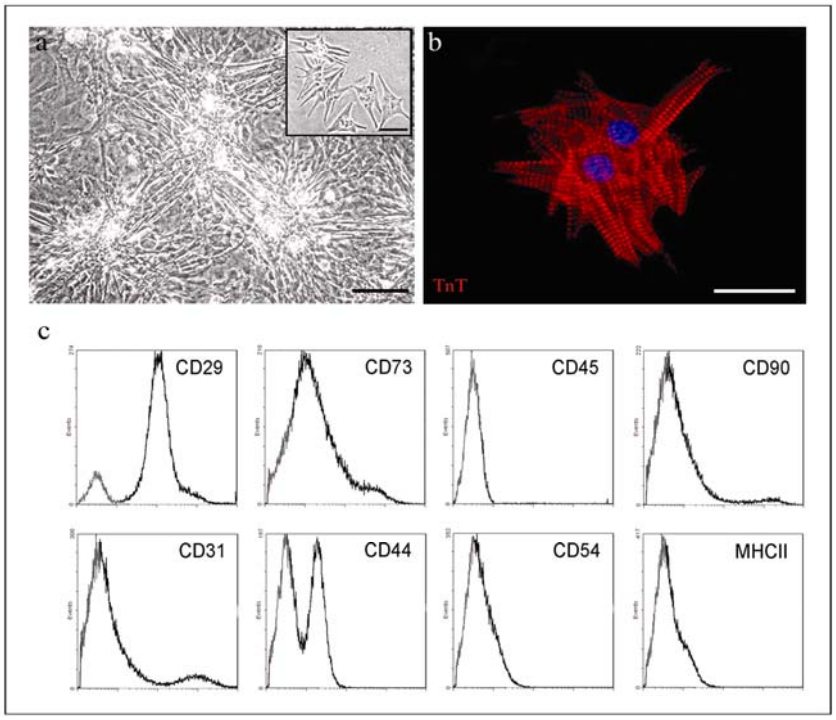

Figure 11. Neonatal rat cardiomyocytes phenotype. In **a** and **b**: cells morphology and immunostaining for the sarcomeric structural protein troponin T, magnification 20x and 100x, bar 100um and 25um respectively, inlets 40x, bar 75um; in **c**: flow cytometry profile.

Table 3. Summary of cell immunophenotyping. Percentage of cells expressing the relevant antigent was expressed as follows:

-	0%
- and +	heterogeneous population
+/-	‹ 10%
+	10-30%
++	30-60%
+++	60-90%
++++	› 90%

Markers	Immunophenotyping		
	hAFS	**gfp^{+}rAFS**	**rCM**
CD117	-	-	-
Oct 3/4	+++	+	n.a.
SSEA-4	+++	++++	n.a.
Nanog	+/-	n.a.	n.a.
CD34	-	-	n.a.
CD44	++++	n.a.	- and ++
CD45	-	-	-
CD29	++++	++++	- and +++
CD105	++++	++++	n.a.
CD90	+++	+/-	++
CD73	++++	+/-	-and+++
CD54	n.a.	n.a.	++
CD166	+++	n.a.	n.a.
Stro-1	-	-	n.a.
NGFr	++	+++	n.a.
CD31	-	n.a.	+
Flk1	+++	++++	n.a.
Smooth Muscle α Actin	+	+++	+/-
vonWillebrand factor	+	+	+/-
Cardiac Troponin T	-	-	+++
α Prolyl Hydrosilase	n.a.	n.a.	+
Vimentin	++++	++++	++++
Pancytokeratin	+	-	n.a.
MHC II	-	+/-	+

2. *In Vitro* Differentiation.

2.1. Patch Clamp analysis on Co-Culture on plastic dishes.

For single cell electrophysiology, cells were put in co-culture 3-4 days prior to experimental procedure. The best results were obtained when the cardiomyocytes were

beating in the co-culture. We could only record electrical activity on co-cultured cells that were beating.

The neonatal cardiomyocytes showed pacemaking activity, with an APD50 = 95.58 ± 12.89 ms and APD90 = 174.65 ± 33.25 ms (n=9).

gfp^+rAFS and hAFS cells that were never put in co-culture have a depolarised membrane potential (-10 to -20 mV) and were never able to develop an action potential when excited with a 5 ms current pulse. The same lack of excitability was observed when the cells were held at more hyperpolarised membrane potential (around -70 mV).

In contrast, when AFS cells were co-culture with neonatal cardiomyocytes, they developed a pacemaking activity as illustrated in Figure 12 and 13. We observed that only AFS cells that were in close contact with beating neonatal cardiomyocytes were able to develop electrical excitability.

In particular, when gfp^+rAFS cells were challenged with 10 □M isoprenaline (Figure12c), there was a reduction of APD50 and APD90, showing acceleration of the pacemaking activity.

The action potential recorded on co-cultured gfp^+rAFS cells fell into two categories that we named “immature” and “mature”, according to their electrophysiological specificities.

Immature AFS cells have a membrane potential of -30±2.78 mV. The action potential have an APD50 = 193.71±14.00 ms, and an APD90 = 322.66 ± 33.61 ms (n=6), while the membrane depolarisation reached a maximum of 42.21 ± 3.44 mV.

In mature AFS cells the membrane potential was -53.61±3.32 mV, APD50 = 213.66±15.77ms, APD90 = 357.22 ± 24.33ms (n=6), and membrane depolarisation during action potential was 82.14 ± 5.95 mV.

During the action potential, the immature cells showed smaller membrane depolarisation and shorter APD50 and APD90.

The neonatal cardiomyocytes (n=7) have similar membrane potential as the mature AFS cells but in general the action potential of the cardiomyocytes has a shorter APD50 and APD90.

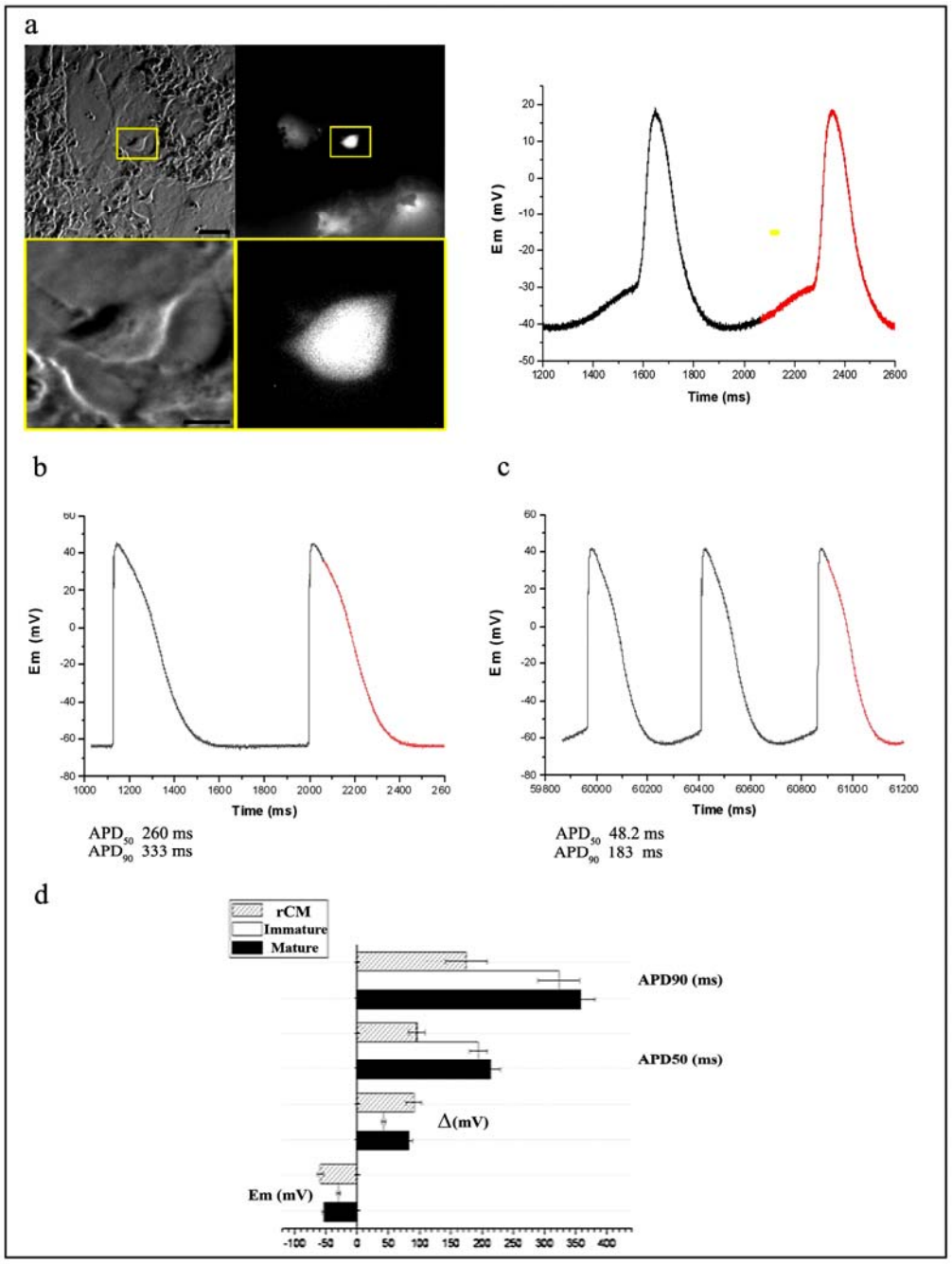

Figure 12. Patch clamp analysis on gfp^{+}rAFS and rCM cells co-cultured cells. In **a**: panel on the right, bright field and GFP fluorescence of a patch-clamped cell, magnification 20X above, bar 100um, and 40x below, bar 75um; panel on the left: the action potential was spontaneous, showing a typical pacemaking activity. In **b** and **c**: gfp^{+}rAFS cells in coculture as control and challenged with 10 μM isoprenaline, these ones showing acceleration of the pacemaking activity in c compared to b: isoprenaline decreases both APD_{50} and APD_{90}. In **d**: summary of the electrical parameters recorded on cells: membrane potential (Em), membrane depolarisation during action potential (Δ), time to 50% repolarization of the action potential

(APD_{50}) and time to 90% repolarization of the action potential (APD_{90}) are shown for rCM and AFS cells in co-culture. AFS cells were sorted into two categories immature (n=7) and mature (n=9). During the action potential, the immature cells show smaller membrane depolarisation and shorter APD_{50} and APD_{90}. The "mature" ones have a membrane potential similar to cardiomyocytes and APD50 and APD90 are longer than "immature" AFs cells. The rCM cells (n=7) have similar membrane potential as the mature AFS cells and their action potential has a significantly shorter APD_{50} and APD_{90}.

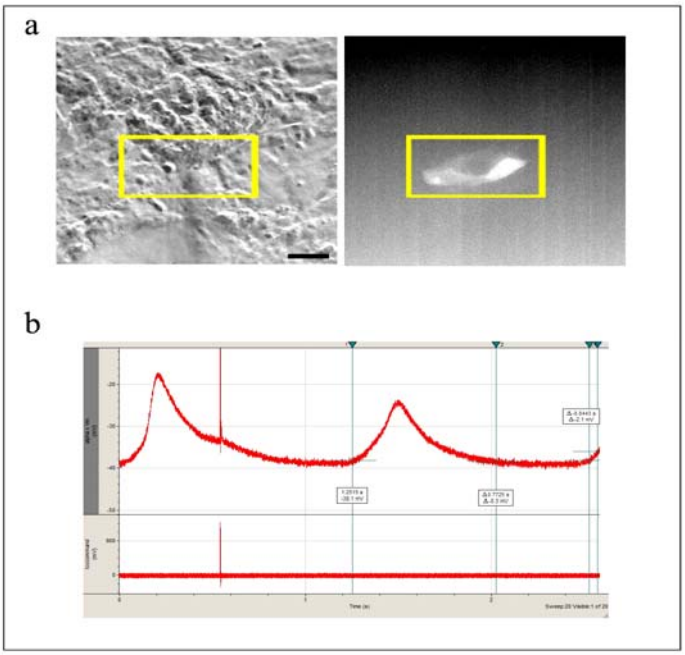

Figure 13. Patch clamp analysis on gfp^+hAFS and rCM cells co-cultured cells. In **a**: panel on the right, bright field, magnification 20X, bar 100um, on the left fluorescence signal of the patch-clamped GFP cell; in **b**: gfp^+hAFS cells showing pacemaker-like activity.

3. *In Vitro* Tissue Engineering.

3.1. rCM cells Culture on Hydrogel films.

rCM cells seeded on hydrogel films created aligned and organized cardiac myofibers expressing peculiar functional properties, i.e. synchronous contractile activity after few days and the culture was maintained up to 10 days. The extreme selectivity obtained in cell adhesion was underlined by the staining for cardiac troponin I: the protein was uniformly expressed and higher magnification a contractile apparatus was observable.

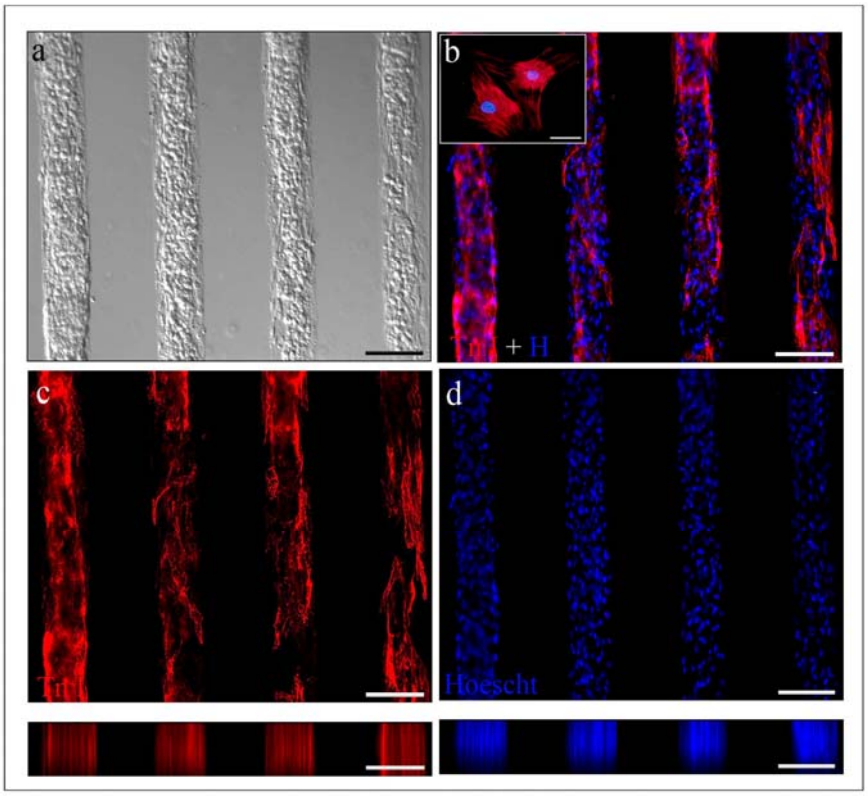

Figure 14. Cardiomyocytes cultured on hydrogel scaffold. In **a**: phase contrast bright field image of cardiomyocytes after 4 days in culture, magnification 10X, bars 250um. In **b**: cultured cardiomyocytes express troponin I (red), a typical structural sarcomeric marker; nuclei were counterstained with Hoechst (blue), magnification 10X, bar 250um. In the inset immunostaining for troponin I showing the typical phenotype of rCM, magnification 40X, bar 75um. Unmerged images are reported in panel **c** and **d**, magnification 10X, bars 250µm.

3.2. AFS and rCM cells Co-Culture on Hydrogel Films.

Both gfp^{+}rAFS and $cmtmr^{+}$hAFS cells cultured with rCM cells on hydrogel films showed adhesion problems due to the high cellular density on the polymer surface. Cells weren't able to adhere properly and in a well aligned organization and they started detaching soon after seeding. Because of that, it wasn't possible doing any analysis and the hydrogel film was discarded as bidimensional polymeric scaffold to be employed in the *in vitro* co-culture experiment.

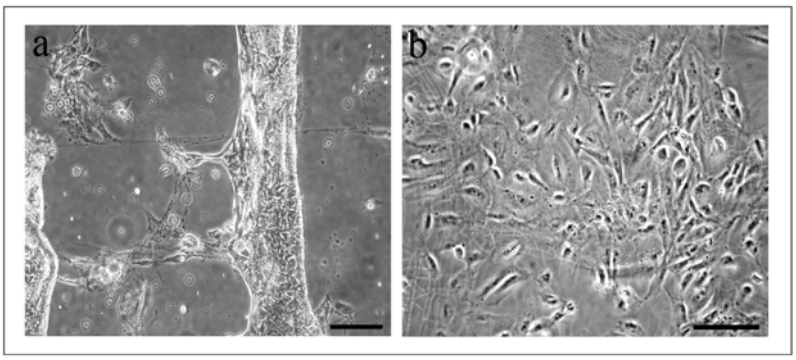

Figure 15. cmtmr^{+}hAFS cells with rCM cells on hydrogel films showing disorganized structure. In **a**: rCM cells detaching, magnification 10X, bar 250um; in **b**: AFS cells randomely attached, magnification 20X, bar 100um.

3.3. rCM cells Culture on PDMS microstruttured membrane.

We analized the viability and the biocompatibility of the poly (dimethylsiloxane) (PDMS) scaffold on the cardiomyocyte culture alone to obtain a more spatially organized *in vitro* culture. rCM cells seeded on the 2D silicone scaffold showed to align following the orientation with a well defined spatial organization, as reported by figure, for troponin T staining, and were able to express synchronous beating activity. Moreover, the thinner micropattern of the textured silicon surface was able to improve cardiomyocyte organization in culture at the single cell level.

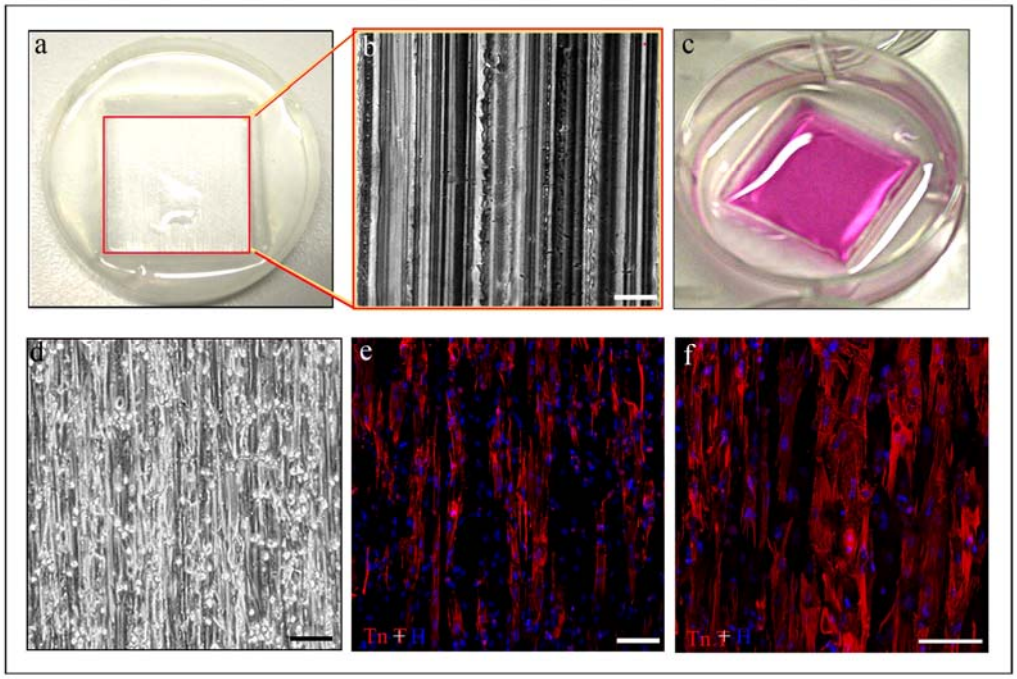

Figure 16. rCM cells cultured on PDMS membranes. In **a** and **b**: gross appereance of the membrane, magnification 20X, bar 100um; in **c**: rCM culture on the scaffold; in **d**: bright field of rCM cells on PDMS scaffold, magnification 20X, bar 100um; in **e** and **f**: immunostaining for cardiac troponin T (red), showing the organization and orientation of the cells on the membrane, magnification 20X and 40X, bars 100um and 75um.

3.4. AFS and rCM cells Co-Culture on PDMS microstruttured membrane.

gfp^+rAFS cells were seeded in co-colture with rCM cells on silicon membrane to analyze the topological stimulation of the 2D support on the stem cell in co-culture. gfp^+rAFS cells were found growing closely related to rCM cells on the silicon membrane, following the longitudinal orientation given by the micropattern; besides, some of gfp^+cells seemed to express the cardiomyocyte marker troponin T and beating activity as well. These results suggest that the microtextured PDMS surface model could be a good approach to get a better defined spatial organization and orientation of the co-culture *in vitro* and to improve the mechanical stretch and all the physical and chemical stimulation of cardiomyocytes on the surrounding AFS cells, in respect of the standard conditions using plastic culture dishes.

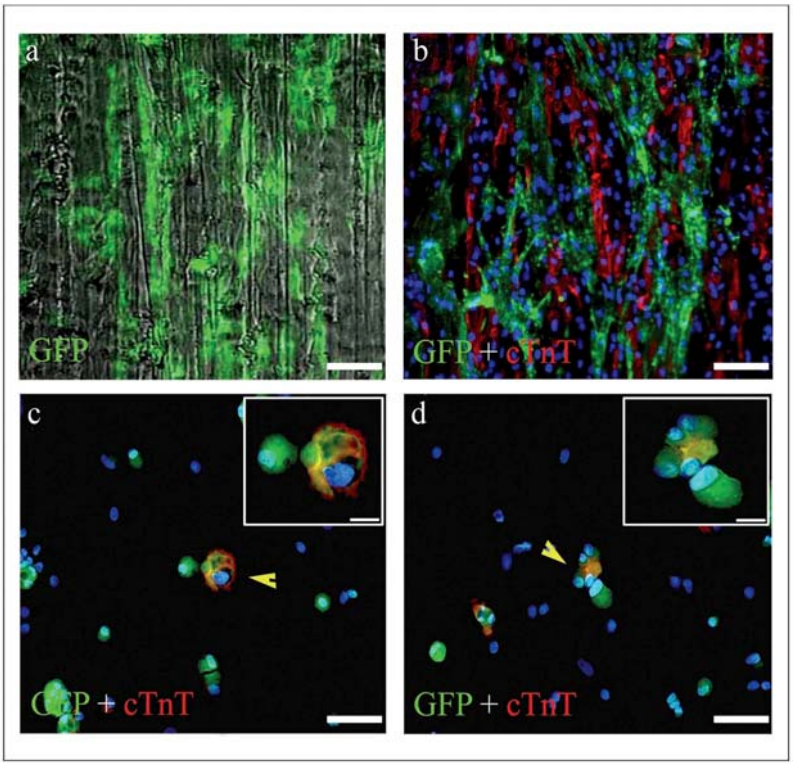

Figure 17. gfp$^+$rAFS and rCM cells co-culture on PDMS scaffold. In **a**: merge of bright field and GFP fluorescence of the co-culture after 4 days: gfp$^+$rAFS cells (in green) grew close related to rCM cells (in grey) and aligned following the micropattern, magnification 20X, bar 100 um; in **b**: immunefluorescence for GFP (in green) and cardiac troponin T (in red) of gfp$^+$rAFS and rCM cells after 4 days, magnification 20X bar 100 um; in **c** and **d**: immunefluorescence for GFP (in green) and cardiac troponin T (in red) of cytospun cellular spots of gfp$^+$rAFS and rCM cells co-culture on PDMS scaffold after 4 days: arrows showing some gfp$^+$rAFS cells in yellow, as both positive for GFP and cardiac troponin I expression, magnification 20X, bar 100 um; inlet magnification 40X, bar 75 um.

hAFS cells co-cultured with rCM cells were also found growing closely related to rCM on the PDMS membrane, following the longitudinal orientation given by the micropattern. Here we tested two different conditions of co-culture on the bidimensional micropattern scaffold: hAFS cells seeded at 1000 and 4000 cells/cm^2.
Immunostaining analysis after 6 days revealed some hAFS cells positive for the expression of the cardiac marker troponin T. As reported in Figure 18, in the co-culture referred to as control, after 6 days the troponin T-positive hAFS cells were 5,06±2,8% of cells seeded at 1000 cells/cm^2 and 2,1±0,08 % of the cells seeded at 4000 cells/cm^2;

after 10 days none of hAFS cell expressing TnT was found in the control coculture at 1000 cells/cm^2, whereas in the one with hAFS cells at 4000 cells/cm^2 were 4.97±2,5%. The coculture seeded on the micropatterned membrane showed that after 6 days about 2,5±2,4% of hAFS cells seeded at 1000 cells/cm^2 and 6,73±2% of the ones seeded at 4000 cells/cm^2 were expressing the cardiac marker TnT. After 10 days these values increased to 11±4,7% of hAFS cells seeded at 1000 cells/cm^2 and 13±4,2% of the ones seeded at 4000 cells/cm^2. Even if the percentages of hAFS cells expressing the cardiomyocytes marker dramatically improved after 10 days in the culture on the bidimensional scaffold compared to the standard culture conditions on petri dishes, these results were not statistically significative (p>0,05).

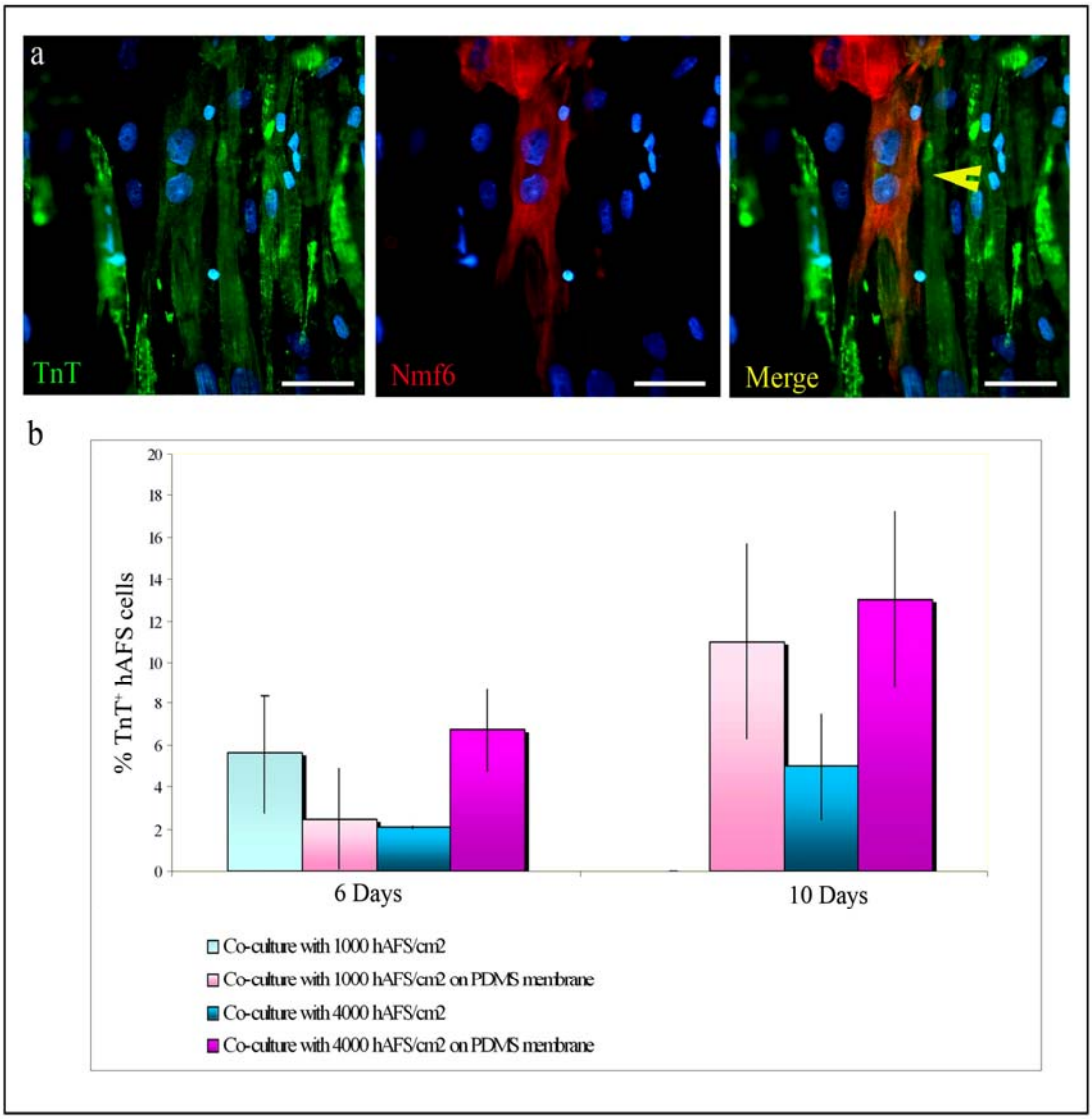

Figure 18. hAFS and rCM cells co-culture on bidimensional biocompatible PDMS scaffold. In **a**: cardiac troponin T immunostaining (in green) for rCM cells co-culture after 6 days on the left, human specific platelet-derived non muscle myosin (Nmf6, in red) detecting hAFS cells in the centre, merge on the right: the hAFS cell expressing cardiac troponin T, as demonstrated by the yellow co-staining, is pointed out by the arrow, magnification 40X, bar 75 um. In **b**: comparison of troponin T-positive hAFS cells cocultured with rCM at 1000 and 4000cells/cm^2 on plastic dish and on PDMS membrane. In the co-culture referred to as control, after 6 days the troponin T-positive hAFS cells were 5,06±2,8% of cells seeded at 1000 cells/cm^2 and 2,1±0,08 % of the cells seeded at 4000 cells/cm^2; after 10 days none hAFS cell expressing TnT was found in the control coculture at 1000 cells/cm^2, whereas in the one with hAFS cells at 4000 cells/cm^2 were 4.97±2,5%.
The coculture seeded on the micropatterned membrane showed that after 6 days about 2,5±2,4% of hAFS cells seeded at 1000 cells/cm^2 and 6,73±2% of the ones seeded at 4000 cells/cm^2 were expressing the cardiac marker TnT. After 10 days these values increased to 11±4,7% of hAFS cells seeded at 1000 cells/cm^2 and 13±4,2% of the ones seeded at 4000 cells/cm^2.

In conclusions, the results obtained in the in vitro work showed that AFS cells were able to acquire a functional “cardiomyocyte-like” phenotype, in co-culture with rat neonatal cardiomyocyte, with the expression of pace-making cells action potential.
AFS cells were also demonstrated to grow on micropatterned scaffold showing a well defined spatial organization in co-culture, improving the intercellular and cross-talks interactions that drive the differentiation towards rCm cells.

Chapter 3 *In Vivo* Study.

METHODS

1. Cardiac Cryoinjury Rat Model.

1.1. Animals.

27 male immunodeficient nude rats (rNu, Harlan, Milan, Italy) weighing about 190-200g and 11 weeks old were housed and maintained in a sterile controlled environment.

1.2. Three-dimensional Collagen Scaffold.

A biocompatible three-dimensional polymer scaffold (patch) from porcine derm-derived collagen type I was used as described previously in Callegari et al. [113]. Sterilized and endotoxin-free collagen scaffolds were cutted in small samples (0.8 x 0.8 x 0.3cm; h x w x t) and conditioned in PBS 1X for 2 hours before the *in vivo* experiments.

1.3. Experimental model of cardiac *cryoinjury* and biomaterial application.

All surgical and pharmacological procedures were performed in accordance with regulations expressed in the Guide for Care and Use of Laboratory Animals by the Institute of Laboratory Animal Resources, National Research Council, published by the National Academy Press, revised 1996 (NIH Publication No. 85-23) and the Italian Health Minister Guidelines for Animal Research. The protocol was approved by the University of Padua Animal Care Committee.

The surgical procedures were carried out as previously set in Callegari et al. [113]. Briefly, rNu rats were anesthetised by i.m. injection of zoletil (4 mg/100 g body weight) along with atropin (s.c. 5 uL/100g) and xylazin (i.p. 0.4 mg/ 100 g) and subsequently intubated and ventilated mechanically with room air (Harvard, South Natick, MA). The

heart was exposed through a left thoracotomy (third or four intercostals space) and a left ventricular ANI (*Acute Necrotizing Injury,* a freeze-thaw procedure in this case) was created by three sequential exposures (60s each, 20s of non-freezing interval) of liquid nitrogen-cooled cryoprobe (a stainless steel cylinder, 8 mm of diameter). Instauration of ANI was confirmed by wall blanching followed by hyperemia. Within 10 min form the injury, the collagen scaffold (patch) was placed on the epicardial anterolateral region corresponding to the cryoinjured area (about 12 mm^2) identified by the pale appearance respect to the surrounding myocardium. The scaffold was fixed to the epicardium with a cranially positioned 7-0 prolene suture. The chest was then closed and the animals weaned from the respirator, extubated and treated with antibiotics for 24 hours (20 mg/100 g; Baytrill, Bayer, Milan).

1.4. Cells injection.

According to the cells injection, animals were then divided into the following groups:

a. animals receiving injection suspension medium, as control;
b. animals receiving wt and gfp^+rCM cells injection into the patch, as control;
c. animals undergoing cryoinjury and $cmtmr^+$hAFS cells injection without patch applications, as further control;
d. animals receiving $cmtmr^+$hAFS cells injection, further subdivided into rats injected locally into the patch (Model I) or systemically i.v. (Model II).

Regarding cell processing, stem cells and neonatal cardiomyocytes were detached from culture plastic dishes with Trypsin 0.05-EDTA 0.02 w/v (Biochrom AG, Germany) sterile solution and centrifuged 5 min at 310g (1200 rpm).

$5x10^6$ $cmtmr^+$hAFS (labelled in red) and wt or gfp^+rCM cells/animal were injected in 90ul of DMEM high glucose medium (Gibco, Italy) and rNU serum 1:100 solution (injection medium), on the collagen scaffold, 15 days after its *in vivo* application on the heart cryoinjury. Animals were sacrificed at 24 hours, 15 and 30 days (this last time point only for the stem cells not for rCM) in Model I and 30 days after the cells injection in Model II.

Animals from control group receiving injection suspension medium and $5x10^6$ $cmtmr^+$hAFS cells/animal injection, on cryoinjury area without scaffoldapplication, were analyzed 30 days after injection, as in Model II.

1.5. Histology and Immunostaining analyses.

Eight-micron thick frozen sections were cut from hearts of animals embedded in OCT and snap frozen in 2-metyl butane and liquid nitrogen and processed with hematoxylin-eosin and Masson's trichrome staining, following manufacturer's instruction (Bioptica, Italy). Further cryosections were processed by immunofluorescence protocol for cardiac, immune response and inflammatory markers such as anti-cardiac troponin T (cTnT mouse IgG, 1:500, Abcam, UK), anti-α Smooth Muscle Actin (α-SMA, mouse IgG 1:1000 Sigma, Italy), anti-von Willebrand's Factor (vW, rabbit IgG, 1:100, Abcam, UK), anti-CD31 (mouse IgG 1:100 bot from Chemicon, Italy) and anti-macrophages (ED2 mouse IgG 1:400 Chemicon, Italy). The anti-human mitochondria antigen antibody (IgG, mouse, 1:50 Abcam,UK) was to detect and track hAFS cells in the host tissue.

Briefly, tissue slides were fixed in PFA 4% for 5 minute at room temperature, and incubated at 37°C for 25 minutes with the appropriate dilution of the primary antibody in PBS+1% bovine serum albumin (Gibco and Sigma, Italy). Cells were then re-incubated at 37°C for 25 minutes with the appropriate dilution of the secondary antibody (donkey anti-mouse IgG coniugated with Alexa Fluorescence 564 IgG 1:150, Molecular Probes; goat anti-rabbit coniugated with Alexa Fluorescence 488 IgG 1:150, Molecular Probes, Invitrogen, Italy) in PBS+1% bovine serum albumin with human and rat serum (1:100). Cell nuclei were stained with a Hoescht solution diluited 1:5000 in PBS 1X for 5 minutes at room temperature.

Apoptosis analysis was made using apoptag detection kit (Chemicon, Italy) following manufacterer's instructions. Observations were made using a Zeiss Axioplan epifluorescence microscope (Zeiss, Oberkochen, Germany), a Leica TCS SP5 confocal microscope and images were obtained using a Leica DC300F digital videocamera. Optical images were acquired by a Leica DMR microscope connected to a Leica DC300 videocamera.

1.6. Statistical analyses

All values were expressed as mean ± standard error. The amount of the hAFS cells and the host immune response system cells detected *in vivo*, the density of capillaries and arterioles, as well as differentiation patterns data, were evaluated for statistical analyses using Graph Pad Instat (for assessing data normal distribution) and Prism4 softwares. Statistical significance was evaluated by One-way and Kruskal-Wallis ANOVA and Student T-test. A probability of <0.05 was considered significant.

2. Acute Myocardial Infarct Rat Model.

2.1. Animals.

42 male wild type Wistar rats (Charles River, UK) weighing about 250-300g and 8 weeks old were housed and maintained in a controlled environment.

2.2. Experimental model of Acute Myocardial Infarct.

All surgical and pharmacological procedures were performed in accordance with regulations expressed in the Animals (Scientific Procedures) Act 1986 in accordance to the rules about research and testing using animals established by the Home Office, Science, Research and Statistics Department, in UK.
Rats were anesthetised by i.p. injection of thyopentone (120 mg/kg body weight, Intraval, Merial UK) and body temperature was monitored using a rectal probe. Animals underwent tracheotomy to insert an endotracheal tube to support mechanical breathing with room air (Harvard, South Natick, MA). Common carotid artery was then cannulated and connected to a transducer to monitor blood pressure by the Chart software. External jugular vein was cannulated providing an i.v. access for cell injection. A thoracotomy was performed, heart exposed and the left anterior descending coronary artery occluded (coronary artery ligation, LAD) by a 6/0 silk suture connected to the snare. The snare was tightened against the myocardium creating an ischemic

insult. Snare was kept in position for 30' and then released to allow reperfusion for 2 hours.

2.3. Cells injection.

According to the cells injection, animals were divided into 3 main groups:

a. animals (n=12) receiving 500ul PBS injection as control;
b. animals (n=12) receiving gfp^+rAFS cells injection, further subdivided into rats (n=6) injected with a 500ul solution of 10^7cells/animal in PBS and rats (n=6) injected with a 500ul solution of 10^6cells/animal in PBS;
c. animals (n=18) receiving hAFS cells injection, further subdivided into rats (n=6) injected with a 500ul solution of 10^7cells/animal in PBS and rats (n=12) injected with a 500ul solution of $5x10^6$cells/animal in PBS.

Stem cells were detached from culture plastic dishes with Trypsin 0.05-EDTA 0.02 w/v (Biochrom AG, Germany) sterile solution and centrifuged 5 min at 310g (1200 rpm). 10^7 or 10^6 cells/animal gfp^+rAFS or 10^7 and 5 x 10^6 hAFS and were injected in 500ul of PBS 1X in the 2 minutes following snare release. Animals were sacrificed 2 hours after the injection.

2.4. Assessment of Area at Risk (AAR) and Infarct Size (IS) by Planimetry.

After reperfusion, snare was re-tightened to re-occlude LAD. 2ml of 2% Evans Blue PBS solution (Sigma, UK) was injected trough external jugular vein cannula for at least 30 seconds. As soon as normal and ischemic myocardium was delineated, heart was cut through the main vessels; pericardium was removed and freezed at -20°C for 2 hours. Heart was then chopped into 2mm-thick slices, from and perpendicular to apex, and then flatted in filter papers, incubated in 10% TTC (2,3,5-Triphenyl Tetrazolium Chloride solution, Sigma-Aldrich, UK) PBS solution at 37°C for 15 minutes. Slices were then fixed in PFA 4% at 4°C overnight, drained off, placed between glass slides and digitised for quantification using a flat-bed scanner, with a minimal resolution of 600 dpi. Images were processed using ImageJ software. The ischemic area at risk of

necrosis (AAR, showed in red as result of TTC staining) and the infarct area (In, showed in white as result of TTC staining) sizes were measured by planimetry with the software ImageJ for segmenting AAR and In, using different channels for the regions analyzed and adjusting the threshold limit to include the area of interest comparing full-colour images as reference. Two different threshold channels were used for evaluating AAR (channel red) and In areas (channel grey). The ischemic area at risk of necrosis was expressed as the percentage ratio between the volumes of non reperfused area at risk (AAR) and viable left ventricle myocardium, Infarct Size (IS) was expressed as the percentage ratio between the volumes of the infarct area (In) and the area at risk of necrosis (AAR).

2.5. Immunostaining analyses.

Heart, lungs, liver and spleen were taken from animals soon after reperfusion time ended. Tissues were fixed in PFA 4%, incubate into 30% Sucrose-PBS solution (Sigma, UK) and then embedded in OCT solution (Sigma, UK) and snap-frozen in 2-metyl butane and liquid nitrogen. Eight-micron thick frozen sections were cut from organs and processed for immunostaining as previously described in paragraph 1.5. Human cells were detected using a human specific anti-mitochondria antibody (mouse monoclonal IgG 1:50, Abcam) and a donkey anti-mouse Alexa Fluorescence 594-conjugated as secondary antibody (donkey IgG, 1:150, Molecular Probes, Invitrogen, UK).

2.6. Statistical analyses.

All values were expressed as mean ± standard error. The amount of hAFS cells detected *in vivo* and the significance among the different treatment groups were evaluated using SPSS 15.0 software for statistical analyses. Statistical significance was evaluated by One-way ANOVA test. A probability of <0.05 was considered significant.

2.7. Analysis of AFS cells cardioprotective potential.

2.7.1. Analysis of Cardiac Progenitors in hAFS cells by RT-PCR.

As previously shown [94], hAFS are positive for the expression of cardiac commitment markers as Nkx 2,5 and GATA4; to further evaluate if human AFS could contain a cardiac progenitor subpopulation, their gene expression profile was evaluated, in standard culture conditions, by RNA extraction and RT-PCR for the cardiac markers Isl1 and Kdr. Total RNA was isolated from cells with TRIzol™ B (Tel-Test Inc., Texas, USA) solution and 1μg of RNA was reverse-transcribed into first strand cDNA with Superscript II reverse transcriptase (Life Technologies, MD, USA) using Oligo-dT primer (Invitogen) following manufacturer's instructions. Both RT and PCR were done using an Eppendorf® PCR Mastercycler (Eppendorf, AG, Germany). For each PCR reaction cDNA was used in a final volume of 25μl with 200nM dNTP, 10pM of each primer, 0.3U Taq-DNA-polymerase, reaction buffer, and $MgCl_2$ (Invitrogen, UK). Cycling conditions consisted of 94°C for 2 minutes, annealing at 63°C for 40 seconds and elongation at 72°C for 1 minute. Primer sequences are listed in Table 3. cDNA from adult human heart (courtesy of Prof. Gerosa, University of Padua, Italy), fetal human heart (courtesy of Dr. Monk, UCL, London), mouse fetal heart (courtesy of Dr. Risebro, UCL, London) and mouse ES G_2G_4 cells (courtesy of Dr. Cananzi, UCL, London) were used as control. βActin was used as housekeeping gene. PCR reactions were performed on 2% agarose gel electrophoresis and picture acquired by Quantity One® software. Primers sequences were build using the PrimerExpress software, checked by Blast sequences aligning software and purchased from Operon Technologies (UK). Experiments were done in triplicates.

Table 4. Primers details.

Gene	Primer Sequence	Amplicon	T/Cycles
βActin	Fw: 5'TCATGAAGTGTGACGTTGACATCCGT 3' Rv: 5'CCTAGAAGCATTTGCGGTGCACGATG 3'	285 bp	65°C/40
Isl1	Fw: 5' CACTGTGGACATTACTCCCTCTTA 3' Rv: 5' AAGTCGTTCTTGCTGAAGCC 3'	301 bp	56°C/40
Kdr	Fw: 5' ACCTGGAGAATCAGACGACAAGT 3' Rv: 5' CGGTCCGTAGGATGATGACAA 3'	351 bp	58°C/40

2.7.2. Analysis of Thymosin β4 secretion by AFS cells.

To evaluate if AFS could exert any paracrine effect releasing anti-inflammatory cytokines, ELISA analysis for thymosiņβ4 expression were performed on cell conditioned medium. The analysis was carried out using a ELISA kit for detection of thymosin β4 in cell conditioned medium (Immunodiagnostik, Biocompare, Germany). AFS cells were cultured *in vitro* at the same cell density used for the *in vivo* experiments. Conditioned medium was collected after 72 hours from seeding, centrifuged to get rid of all debris and then analyzed by the ELISA kit according to the manufacture's instructions. Briefly, samples were incubated with anti-thymosin-β4 antibody solution for 1 hour, washed with buffer solution, incubated with conjugate solution, washed again and incubated with substrate solution. Absorption was determined with an ELISA reader at 450 nm against 620 nm (or 690 nm) as a reference. The samples values were compared to a calibration curve and expected values determined. Experiments were done in triplicates. Data collected were evaluated for statistical analysis using GraphPad Instat (for assessing data normal distribution) and Prism4 softwares by one-way anova test. A probability of <0.05 was considered significant.

RESULTS

1. Cardiac Cryoinjury Rat Model.

In a previous work we demostrated that the 3D type I collagen scaffold, implanted into wild type Wistar rat intact and cryoinjured hearts, was able to evoke a powerful angiogenetic and arteriogenetic response 15 days after its *in vivo* application, representing an ideal tool for therapeutic angio-arteriogenesis and a potentially useful substrate for stem cell seeding [113]. Here we combined these previous results with hAFS cells injection.

The experimental design is reported in Figure 19: cmtmr^{+}hAFS were injected into the animals two weeks after cryoinjury and patch application, considering two groups of Nude Immunodeficient Rats (rNu):

- Model I, with cell injected locally in the patch via thoracotomy and time points analysis at 24 hours, 15 days and 30 days after cell injection;
- Model II, with systemic injection via iliac vein injection and time point analysis 15 days later.

The microfibrillar, highly porous structure of the collagen scaffold is illustrated in Figure 19b. The necrotizing ischemic insult by cryoinjury was obtained following the procedure already described in callegari et al. [113] and illustrated in Figure 19c.

As control, cryoinjured heart of rNU with patch application and injection of wt and gfp^{+}rCM, with cell suspension medium only injection and with cryoinjury without scaffold application but with cmtmr^{+}hAFS cells injectio were used.

We used two different approaches (Model I and Model II) to evaluate two different aspects: in Model I the capability of the collagen patch of sustaining and improving cell engraftment locally and in Model II the patch trophic properties in homing hAFS injected systemically to the ANI site.

From the 27 rats at the beginning, 9 died during surgery procedure. The remaining were randomly subdivided into 6 groups: 2 with wt rCMcells injection (model I), 2 with gfp^{+}rCM cells injection (model I), 2 only with cryoinjury and cmtmr^{+}hAFS cells application without patch (model I), 2 with injection suspension medium (model II), 5

with cmtmr^{+}hAFS cells injection in Model I and 5 with cmtmr^{+}hAFS cells injection in Model II.

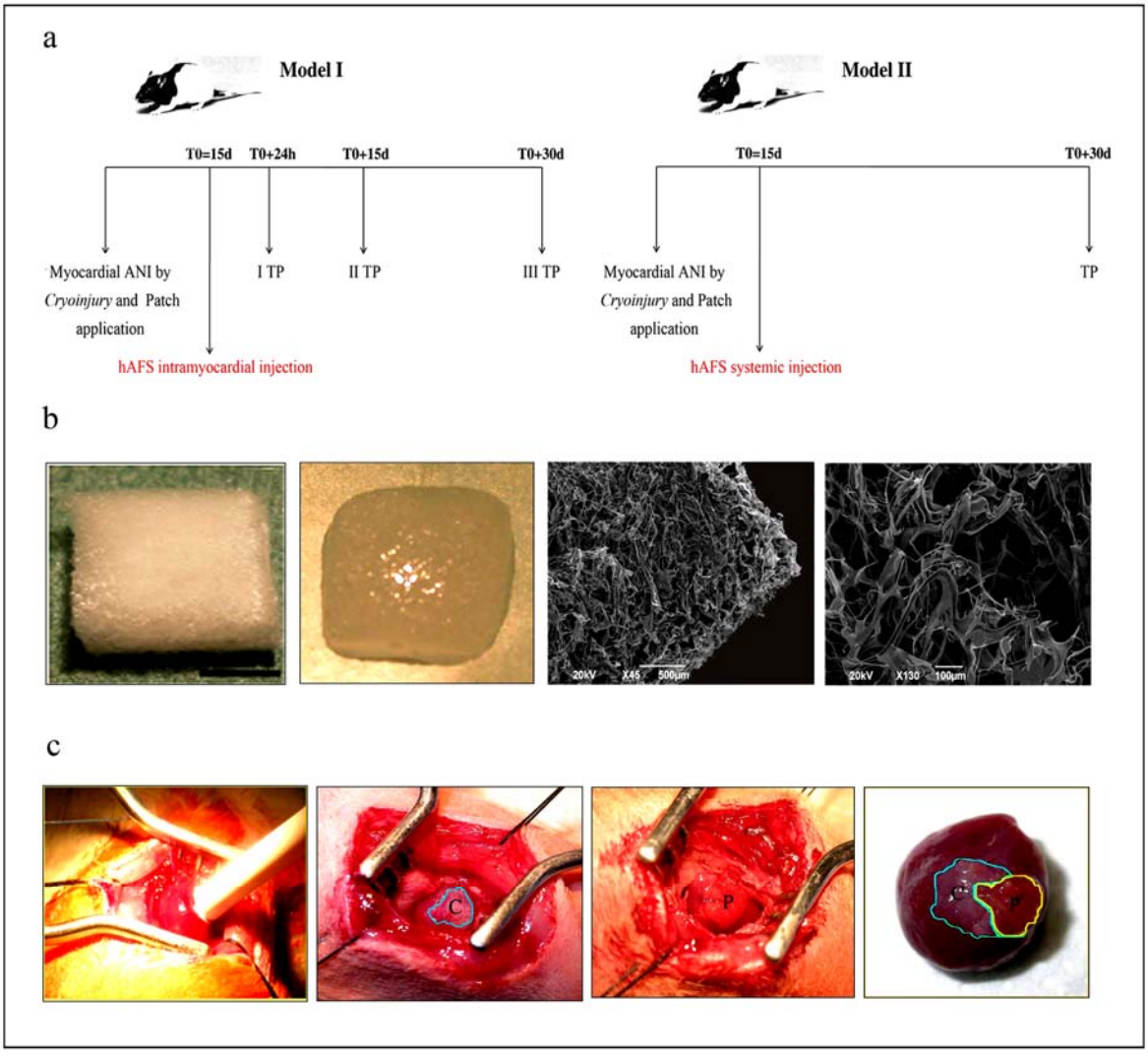

Figure 19. In **a:** cartoon of the experimental models; Model I: cryoinjury and patch application, 15 days later animals underwent cell injection into the patch. Three different time points were chosen. Model II: cryoinjury and patch application, 15 days later cells were injected via iliac vein and one time point was chosen. In **b**: on the left, collagen scaffold (patch, 0.8x0.8x0.5cm) dry and after PBS conditioning; on the right, electron scansion microscopy (SEM) images of collagen scaffold. In **c**: the cryoinjury procedure in NuRat LV as reported in Callegari et al. [113]; on the right corner gross appearance of heart with cryoinjury (C) and patch application (P), after 30 days.

As in the previous work [113], we then analysed several locations in the heart: the patch area, the cryoinjury area (just underneath the first one), the border area (between the lesion and the viable myocardium) and the intact myocardium, surrounding the border zone.

1.1. Model I: cmtmr^{+}hAFS cells locally injected into the collagen patch.

As illustrated in Figure 20b, 15 and 30 days after the injection, cmtmr^{+}hAFS were still in the patch and moved from the site of the injection (patch area) towards the cryoinjured area in the heart and, moreover, to the intact myocardium close to big vessels.

None of cmtmr^{+}hAFS cells expressing cardiomyocyte markers was found, even if most of the stem cells were found very closely related to smooth muscle and endothelial rat cells.

In particular after 24h about 50% of cells, both cardiomyocytes used as control and cmtmr^{+}hAFS cells were found inside the patch, but, interestingly, after 15 days cardiomyocytes were still in the patch, as reported by Figure 21b, while most of the hAFS cells had moved.

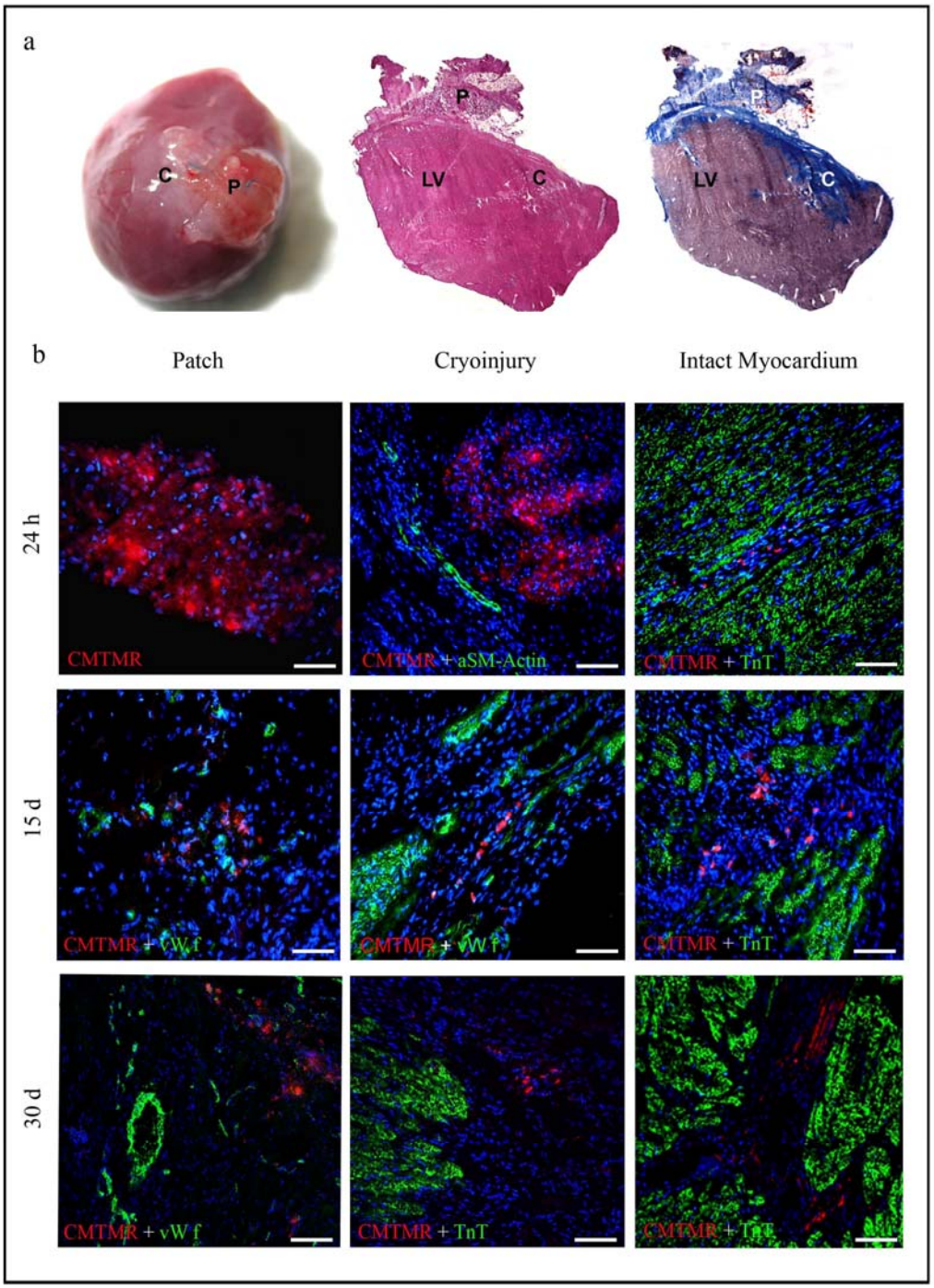

Figure 20. Model I. In **a:** gross appereance of the heart with cmtmr^{+}hAFS cells injection (on the left), c = cryoinjury area, p = collagen patch; Haematoxylin and Eosin (high centre, cryoinjury site reported as pale area) and Masson's Tricrome (high right, cryoinjury and patch area represented in blue, as high in collagen content), LV= left ventricle. In **b**: immunostaining for cmtmr^{+} cells (in red) and smooth muscle actin (in green), cardiac troponin T (in green) and vonWillebrand's

factor (in green) in the patch, cryoinjury and intact myocardium area at 24 hours, 15 days and 30 days after injection. Magnification 20X, bar 100um.

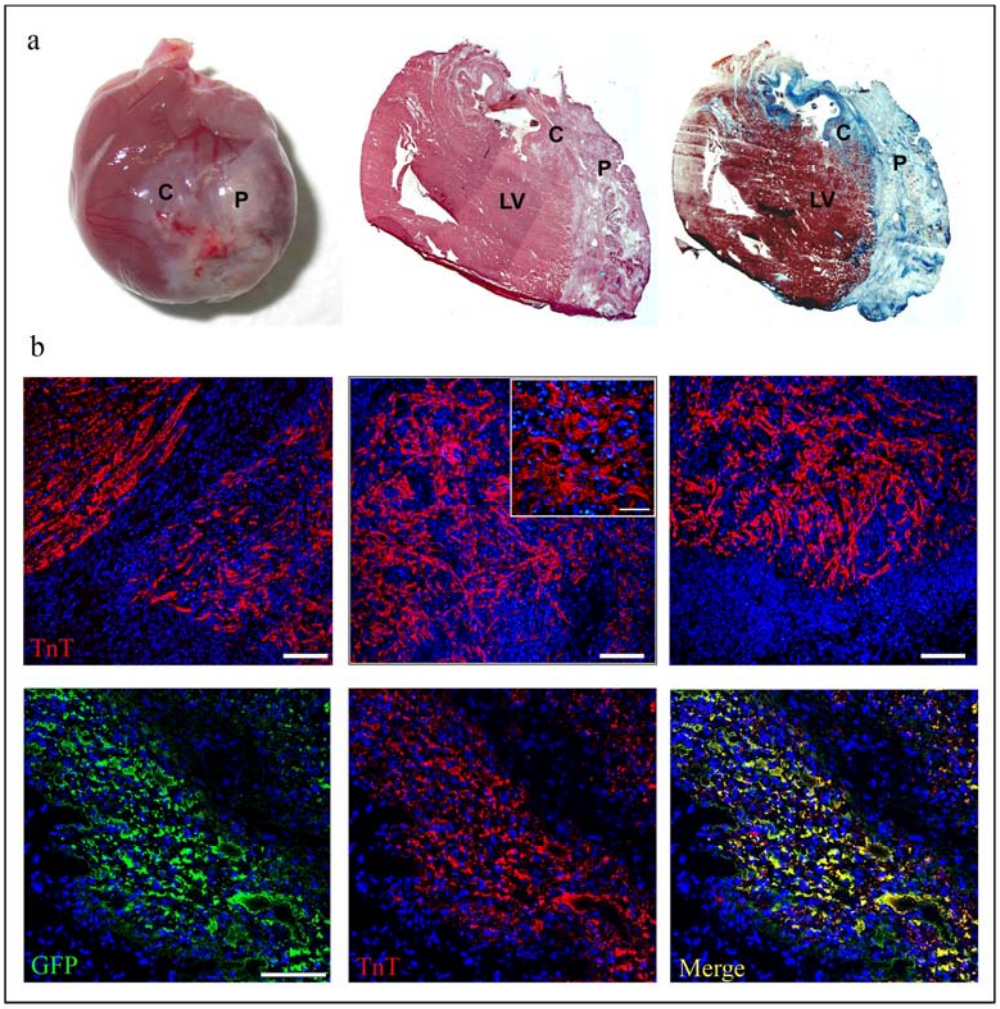

Figure 21. Model I. In **a**: gross appereance of the heart with rCM local injection, c = cryoinjury area, p = collagen patch. Haematoxylin and Eosin (high centre, cryoinjury site reported as pale area) and Masson's Tricrome (high right, cryoinjury and patch area represented in blue, as high in collagen content) LV = left ventricle. In **b**: immunostaining for cardiac troponin T of wt rCM (in red, magnification 20X, bar 100um, inlet magnification 40X bar 75um) and gfp^+rCM (GFP, in green; troponin T in red, merge, magnification 20X, bar 100um). After 15 days post cardiomyocytes injection, TnT staining highlight most of the cardiomyocytes still in the patch area.

In Figure 22 is reported the amount of $cmtmr^+$ hAFS found in the heart at different time points. In 22a $cmtmr^+$ hAFS are clearly showed to decrease from 186,15±66,76 cells/mm^2 after 24 hours from the *in vivo* local injection in the patch to 8,12±2,22

cells/mm^2 after 15 days and 9,27±4,12 cells/mm^2 after 30 days. The difference in the amount of hAFS cells *in vivo* detected among the first time point at 24 hours and all the others, was statistically significant ($p<0,05$).

To investigate the causes of this dramatic decrease, apoptag assay was carried out to evaluate the amount of cells dead by apoptosis: in Figure 22b it's showed as small the number of cells died by apoptosis was: after 15 days they were about 15,58±4,72 cells/mm^2 and 6,49±1,84 cells/mm^2 after 30 days post injection into the collagen scaffold. As control, we analyzed also apoptosis in animals which underwent cryoinjury, without patch application but with cmtmr$^+$ hAFS injection: after 30 days dead cells were a very little amount as well, 3,90±1,43 cells/mm^2. A much bigger amount of cells died by apoptosis was seen after at 15 dayst, this value, indeed, was statistically significant, compared to the amount of cells dead in the control setting ($p<0,05$).

As the cells positive for apoptosis staining were all negative for CMTMR expression and, at the same time, the amount of cmtmr$^+$ cells present in the heart remarkably decreased during time, they should have chosen different mechanism of cell death.

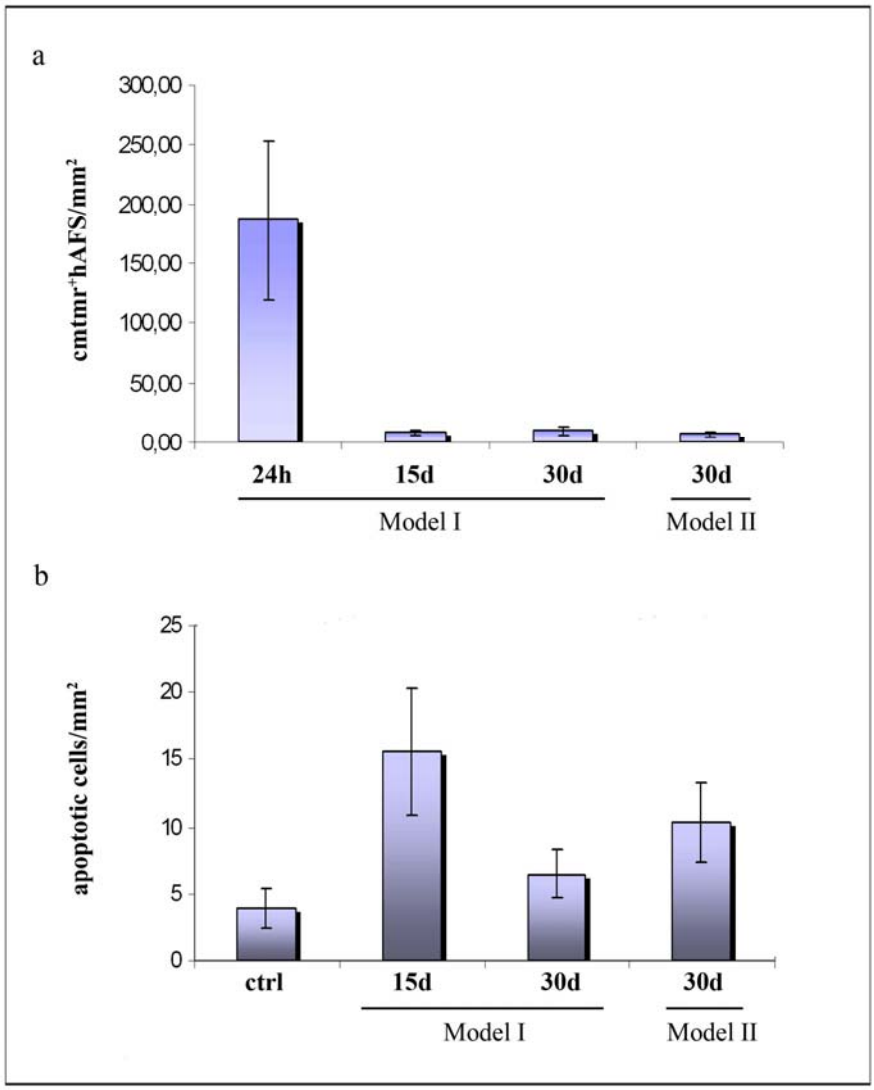

Figure 22. cmtmr$^+$hAFS cells distribution in the heart after injection. In **a**: in Model I 24h after injection cmtmr$^+$cells were 186.15±66.76 cells/mm^2, 15 days after were 8.17±2.22 cells/mm^2, 30 days after they were 9.27±4.12 cells/mm^2; in control animal; in Model II cmtmr$^+$ cells were 6.49±2.62 cells/mm^2 after 30 days. In **b**: amount of cells positive for apoptosis staining in the heart at different time points after cmtmr$^+$hAFS cells injection. "Ctrl" represents samples from cryoinjured heart without patch application but with cells injection 30 days after ANI instauration, apoptotic cells were 3.89±1.42 cells/mm^2; in Model I after 15 days from hAFS injection apoptotic cells were 15.58±4.71 cells/mm^2, after 30 days 6.49±1.84 cells/mm^2; in Model II, 30 days after i.v. injection dead cells were 10.34±2.96 cells/mm^2. Interestingly, none of these cells was cmtmr$^+$.

After 15 and 30 days from the cells injection, serial slides of heart specimens were processed by immunostaining for endothelial markers such as von Willebrand factor and smooth muscle α actin, to analyse presence of new and mature vessels.

The collagen patch potential of attract new vessels in cryoinjury site and in itself had been already demonstrated [113]: here we confirmed those data in our model with cells injection, by the quantitative analisys of the vases in patch area, cryoinjury and myocardium. This aspect highlighted the strong capacity time-dependent of the collagen to recruit endothelial cells to form new vases, as in Figure 23: after 15 days from cells injection, von Willebrand factor-positive vessels were 20,92±6,98 vessels/mm^2 in the intact myocardium, 33,28±4,65 vessels/mm^2 in the cryoinjury area and 19,48±3,63 vessels/mm^2 in the collagen patch; smooth muscle α actin-positive vessels were 10,39±6,52 vessels/mm^2 in the intact myocardium, 16,88±5,39 vessels/mm^2 in the cryoinjury area and 29,87±7,02 vessels/mm^2 in the collagen patch. At the first time point after cells injection, the amount of capillaries and arterioles were not significantly different in these 3 areas considered ($p>0,05$). After 30 days from cells injection, von Willebrand factor-positive vessels were 42,67±11,65 vessels/mm^2 in the intact myocardium, 89,98±27,59 vessels/mm^2 in the cryoinjury area and 38,03±6,99 vessels/mm^2 in the collagen patch; smooth muscle α actin-positive vessels were 17,63±6,11 vessels/mm^2 in the intact myocardium, 21,34±5,52 vessels/mm^2 in the cryoinjury area and 24,12±2,85 vessels/mm^2 in the collagen patch. As seen in the first time point, even in this one the amount of detected vessels was not significantly different in these 3 areas after cells injection ($p>0,05$).

The density of von Willebrand factor-positive capillaries at 30 days in the patch and cryoinjury area was significantly higher than the one detected after 15 days from cells injection ($p<0,05$), whereas the density of smooth muscle α actin-positive cells at 30 days, both in patch and cryoinjury area, was not significantly different from the one detected after 15 days from cells local injection ($p>0,05$). According to these results and to the ones previously achieved [113], after patch application and cells injection, new vessels formed: new capillaries were formed during 30 days, whereas arterioles increased after 15 days and then reached a plateau.

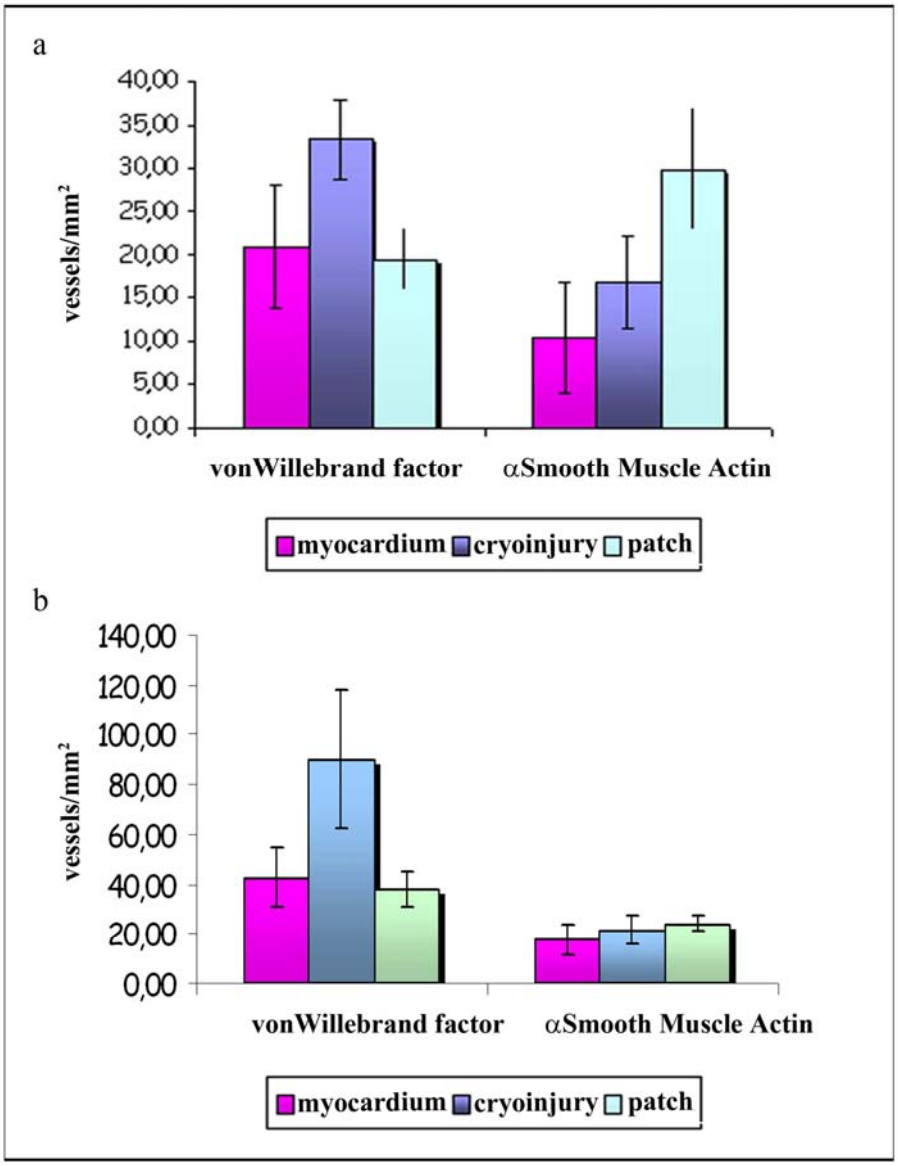

Figure 23. Number of vases after cmtmr^{+}hAFS cells injection in Model I in intact myocardium (pink), cryoinjury area (blue) and collagen patch area (light blue) after 15 and 30 days. After patch application and cells injection, new vessels formed: new capillaries were formed during 30 days, whereas arterioles increased after 15 days and then reached a plateau. In **a**: vessels amount 15 days after cells injection; von Willebrand factor-positive vessels were 20,92±6,98 vessels/mm^2 in the myocardium, 33,28±4,65 vessels/mm^2 in the cryoinjury and 19,48±3,63 vessels/mm^2 in the patch; smooth muscle α actin-positive cells were 10,39±6,52 vessels/mm^2 in the myocardium, 16,88±5,39 vessels/mm^2 in the cryoinjury and 29,87±7,02 vessells/mm^2 in the patch. In **b:** after 30 days von Willebrand factor-positive cells were 42,67±11,65 vessels/mm^2 in the myocardium, 89,98±27,59 vessels/mm^2 in the cryoinjury and 38,03±6,99 vessels/mm^2 in the patch; smooth muscle α actin-positive cells were 17,63±6,11 vessels/mm^2 in the intact

myocardium, 21,34±5,52 vessels/mm^2 in the cryoinjury and 24,12±2,85 vessels/mm^2 in the collagen patch.

As mentioned before (Figure 20b), hAFS cells were found just as scattered red cells close to the vases, particularly after 30 days, nevertheless immunoflurescence assays did not reveal integration cmtmr$^+$cells in capillaries or arterioles.

Considering that cmtmr$^+$hAFS cells dramatically decreased during time, we analyzed if the relatively paucity of the hAFS cells could have been the result of the intervention of the innate immune system cells, macrophages in particular.
We analyzed heart slices by immunostaining for ED2, macrophages marker. As reported in Figure 24 both in crioinjured area and in the intact myocardium few cells co-staining for CMTMR and ED2 were found, as illustrated in Figure 24.

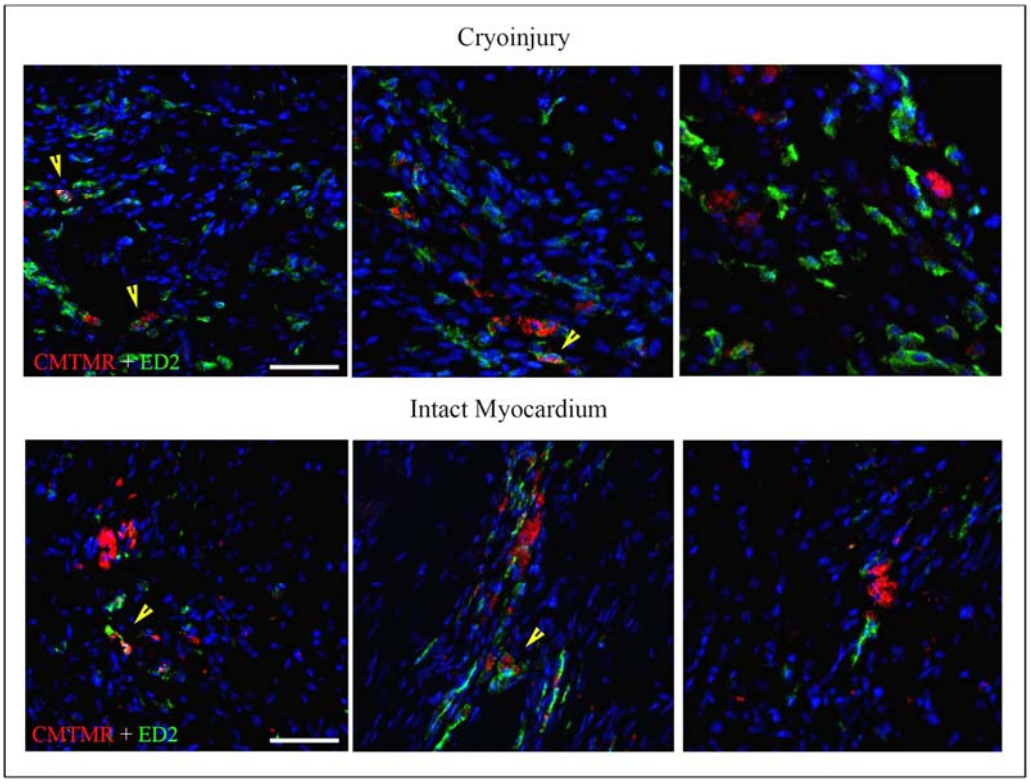

Figure 24. Model I. Immunostaining for cmtmr$^+$ cells (red) and macrophage ED2$^+$ cells (green) in model I, after 30 days from cmtmr$^+$hAFS cells injection, in cryoinjury (above) and intact myocardium (below) area, magnification 40X, bar 75um. Arrows pointing at cells co-stained for CMTMR and ED2, indicating some macrophages adsorbing CMTMR particles.

1.2. Model II: cmtmr^{+}hAFS cells systemically injected i.v.

In this model we analyzed cells delivered *in vivo* 15 days after patch application and cryoinjury instauration by systemic injection in the iliac vein.

As illustrated in Figure 25, 30 days after the i.v. injection few cmtmr^{+}hAFS were found in the patch close to the cryoinjured area and border zone, between cryoinjury and viable myocardium and near vessels (Figure 25); no co-staining for cardiac or endothelial marker was found. As expected a small amount of cmtmr^{+} hAFS cells were also detected into the spleen. cmtmr^{+} hAFS cells in the heart after 30 days from systemic administration were about 6.49±2.62 cells/mm^2 (Figure 22a).

In this model, cells dead by apoptosis were few, 10.34±2.96 cells/mm^2 (Figure 22b). Even if none of cmtmr^{+}hAFS cells found co-stained for cardiac or endothelial markers, both the total amount of cells detected and the apoptosis value were comparable to ones obtained with Model I at 30 days , suggesting that the patch could be able to exert a trophic effect improving homing to the heart of i.v. injected stem cells .

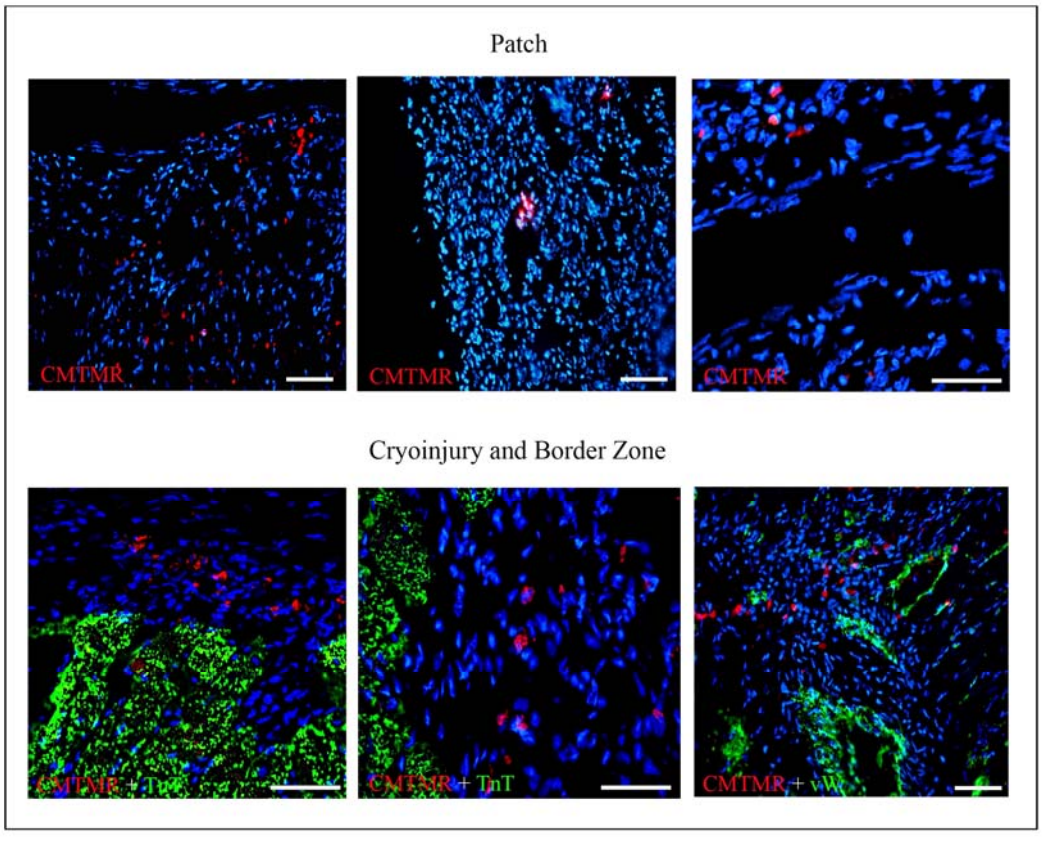

Figure 25. Model II: immunostaining of cmtmr^{+}hAFS cells (in red) found in patch and cryoinjury/border zone 30 days after i.v. delivery. Few scattered cells were detected in the patch area (panel above, magnification 20x, bar 100um and 40x, bar 75um) and in the cryoinjured area, close to the border zone (panel below, from left to right: staining for Troponin T, in green, von Willebrand factor in green, magnification 20x, bar 100um and 40x, bar 75um). None of cmtmr^{+}hAFS cells costaining for cardiac or endothelial markers was found.

Considering the host immune response against cmtmr^{+} human cells after 30 days from i.v. delivery, macrophage labelled with red spots of CMTMR were found, in this model as well, mainly in the patch area, as showed in Figure 26.

Considering both models, I and II, we could see number of macrophages containing CMTMR particles increasing during time: they were 9.19±6,13% in Model I 24 hours after hAFS cells injection, after 15 days they reached 11,94±3,24% and after 30 days they were 21,30±9,2% and 55,45±15,30% in Model II, as shown in Fgure 27. As control we also used samples from cryoinjured heart without patch application, but with cells injection at 30 days, in which costaining cells were 27,75±6,24%. The amount of macrophages containing CMTMR particles in Model II after 30 days from systemic hAFS cells injection was significantly higher compared to the value of Model I, 24 hours from cell injection ($p<0,05$), but not significantly different compared to the other time points ($p>0,05$).

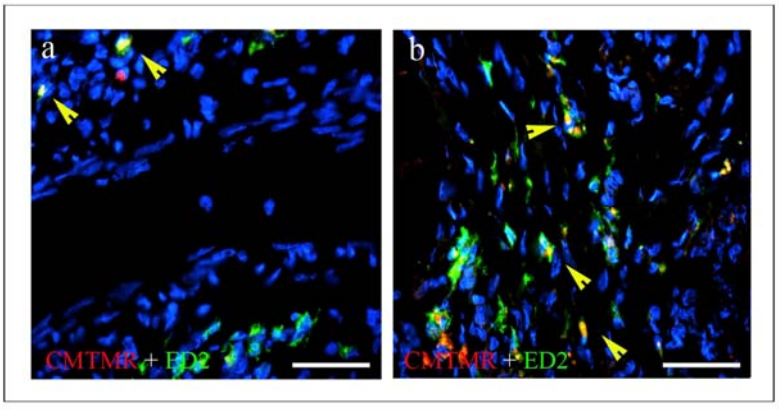

Figure 26. Model II: immunostaining of cmtmr^{+}hAFS cells (in red) and macrophage marker ED2 (in green) found in patch and cryoinjury/border zone 30 days after i.v. delivery. Some macrophage cells containing CMTMR particles are showed, pointed by yellow arrows, magnification 40x, bar 75um. In **a**: patch area, in **b**: cryoinjury area.

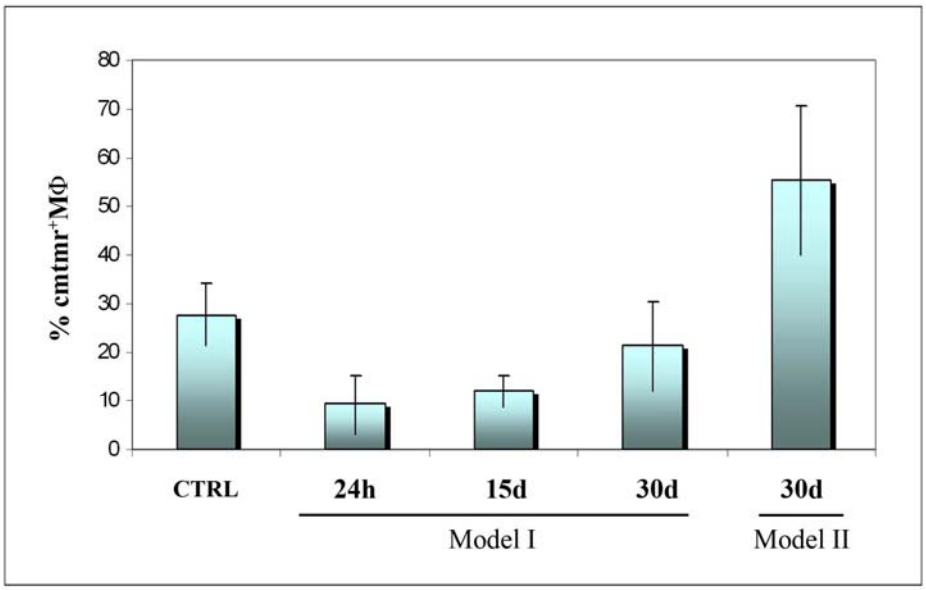

Figure 27. Evaluation of percentage of cmtmr^{+}macrophages (stained for ED2 expression) in Model I and II at different time points. "Ctrl" represents sample from cryoinjured heart without patch application but with cells injection 30 days after ANI instauration. Macrophages contaning CMTMR particles were about 27,75±6,24% in control hearts undergoing cryoinjury and cells injection (without patch) after 30days; in Model I after 24 hours from the injection they were 9.19±6,13%, after 15 days they increased to 11,94±3,24%, after 30 days up to 21,30±9,2% and 55,45±15,30% after i.v. delivery in Model II.

1.3. *In vivo* tracking of hAFS cells by human specific marker.

In both cell delivery approaches used in this sperimental model in rat (Model I and II), hAFS cells were detected using an intracellular red fluorescent marker, named CMTMR. Generally speaking, as this is a dye, subjected to dilution when cells replicate, we have seen that sometimes it has been misleading, as we found host macrophage cells positive for its expression, due to an immune response towards human cells or because of dead cells releasing it.

Considering this aspect, we decided to use a human specific marker, such as an antibody raised against human mithocondria, to accurately identify hAFS cells *in vivo* injected in both models *(the proof of this antibody specificity is reported later on in Figure 37).*

In Figure 28 the validation of this marker *in vivo* targeting hAFS has been successfully compared to CMTMR labelling: it was clearly demonstrated, indeed, that cmtmr^{+}hAFS cells costained with human specific anti-mithocondria antibody as shown by the merge picture in Figure 28.

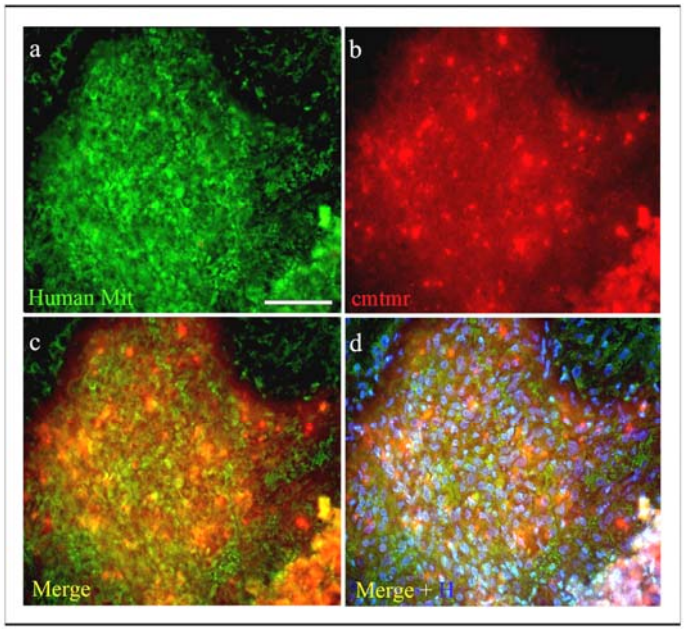

Figure 28. Immunostaining for cmtmr^{+}cells (red) and human mitochondria antigen (Hum Mit, green) on hAFS cells after 24 hours from injection in the collagen patch in Model I, magnification 40x, bar 75um. Cmtmr^{+} hAFS cells costained with human specific anti-mithocondria antibody, as showed by the merge pictures, in **d**.

We then repeated the analysis of the amount of hAFS cells detected *in vivo* by tracking them using this human-specific antibody. Using the anti-human mitochondria antibody we were able to find a bigger amount of hAFS cells *in vivo*, compared to the previous analysis. The trend of the amount of cells present in the heart in both models at different time points, represented here in Figure 29, is comparable to the one previously shown in Figure 22, when considering only CMTMR as *in vivo* cells tracker.

hAFS cells were mostly found after 24 hours post injection, as they were about 1206±482,46 cells/mm^2. They then dramatically decrease 30 days after to 160,42±64,53 cells/mm^2 in Model I and 75,20±21,44 cells/mm^2 in Model II. The difference among the amount of hAFS cells after 24 hours from local injection and all the other time points

was statistically significant ($p<0,01$). The other remaining values were comparable and similar among them.

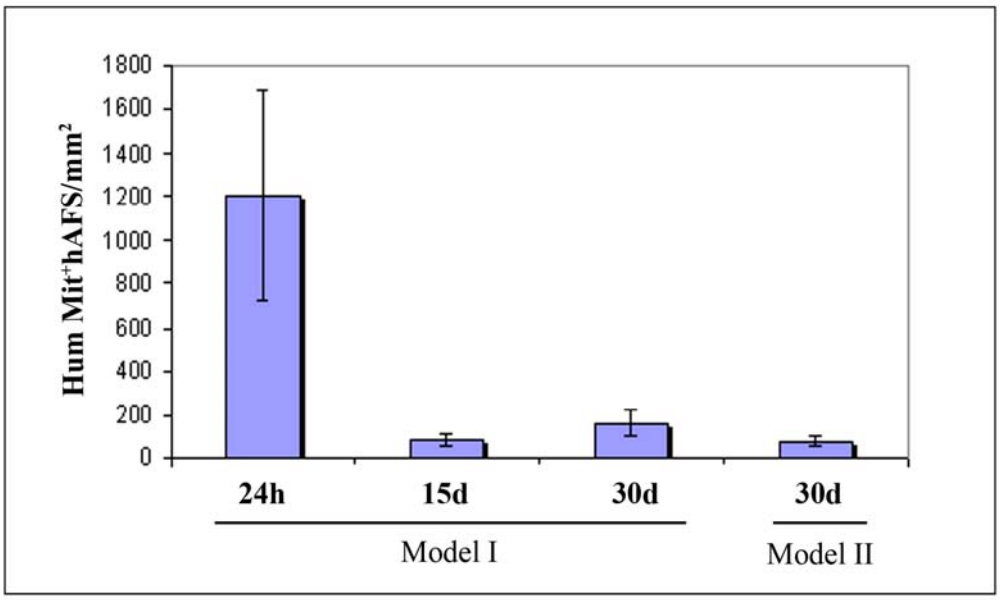

Figure 29. Quantification of hAFS cells detected in the rat heart by anti-human mitochondria staining in both models, Model I and II. In Model I, 24 hours after local injection, hAFS cells were 1206±482,46 cells/mm^2, 15 days after they were 80,21±25,76 cells/mm^2 and 30 days after 160,42±64,53 cells/mm^2. In Model II, after 30 days from systemic delivery hAFS cells were 75,2±21,44 cells/mm^2. In control animals with cryoinjury and hAFS cells injection only, human cells detected were 164,88±61,90 cells/mm^2.

The next immunostaining analysis for human mitochondria antigen, (green) and von Willebrand's factor (red) on hAFS cells, after 24 hours from injection in the collagen patch in model I, revealed some human cells co-expressing the endothelial marker, as shown in Figure 30.

More interestingly, hAFS cells injected i.v. after 30 days were found co-staining for endothelial markers, as von Willebrand factor and smooth muscle α actin, in close relationship with host endothelial cells forming vessels, Figure 31.

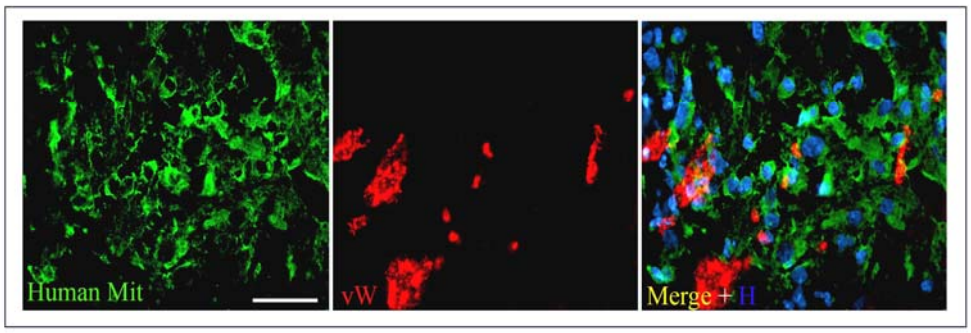

Figure 30. Immunostaining for human mitochondria antigen, (green) and von Willebrand's factor (red) on hAFS cells after 24 hours from injection in the collagen patch in model I, magnification 40x, bar 75um. Some hAFS cells costained with von Willebrand's Factor, endothelial marker.

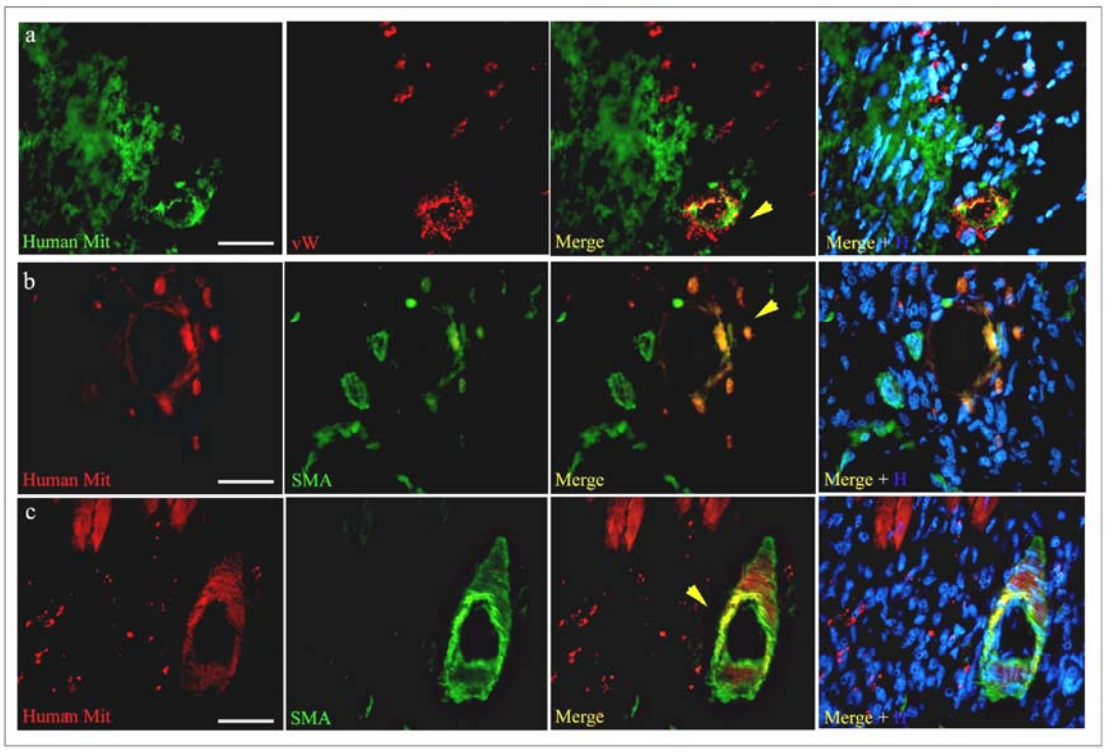

Figure 31. Immunostaining for human mitochondria antigen, von Willebrand's factor and smooth muscle α actin on hAFS cells in patch and cryoinjury area after 30 days from systemic injection in Model II, magnification 40x, bar 75um. In **a** and **b**: some hAFS cells (in green) costained with von Willebrand's factor^{+}endothelial cells (in red) forming chimeric capillaries, as pointed by arrows. In **c** and **d**: some hAFS cells (in red) co-stained with smooth muscle α actin^{+} cells (in green) forming chimeric arterioles, as pointed by arrows.

The amount of the chimeric capillaries and arterioles formed by hAFS cells, after 30 days, in both models (Model I and II), in the patch and cryoinjury area, is reported in Figure 32.

The number of chimeric vessels, positive for the expression of both human mithocondria antigen and vonWillebrand's factor was 11,35±3,59 vessels/mm^2 in Model I and 14,19±5,23 vessels/mm^2 in Model II. The whole population of chimeric and non-chimeric capillaries (vessels positive for vonWillebrand's factor expression), formed in the patch was 70,96±11,13 vessels/mm^2 in Model I and 73,79±16,25 vessels/mm^2 in Model II.

Chimeric vessels were 20,83±8,0% of the whole vessels population after 30 days in Model I and 19,30 ±8,1% in Model II.

The density of chimeric arterioles, positive for the expression of both human mithocondria antigen and smooth muscle α actin was 8,51±3,80 vessels/mm^2 in Model I and 2,83±2,83 vessels/mm^2 in Model II. The whole population of chimeric and non-chimeric arterioles (vessels positive for smooth muscle actin expression) formed in the patch was 59,6±20,5 vessels/mm^2 in Model I and 39,74±12,17 vessels/mm^2 in Model II.

Chimeric arterioles were 26,38±14,48% of the whole vessels population after 30 days in Model I and 16,67±16.67% in Model II.

Considering these data, the amount of new capillaries and arterioles formed by hAFS delivered by the two different approaches was demostrated to be comparable as there was not any significant difference regarding the chimeric vessels content between the two different approaches ($p>0,05$).

In conclusions, the results obtained regarding this part of the *in vivo* work demostrated that hAFS cells, injected on a cryoinjured rat heart locally on a vascularized 3D scaffold or systemically i.v., seemed to be refractory to transdifferentiate in cardiomyocytes, whereas they showed a propensity for a phenotypic vascular maturation. In this settings hAFs cells demostrated to take part in formation of chimeric vessels in the heart lesioned area and in the tissue engineered vascularized colagen scaffold, independently from the delivery strategy.

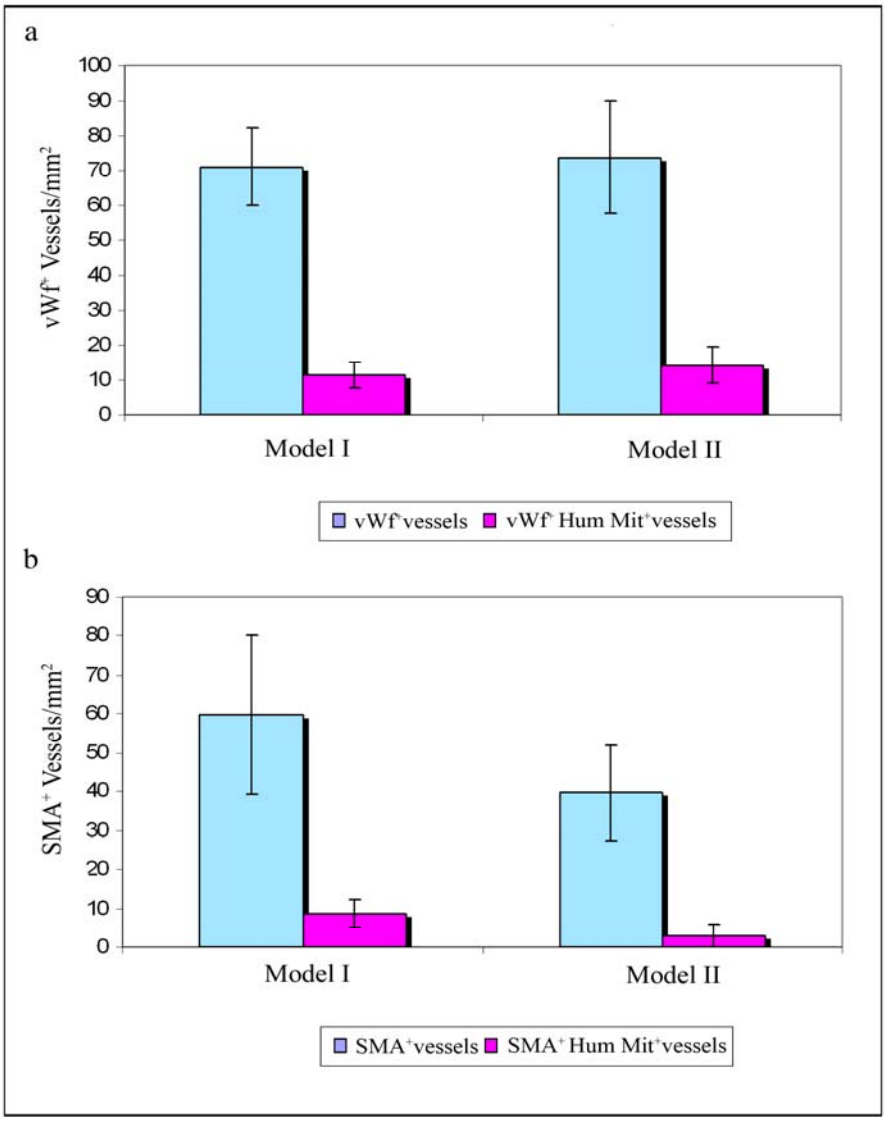

Figure 32. In **a**: evaluation of total amount of vonWillebrand's factor$^+$chimeric capillaries compared to the whole population of capillaries formed in Model I and II. The number of chimeric capillaries (vWf$^+$ Hum Mit$^+$ vessels) was 11,35±3,59 vessels/mm^2 in Model I and 14,19±5,23 vessels/mm^2 in Model II (in pink). The whole population of chimeric and non-chimeric capillaries (vWf$^+$vessels) was 70,96±11,13 vessels/mm^2 in Model I and 73,79±16,25 vessels/mm^2 in Model II (in blue). In **b**: evaluation of total amount of smooth muscle α actin-positive chimeric arterioles compared to the whole population of arterioles formed in Model I and II of hAFS cells delivery. The density of chimeric arterioles (SMA$^+$Hum Mit$^+$vessels) was 8,51±3,8 vessels/mm^2 in Model I and 2,83±2,83 vessels/mm^2 in Model II (in pink). The whole population of chimeric and non-chimeric arterioles (SMA$^+$vessels) was 59,6±20,5 vessels/mm^2 in Model I and 39,74±12,17 vessels/mm^2 in Model II (in blue).

2. Acute Myocardial Infarct Rat Model.

In a previous work it has been demostrated that freshly isolated bone marrow derived mononuclear cells injected i.v. into an acute model of myocardial infarct in rat were able to decrease significantly the infarct area, compared to animals receiving only PBS solution injection *(data not published yet)*. Here we used the same model, in an acute myocardial infarct setting, with AFS cells injection.

The experimental design is reported in Figure 33: AFS cells were injected into the animals soon after the ischemic insult, obtained by ligation of the anterior descendant coronary artery (LAD) for 30 minutes, following 2 hours reperfusion. After reperfusion the rats were sacrificed and the heart processed.

According to the cell injection animals were divided into the following groups:

a. animals receiving systemic injection of 500 ul of PBS solution;
b. animals receiving systemic injection of 10^7 gfp^+rAFS cells in 500ul of PBS solution;
c. animals receiving systemic injection of 10^6 gfp^+rAFS cells in 500ul of PBS solution;
d. animals receiving systemic injection of 10^7 hAFS cells in 500ul of PBS solution;
e. animals receiving systemic injection of $5x10^6$ hAFS cells in 500ul of PBS solution.

From the 42 rats at the beginning, 9 died during surgery procedure and cells injection, whereas 6 were not considered due to unstable physiology such as low blood pressure during the procedure. In the end, we had 12 rats with control PBS injection, none with 10^7 gfp^+rAFS cells/animal injection, 4 rats with 10^6 gfp^+rAFS cells/animal injection, 3 with 10^7 hAFS cells/animal injection and 9 rats with 10^6 hAFS cells/animal injection.

The infarct size was assessed by Evans Blue and TTC staining, after LAD ligation and 2 hours reperfusion, as illustrated in Figure 34: the perfused normally supplied myocardium was revealed in blue, the ischemic tissue in red, and the infarct area in the ischemic tissue was represented in white colour.

The stained heart slices were then acquired by the software ImageJ and the ischemic area at risk of necrosis (red) and the infarct area (white) were evaluated by planimetry using two different thresholds channels (red and white respectively).

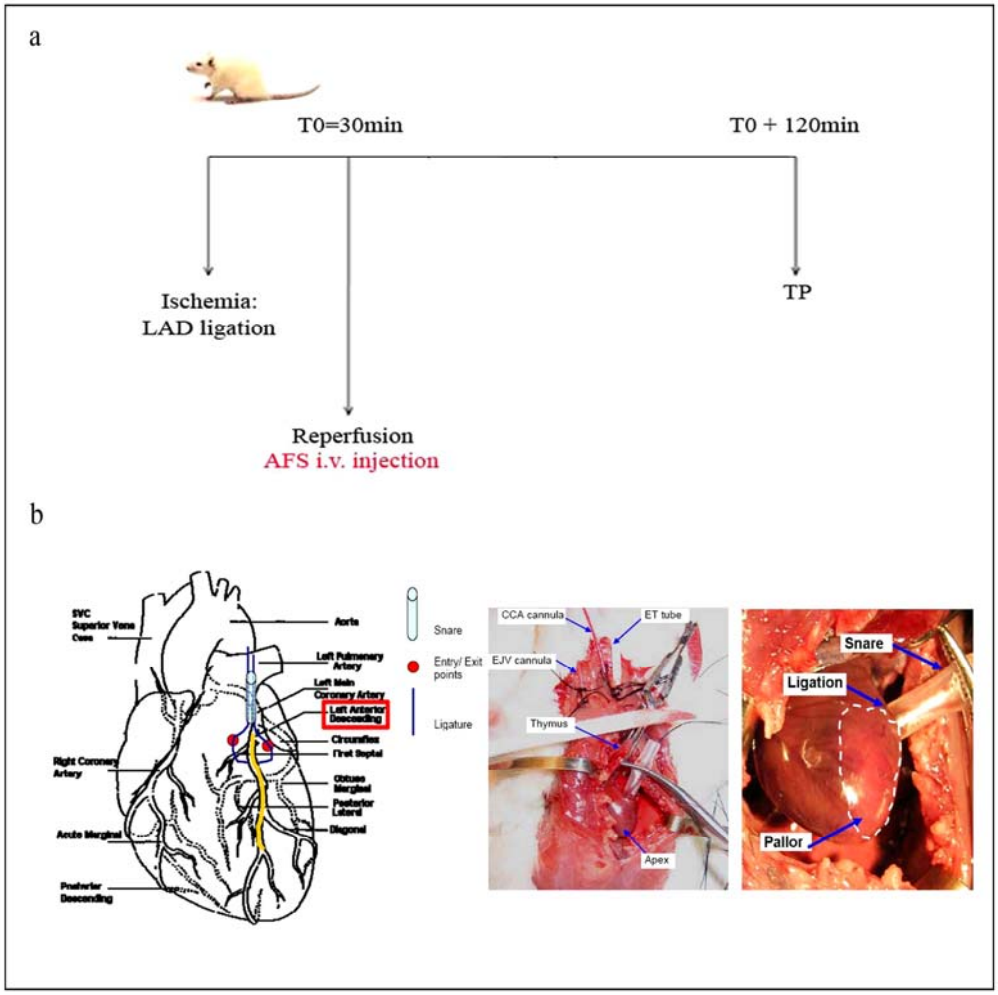

Figure 33. In **a:** cartoon of the experimental models: ischemia insult by coronary artery ligation for 30 minutes, reperfusion, cell injection and sacrifice after 2 hours. One final time point was chosen at the end of the reperfusion period. In **b**: the coronary artery ligation procedure, schematic representation on the left and pictures illustrating the toracotomy and cardiac ischemia obtained after LAD on the right.

Animals treated each with i.v. injection of 10^7 gfp^+rAFS and hAFS cells all died because of pulmonary embolism due to the cell size and the viscosity of the injected cell solution. About 66% of the animals treated each with i.v. injection of 10^6 gfp^+rAFS cells. 50% of the animals receiving each with i.v. injection of 10^7 hAFS cells died for pulmonary embolism, wheras the 75% of the ones receiving each i.v. injection of $5x10^6$ hAFS cells survived.

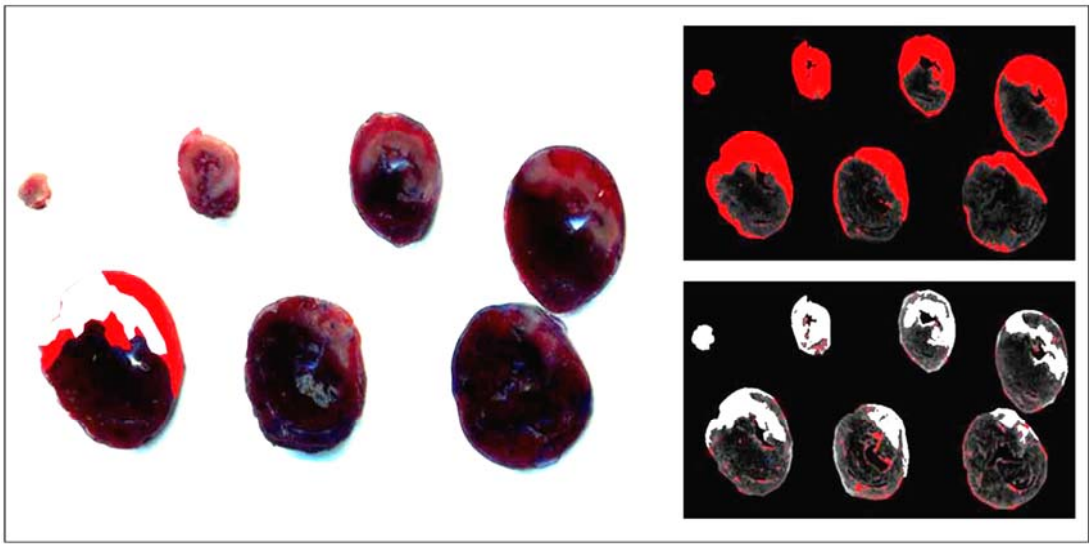

Figure 34. On the left: pictures of heart slices processed by Evans Blue and TTC staining after LAD and reperfusion: in blue the normally supplied myocardium, in red the ischemic area, in white the infarct area. On the right the same images of the heart slices acquired and processed by the software ImageJ, where the ischemic area at risk of necrosis (red) and the infarct area (white) have been evaluated using two different threshold channels (red and grey respectively) for measuring the region of interest.

In Table 5 and Figure 35 the data regarding the calculation of the area at risk of necrosis, (AAR) and the infarct size (IS) of each group are reported.

The ischemic not reperfused area, (expressed as the percentage ratio between the volumes of the Area at Risk of necrosis, AAR, and the left ventricle, %AAR/LV) was 56.8±2.1% of the left ventricle, in PBS control group, in the group receiving 10^6gfp$^+$rAFS cells/animal injection was 53.3±2.8%, in the group receiving 10^7hAFS cells/animal injection was 54.7±3.0% and in the group receiving 5x10^6hAFS cells/animal injection was 55.7±2.2% of the keft ventricle. The values among the 4 groups were comparable and similar one to the other ($p>0,05$), showing the good reproducibility of the procedure, that is each group has had a similar and comparable LAD and myocardium infarct.

The infarct size (IS, expressed as the percentage ratio between the volumes of Infarct area (In) and the Area at Risk of necrosis, %In/AAR) in PBS control group was 53.9±2.3% of the ischemic zone, in the group receiving 10^6gfp$^+$rAFS cells/animal treatment was 48.0±1.5%, in the group receiving 10^7hAFS cells/animal injection was

45.0±7.8% and in the group receiving $5x10^6$hAFS cells/animal injection was 40.0±3.0% of the ischemic zone. The infarct size in animals treated with $5x10^6$hAFS cells/animal i.v. injection, soon after ischemia for 2 hours, was statistically significant lower compared to the control, the PBS group ($p<0,05$).

Table 5. Summary of data about *in vivo* acute myocardial infarct rat model with hAFS cells injection. Dose refers to cells injected in each animal treated.

	PBS	**gfp+rAFS cells**		**hAFS cells**	
Dose	**500ul**	**10^7 cells**	**10^6 cells**	**10^7 cells**	**$5x10^6$ cells**
n	12	-	4	3	9
Body Weight, g	290 ± 6	-	279 ± 4	382 ± 3	305 ± 11
LV Volume, mm^3	474 ± 12	-	462 ± 24	545 ± 38	423 ± 13
AAR volume, mm^3	269 ± 13	-	246 ± 23	299 ± 30	235 ± 7
Infarct Volume, mm^3	144 ± 7	-	118 ± 12	134 ± 21	93 ± 6
AAR/LV %	**56.8 ± 2.1**	**-**	**53.3 ± 2.8**	**54.7 ± 3.0**	**55 7 ± 2.2**
In/AAR %	**53.9 ± 2.3**	**-**	**48.0 ± 1.5**	**45.0 ± 7.8**	**40.0 ± 3.0 ****
In/LV %	30.3 ± 1.4	-	25.5 ± 1.6	25.3 ± 4.9	22.2 ± 1.3

The decrease of infarct size in these animals compared to the control was significantly evident even in the picture of the heart slices soon after TTC staining: in Figure 36b the infarct area of each slice is showed in white and highlighted in blue and looks smaller compared to Figure 36a, where heart slices of control group are reported.

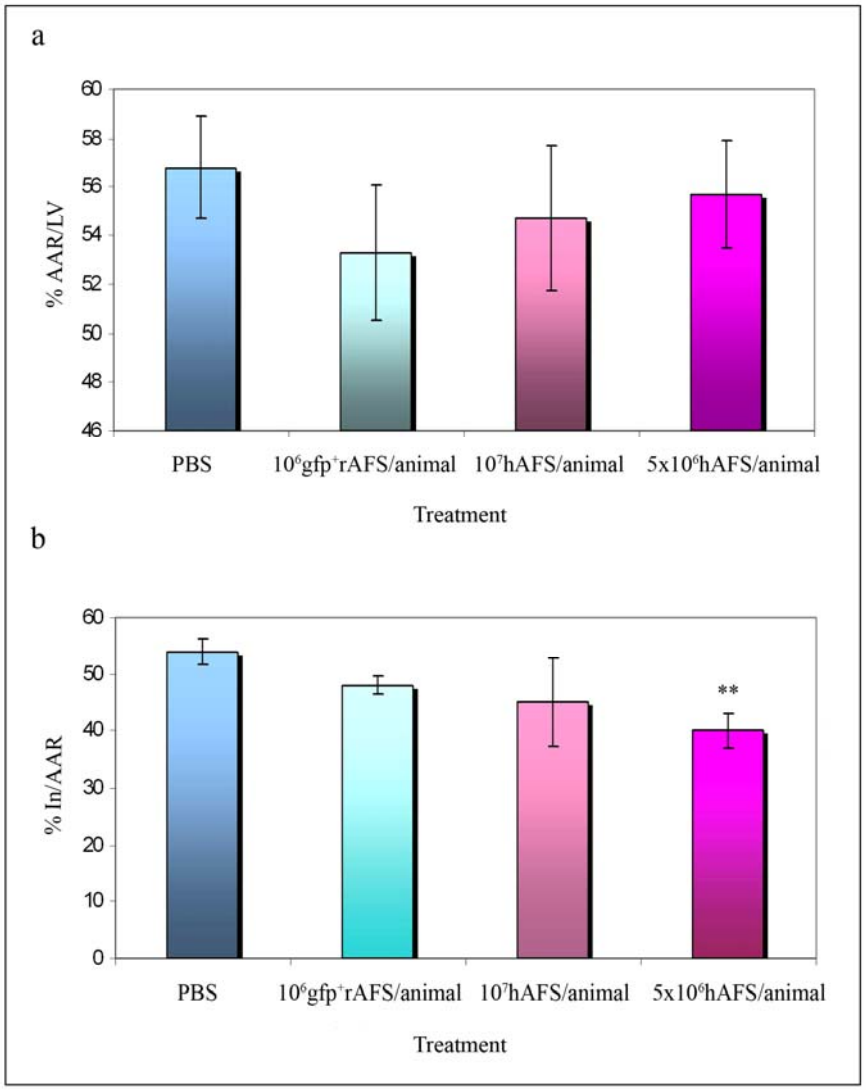

Figure 35. Evaluation of Area At Risk of necrosis and Infarct Size in the 4 different groups: PBS injection as control, 10^6gfp$^+$rAFS cells/animal injection, 10^7hAFS cells/animal injection, 5x10^6hAFS cells/animal injection. In **a**: evaluation of ischemic area, expressed as the ratio in percentage between area at risk (red area by TTC staining) and left ventricular area; % AAR/LV in PBS control group was 56.8 ± 2.1% of the left ventricle, in 10^6gfp+rAFS cells/animal treatment was 53.3 ± 2.8% of the left ventricle, in 10^7hAFS cells/animal injection group was 54.7 ± 3.0% and in 5x10^6hAFS cells/animal injection group was 55.7 ± 2.2% of the left ventricle. The similar values among the group demontrstate the good reproducibility of the procedure, attesting that each group has had a similar and comparable ischemic insult. In **b**: valuation of IS, meseaured as the ischemic area given by the ratio in percentage between infarct area (white area by TTC staining) and area at risk; % In/AAR in PBS control group was 53.9 ± 2.3% of the ischemic zone, in 10^6gfp+rAFS cells/animal treatment was 48.0 ± 1.5%, in 10^7hAFS cells/animal injection group was 45.0 ± 7.8% and in 5x10^6hAFS cells/animal injection group was 40.0 ± 3.0% of the ischemic zone. The infarct size in animals treated with

$5x10^6$hAFS cells/animal i.v. injection soon after ischemia for 2 hours was statistically significant lower than the one in control PBS group.

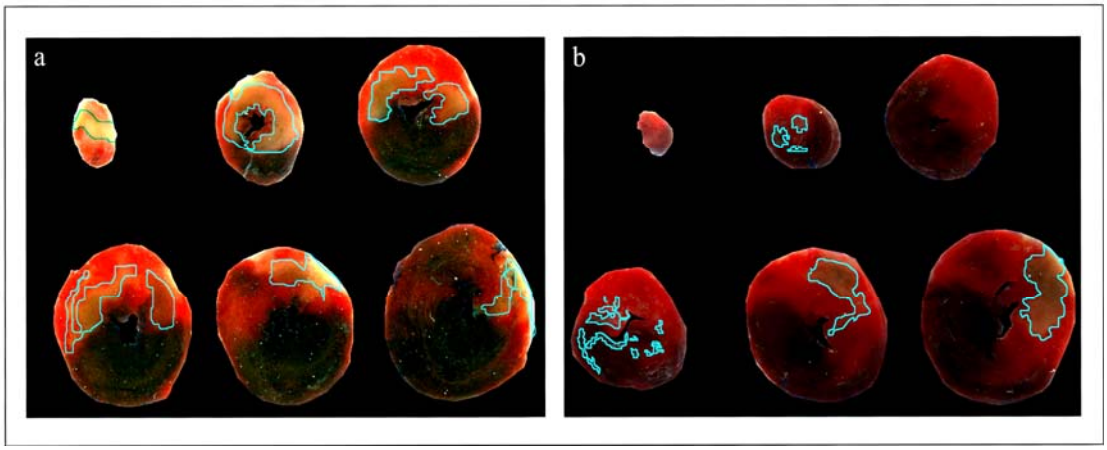

Figure 36. Pictures of heart slices processed by Evans Blue and TTC staining, after LAD and reperfusion. In **a**: slices of control heart injected with PBS, in blue the perfused viable myocardium, in red the ischemic area, in white the infarct area, highlighted in blue.
In **b**: On the right slices of heart injected with hAFS cells, acquired by the software ImageJ, in blue the perfused viable myocardium, in red the ischemic area, in white the infarct area, highlighted in blue.

Heart serial sections from animal injected with $5x10^6$ hAFS cells were also processed by immunostaining to evaluate hAFS cells distribution and localization after 2 hours reperfusion.

Human cells were succesfully detected using a human specific marker, the anti-mitochondria antigen.

In Figure 37 pictures regarding staining for human mitochondria are shown. In Figure 37a is reported the evaluation of specificity of human mithocondria staining on *in vitro* hAFS cytospun spots, compared with the staining on non injected heart rat tissue, as negative control, in 37b.

Very surprisingly, after only 2 hours reperfusion, hAFS cells were detected into the heart tissue as illustrated in Figure 37c and d and as usually expected in lung and spleen tissues as well, Figure 37e and f.

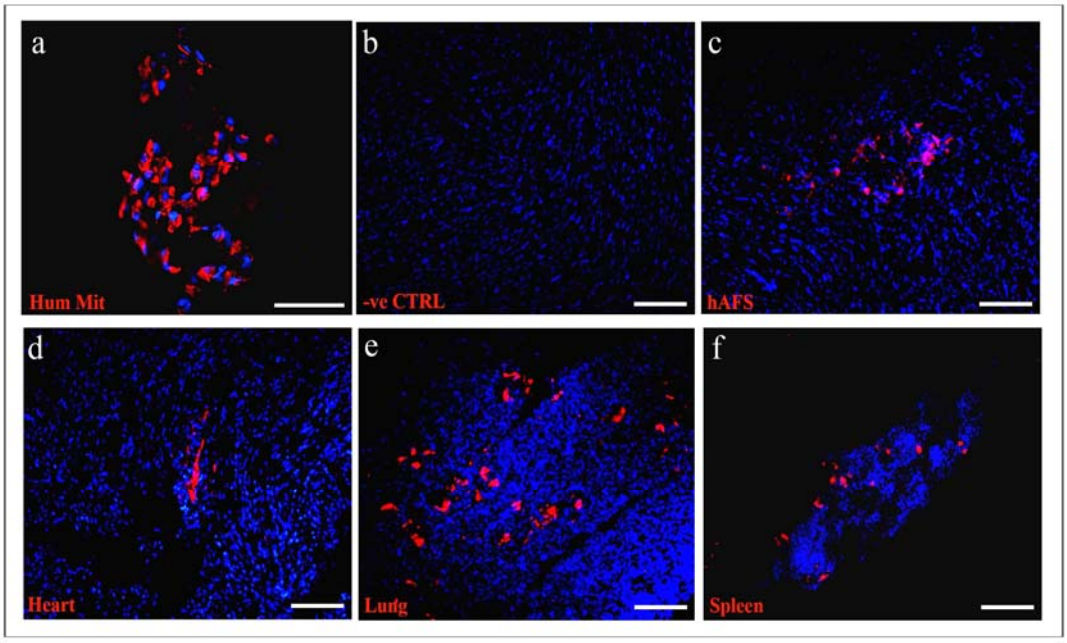

Figure 37. Immunostaining for human mitochondria to track hAFS cells injected i.v. in the rat for 2 hours after ischemia. In **a**: evaluation of human mithocondria staining (red) specificity on *in vitro* hAFS cells cytospun, magnification 40x, bar 75um. In **b**: evaluation of human mithocondria staining (red) specificity on non injected heart rat tissue, as negative control, magnification 20x, bar 100um. In **c** and **d**: hAFS stained for human mitochondria antigen (red) in the myocardium 2 hours after LAD ischemia/reperfusion and i.v. injection, magnification 20x, bar 100um. In **e** and **f**: hAFS cells stained for human mithocondria antigen (red) in lungs and spleen 2 hours after LAD ischemia/reperfusion and i.v. injection, magnification 20x, bar 100um.

Most of the hAFS cells detected in the heart after i.v. injection were found organized in circular "vessel-like" structures as shown in Figure 38a, b, c. 67,9±14,6% of human mitochondria^{+}hAFS cells found in the heart in circular organization were also positive for the expression of vonWillebrand's factor and 81,9±9,8% for the expression of smooth muscle α actin, as showed in Figure38d-q.

After 2 hours, about 2065.63±323.74 hAFS cells/mm^2 were found in the lungs, 1035.29±263.95 cells/mm^2 in the spleen and 601.524±64.41 hAFS cells/mm^2 were found in the heart, whereas almost none in the liver (Figure 39). The amount of cells in lungs and spleen was significantly higher than the amount present in the heart ($p<0,05$).

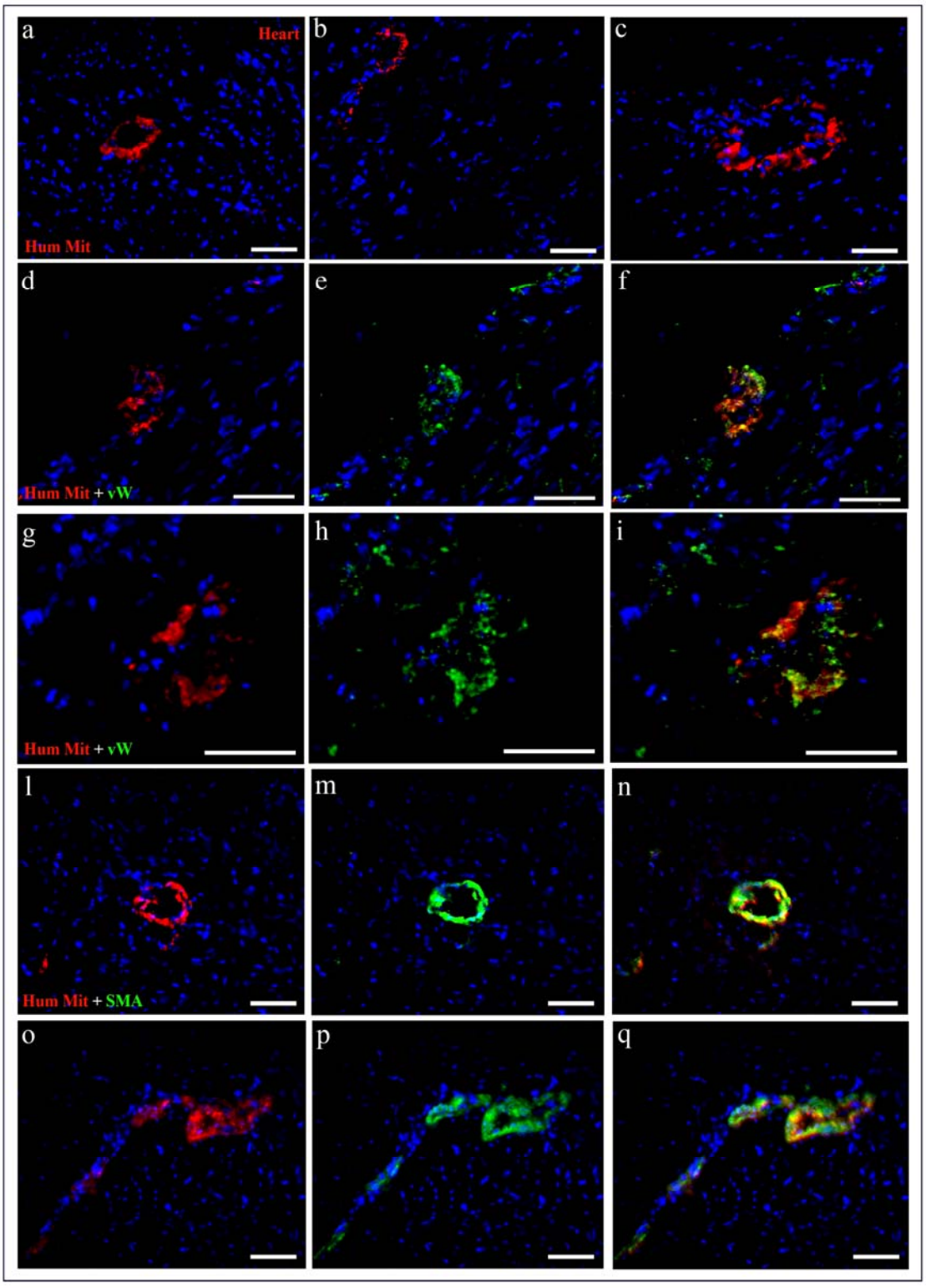

Figure 38. Immunostaining for human mithocondria to track hAFS cells injected i.v. in the rat for 2 hours after ischemia. In **a, b, c**: hAFS stained for human mithocondria antigen (red) in the myocardium 2 hours after LAD ischemia/reperfusion and i.v. injection, magnification 20x, bar 100um. Cells were found organized in circular "vessel-like" structures.

In **d, e, f** and **g, h, i**: hAFS stained for human mithocondria antigen (red) and vonWillebrand factor (in green) in the myocardium, magnification 40x, bar 75um and 63x, bar 50um. The costaining is represent by the merge picture, in yellow.
In **l, m, n** and **o, p, q**: hAFS found in circular structures and stained for human mithocondria antigen (red) costained also for smooth muscle α actin (in green) in the myocardium, merge picture in yellow, magnification 20x, bar 100um.

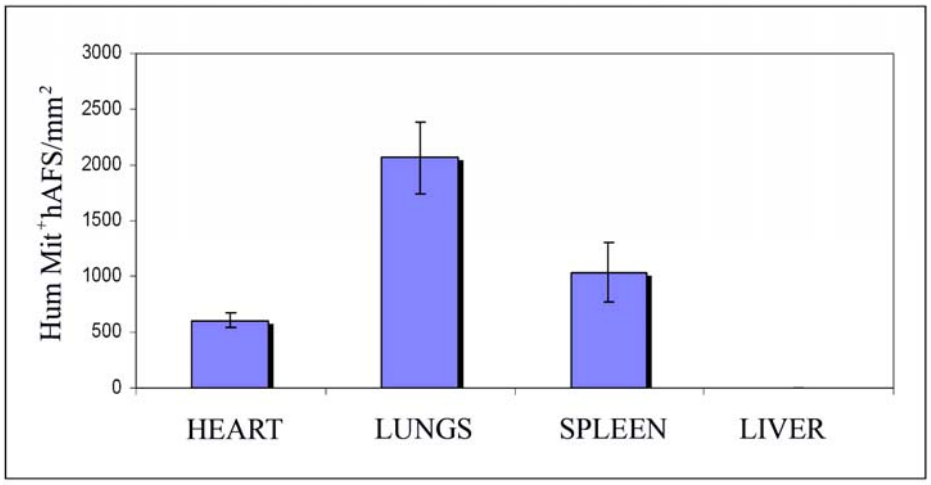

Figure 39. Distribution of hAFS cells found in heart, lungs, spleen, liver after LAD ischemia/reperfusion and i.v. injection. Cells found in heart after 2 hours reperfusion were 601.524±64.41 cells/mm^2; cells found in the lungs were 2065.63±323.74 cells/mm^2; cells found in the spleen were 1035.29±263.95 cells/mm^2. Surprisingly, almost none hAFS cell was found in the liver.

2.1. Analysis of AFS cells cardioprotective potential.

hAFS cells, analyzed by RT-PCR for the presence of a subpopulation of early cardiac progenitor cells, seemed to confirm this hypothesis, showing positive results for the expression of mRNA of cardiac markers as Isl1 and Kdr, in control standard conditions, as illustrated in Figure 40a (lane 5).
AFS cells, cultured *in vitro* at cellular densities resembling the ones used in the *in vivo* acute myocardial infarct model settings, demonstrated to be able to secrete the protein thymosin β4 in the culture medium, as reported in Figure 40b. In particular, human AFS cells showed a higher production of this paracrine factor, compared to the rat ones. The culture medium alone showed to contain the protein thymosin β4 at 0,67±0,11 ug/ml, 10^6

gfp^+rAFS and 10^7 gfp^+rAFS cells were able to secrete, respectively, about 0,95±0,03 ug/ml and 0,94±0,04 ug/ml in the medium, whereas $5x10^6$ hAFS cells were able to secrete about 1,39±0,11 ug/ml in the culture medium. hAFS cells produced an amount of thymosin□4 statistically significantly higher than gfp^+rAFS cells ($p<0,05$).

The results obtained in this part of the *in vivo* work showed that hAFS cells, injected into a model of acute myocardial infarct, were able to get the infarct size reduced of about 14% of its size in a very short period of time (2 hours reperfusion).

The same cells used for the *in vivo* experiments, were also positive for the expression of the early cardiac precursors genes Isl1 and Kdr; moreover, the hAFS cells were demostrated to be able to secrete the cardioprotector paracrine protein thymosin β4 in the culture medium.

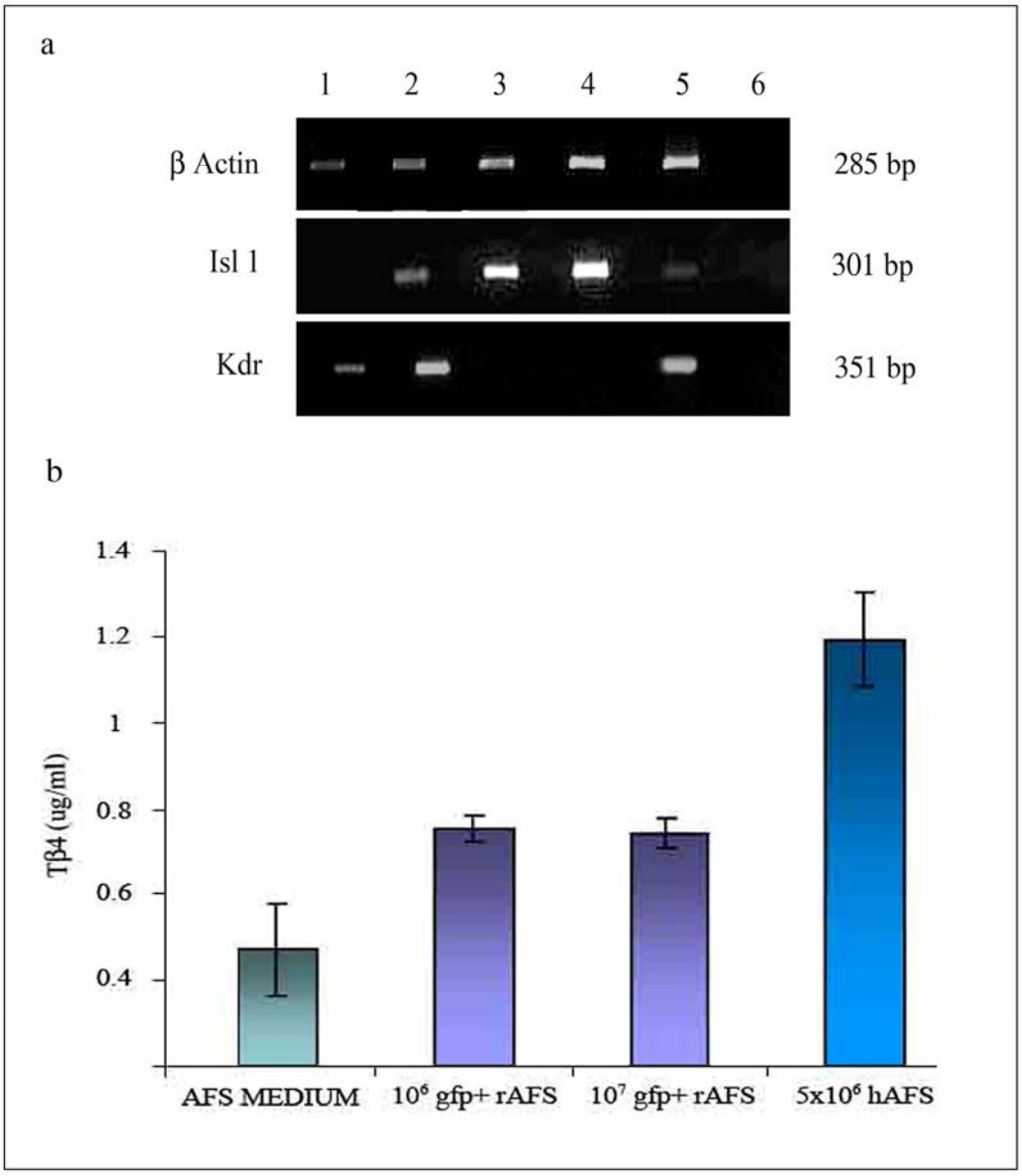

Figure 40. In **a:** RT-PCR of hAFS cells for the early progenitor cardiac markers Isl1 e KDR: lane 1= adult human heart, lane 2= foetal human heart, 3= foetal mouse heart (positive control for Isl1, primers are specific both for human and mouse), 4= mouse ES G_2G_4, 5= hAFS cells, 6= H_2O. hAFS cells showed the molecular signature of cardiac progenitor cells given by the double expression of Isl1 e KDR; **b**: ELISA analysis for thymosin β4 production by AFS cells in the *in vitro* culture medium. The culture medium alone showed to contain the protein thymosin β4 at 0,67±0,11 ug/ml, 10^6 gfp^+rAFS and 10^7 gfp^+rAFS cells were able to secrete, respectively, about 0,95±0,03 ug/ml and 0,94±0,04 ug/ml in the medium, whereas $5x10^6$ hAFS cells were able to secrete about 1,39±0,11 ug/ml in the culture medium. hAFS cells produced an amount of thymosin β4 significant higher than gfp^+rAFS cells.

Chapter 4 Discussion and Conclusions.

1. *In Vitro.*

In the last decade many strategies have been proposed to repair damaged heart and, in this scenario, cell based cardiac tissue engineering has become one of the most challenging fields in modern regenerative medicine.

Congenital heart malformations often require surgical treatment shortly after birth. It would be advantageous to find and employ an autologous source of cell progenitors from the foetus to engineer autologous living heart tissues, ready for use at birth. Foetal tissue could be obtained from a direct biopsy of the fetus during gestation or from foetal membranes; however, both procedures can be associated with a defined mortality and morbidity to some extent

Amniotic fluid could represent an alternative and more accessible source. Foetal cells can be easily collected from amniotic fluid using amniocentesis, a well-established technique, with low risk for both the foetus and mother. Until very recently, cells present in the amniotic fluid were used solely for prenatal diagnosis; however, our group and others have presented studies demonstrating the presence of different progenitors in the amniotic fluid, mainly with mesenchymal characteristics [87, 88,105].

Moreover, we have recently described that it is possible to derive lines of broadly multipotent cells from the amniotic fluid (AFS cells). Using discarded back-up amniocentesis samples, indeed, we isolated AFS cells by selection for the expression of the membrane stem cell factor receptor c-Kit [92]. In previous studies, our group had already analyzed the AFS cells differentiating potential, demonstrating that cloned AFS human lines can be induced to differentiate into cell types representing each embryonic germ layer, including cells of adipogenic, osteogenic, myogenic, endothelial, neuronal and hepatic lineages [92]. Furthermore, we have shown that AFS cells can also acquire a smooth muscle cell-like phenotype *in vitro* and *in vivo* [91]. However, despite the differentiating ability of human amniotic fluid derived cells *in vitro* into cells of cardiovascular lineages (to some extent), we have previously demonstrated that

undifferentiated human amniotic fluid-derived stem cells cells, injected in an ischaemic heart, are unable to transdifferentiate into cardiomyocytes, although they were able to form smooth muscle and endothelial cells [94].

The work done during my PhD period confirmed the data in part already published about the cardiomyogenic potential of the Amniotic Fluid Stem cells [94]. Here, indeed, we analyzed the *in vitro* AFS cells cardiomyocyte differentiating potential, more in details from a functional point of view, by patch clamp analysis and coculture methods.

The single cell electrophysiology study done here, using the patch-clamp method, gives a clear proof of the excitability of AFS cells while in co-culture with cardiomyocyte cells. The AFS cells showed a pacemaking activity that matches with the electrical activity recorded on cardiomyocytes they have been cultured with, although the characteristics of the action potential, measured as APD50 and APD90, are clearly different between the two cell types. When co-cultured AFS cells were challenged with isoprenaline, we observed a shortening of APD50 and APD90, leading to acceleration of their pacemaking activity.

Among the AFS cells, we were able to classify according to their electrophysiological characteristics, into two categories, the less mature and the more mature. The "immature" cells showed a membrane depolarisation during the action potential smaller, and action potential showed shorter APD_{50} and APD_{90} values. The "mature" ones had a membrane potential similar to cardiomyocytes and APD_{50} and APD_{90} were longer than "immature" AFs cells. We therefore believe that the AFS cells, once in co-culture, evolved from the non-excitable phenotype to the mature phenotype under the influence of the surrounding cardiomyocytes.

In order to improve the results obtained by static culture conditions techniques, the use of micropatterned bidimensional scaffolds has also been explored in this work.

In any contractile tissue, such as the myocardium, functional properties are directly related to cellular orientation and elongation; the interactive effects of contact guidance, such as using the abraded surface as a cell seeding support, has been previously demonstrated to drive elongation and organization of cardiomyocytes [115, 6, 7]. In this work, we have tried to create a suitable environment for the AFS-rat neonatal cardiomyocyte cells co-culture as well, in order to promote *in vitro* AFS cells

organization and differentiation by performing bidimensional culture on microstructured matrices.

We tested two different bidimensional scaffolds: hydrogel films and PDMS (silicon) membranes. Before analyzing AFS cells in co-culture, we tested the biocompatibility and viability of the polymers with the neonatal cardiomyocyte primary culture.

Hydrogels films were demonstrated to be highly biocompatible and non-fouling materials; the latter property allowed selectively driving cell adhesion on their surface by means of micro-contact printing technique, used to create protein patterns. We managed to engineer a scaffold with an array of adhesive lanes, with accurate control of shape and size: cell seeding all over the hydrogel surface resulted in an extremely selective adhesion of neonatal cardiomyocytes, with cells only adhering and spreading within the patterned regions and being able to be *in vitro* successfully cultured up to 10 days. Neonatal rat cardiomyocytes were cultured on such patterned elastic substrate and guided to form aligned and organized cardiac myofibers expressing the correct phenotypic markers and spontaneous synchronous contractile activity. These array of fibers showed to maintain the information related to the functionality and structure of cardiac tissue more closely than the traditional *in vitro* cultures or cell array approaches, potentially becoming a useful approach for stem cells differentiating studies by co-culture method. As we were able to obtain a well organized aligned *in vitro* functional cell structure; we thought that hydrogel films could be the ideal scaffold to improve AFS cells organization, interaction and differentiation in co-culture. Unfortunately the high densities of both cell populations used in our co-culture method did not fit with the delicate balance between the available seeding area and the selective adhesion that the polymer film could support. AFS cells weren't able to adhere properly and by a well aligned organization as cardiomyocyte cells, starting detaching soon after seeding.

We then analyzed the PDMS micropatterned membrane. Cardiomyocyte cells seeded on the silicon membrane showed to align following the orientation with a well defined spatial organization and were able to express synchronous beating activity as well. In particular, the thinner micropattern of the textured silicone surface was able to improve cardiomyocyte organization more at the single cell level than at the fiber level, as seen with the hydrogel polymers. To evaluate this aspect in details and to analyze the topological influence of the scaffold, we then tested the gfp^{+}rAFS and rCM co-culture.

gfp^+rAFS cells grew on the membrane in close relation to rCM cells, following the longitudinal orientation given by the micropattern and, moreover, showing rarely functional activity. The PDMS bidimensional scaffold was therefore likely to ameliorate rCM and AFS cells seeding and orientation, allowing better spatial organization of stem cells. These results suggest that the micro textured PDMS surface can be a good approach to improve the close relation between the two cellular populations and their direct intercellular crosstalk and interactions, such as mechanical stretch and physical-chemical stimulations, in respect to standard culture conditions. Unfortunately, even if the spatial organization achieved using the bidimensional scaffolds was definitely better than standard plastic dishes, and the amount of AFS cells acquiring cardiomyocyte markers expression, was bigger than the one resulting from standard culture conditions, the difference was not so statistically significant.

As underlined by Potapova et al. [118], successful *ex vivo* cardiac stem cell therapy must also deal with the balance between achieving cardiomyocyte differentiated phenotype and maintaining cell proliferating ability, to deliver a great number of cells *in vivo*. As a matter of fact, fully *in vitro* cardiomyocyte differentiation of stem cells results in a heterogeneity electrical phenotype that can lead to life-threatening arrhythmias [119]. In this perspective, partial *in vitro* differentiation could be the right compromise before their *in vivo* delivery and complete functional transdifferentiation. Finally, we are aware that co-culture cannot be a suitable method to induce stem cell cardiomyocyte differentiation in clinical application, even if it represents the most similar approach to mimicking *in vitro* the physiological cardiac environment *in vivo*.

In our settings, we had previously demonstrated that cardiomyocyte-conditioned medium is not sufficient to induce AFS cells to express structural cardiac markers, both for human [94] and rat cells. A possible solution could be adopting different culture conditions using chemical stimulation, such as reported by Ventura C et al. [85], who demonstrated that a mixed ester of hyaluronan with butyric and retinoic acid can act as a novel cardiogenic/vasculogenic agent in human mesenchymal stem cells from bone marrow, dental pulp, and also from foetal membranes of term placenta.

In conclusion, for the *in vitro* part of this study, this work results are very encouraging and challenging, suggesting that these cells could have great potential. Further investigations are needed to analyze other differentiating approaches, more suitable than

co-culture method for clinical purposes. More studies are also mandatory to explore the feasibility of the PDMS scaffold as a substrate for human AFS seeding for cardiac tissue engineering and for their *in vivo* delivery and full differentiation.

2. In Vivo.

In these years stem cells have been broadly investigated as the privileged cellular source to be employed in cardiomyoplasty studies. The most suitable way of *in vivo* delivering has been widely studied as well: cells have been administered systematically, intracoronary, or directly injected into the myocardium [(33)].

In this part of the work we mainly focused on improving the cardiovascular conditions after an ischemic lesion using hAFS cells by two different approaches: the first one was about supporting cells engraftment and differentiation using tissue engineering techniques using a biodegradable collagen patch to the site of a chronic cardiac necrotizing cryoinjury; the second one was about analyzing the cardioprotective paracrine effect of the cells into an acute ischemic model by LAD ligation.

In the first part of this study we used the three dimensional collagen scaffold already characterised in Callegari et al. [(113)] and Radisic et al. [(16)] as a feasible tissue engineering support both *in vitro* and *in vivo.* Data from the previous *in vivo* work suggested that collagen scaffold not only can allow the growth and differentiation of cardiovascular cells *in vitro* but, implanted in the intact or cryoinjured rat heart *in vivo*, it can attract a marked neovascularization with formation of capillaries and arterioles. According to that, interesting new applications in the field of tissue engineering of cardiac injuries have been hypothesized for this biomaterial, possibly in association with growth factors and stem or precursor cells.

In this *in vivo* work, one of the hypothesis studied was, therefore, that in the ischemic cardiac scenario the insufficient perfusion and remodelled extracellular matrix environment can negatively influence the engraftment and cardiovascular differentiation of transplanted stem cells. In a purpose of cardiac repair, hAFS cells were delivered to the collagen scaffold 15 days after its application onto a cryoinjured heart of nude rats, when it was supposed to be already vascularised.

Furthermore, we analyzed two different aspects of the scaffold applied *in vivo*: its capability of sustain and improve engraftment of cells delivered by intramyocardial injection, providing a well vascularised cell reservoir (Model I) and its potential of attracting and homing to the injury site systemically injected stem cells (Model II).

As control for AFS cells we used both rat neonatal cardiomyocytes and cell suspension medium. In Model I, soon after the first time point, we could appreciate how hAFS cells were able to migrate from the injection site to the lesioned area in the heart, unlike neonatal cardiomyocyte that were found still as clusters of cells in the injection point in the scaffold. cmtmr^{+}hAFS cells were found very close to endothelial and smooth muscle cells, but not expressing any cardiovascular markers.

Regarding cellular distribution in both model, we noticed that cmtmr^{+}hAFS were easily detected in the heart tissue 24 hours after local injection, but then they dramatically decreased in number and they could only be seen as scattered cells. In both model, despite the administration route, cmtmr^{+}cells detected after 30 days were comparable: 9.27±4.12 cells/mm^2 in Model I and 6.49±2.62 cells/mm^2 in Model II, where, as expected, some cells were also found in the spleen.

Performing apoptag assay to analyze the amount of cells dead by apoptosis we didn't find any significant results, as all the cells positive for apoptotic staining were not expressing CMTMR, demonstrating that the mechanism behind cmtmr^{+} hAFS cells reduction could be a different one. It is also relevant to consider that in both the approaches described, a big amount of cells suspension might have been lost during injection, regarding the difficulties in evaluating the most appropriate area and depth where to inoculate cells in the in Model I and in injecting the cells systemically in Model II.

Comparing the neovascularisation of the scaffold, cryoinjury and viable myocardium area, after 15 and 30 days from hAFS cells local injection, we found that capillaries were more abundant after 30 days in patch and cryoinjury zone, whereas the amount of arterioles was not significantly different. This confirms the previous data found in [113], where new arterioles in the collagen scaffold strongly increased in number after 15 days to then reach a plateu and be stable up to 60 days.

In this work scattered cmtmr^{+}cells were found closely associated to new vessels in both cryoinjury and patch area: these results seem to prove that hAFS cells, even if not able

to differentiate into mature cardiomyocytes in this setting, can exert a positive effect evoking and substaining the local release of chemical signals acting in a paracrine manner on the surrounding ischemic tissue and mediating neoangiogenesis.

As a matter of fact, the *in vivo* paracrine effect possibly acted by stem cells has recently become one of the most suggested hypothesis to explain cardiovascular improvement by cell therapy after ischemic insults: the active role of injected stem cells can be related to the secretion of factors dealing with enhancement of angiogenesis and perfusion, control of matrix remodel and cardiomyocyte apoptosis [(33)]. Besides, looking at the number of macrophage cells found in the patch and cryoinjury areas, the ones containing CMTMR particles strongly increased during time, in particular after 30 days from cells injection. This aspect clearly demonstrated how CMTMR staining wasn't the most suitable approach to target the hAFS cells *in vivo* in this study.

We then repeated the immunostaining analyses using a more specific *in vivo* human cells marker, a human specific mitochondria antibody, already shown to be a reliable tracker to study the in vivo distribution of transplanted human cells [(92)]. Using this approach, we found a much bigger amount of hAFS cells *in vivo* and an interesting number of these co-staining for endothelial markers, as von Willebrand factor and smooth muscle α actin, in close relationship with host endothelial cells forming vessels, in both delivery models. It has been already showed that human amniotic fluid-derived stem cells cells can express these endothelial markers [(94)] in standard conditions, but, here, the relevant aspect is not only about the expression but more about the organization and interaction of the von Willebrand's factor- and smooth muscle actin-positive hAFS cells with the surrounding endothelial host cells, forming chimeric vessels. These vessels (capillaries and small arterioles) were composed of rat and human cells and are, hence, chimeric vascular structures with a variable number of human cells. Along with cells incorporated in the new vessels, some hAFS cells appeared dispersed as single cells or small clusters in between.

More relevant, the amount of new "chimeric" vessels formed by hAFS cells delivered by the two different approaches was comparable (chimeric capillaries were about 11,35±3,59 vessels/mm^2, in local hAFS cells injection and 14,19±5,23 vessels/mm^2, in systemic hAFS delivery, with no significant difference), demonstrating how the scaffold

was able to exert on stem cells injected both effects: support engraftment and homing to the cardiac injury site.

These data are in concordance with some other recent studies. Foetal stem cells, like mesenchymal stem cells from term placenta, have, indeed, been recently demonstrated to be suitable to face the uncomfortable environment of ischemic myocardium. Ventura and colleagues [85] reported that transplantation of human mesenchymal stem cells, from fetal membranes of term placenta, into infarcted rat hearts, was associated with increased capillary density, normalization of left ventricular function and significant decrease in scar tissue. Furthermore, regarding the efficiency of the use of the collagen scaffold, Simpson et al.[120] applied human mesenchymal stem cells, embedded in a "collagen cardiopatch", on the epicardial surface of infarcted rats with improvement in myocardial remodeling, but lost of cell detection at 4 weeks after patch application; Suuronen and colleagues [121] used peripheral blood progenitors cells, in combination of a collagen matrix, to be injected in the ischemic hind limb of athymic rats, resulting in incorporation into vascular structures, with the matrix itself also vascularized.

On the whole, the results obtained in this study demonstrate that hAFS cells can be more prone to differentiate into endothelial and smooth muscle cells than to cardiomyocytes *in vivo*: in our model, in fact, both local injection and systemic delivery of stem cells contribute to the formation of new chimeric capillaries and arterioles, but not of new myocardial tissue. This might be due to the fact that transplanted cells, which survived the immune attack from the host, did not find their way in the new oxygenated environment to start a cardiomyocyte committed program.

Even more, what was unexpected is that the amount of chimeric capillaries and arterioles, formed by hAFS cells delivered systemically and by intrapatch injection, were comparable: this is quite surprising, if considering that hAFS cells injected i.v. were in part sequestered in filter organs such as lung, liver and spleen. Probably cells injected in the patch were prone to be influenced by local paracrine factor from the lesion area, whereas cells delivered i.v. could have experienced a contact with circulation, able to influence their commitment for angiogenesis/arteriogenesis before they crossed the vessel wall and accumulated in the patch area to be then subsequentely incorporated, along with rat progenitor cells, in new capillaries and arterioles.

In conclusion, for this chronic study we showed that in a rat model of cardiac necrotizing lesion by cryoinjury, there is no significative difference in local and systemic cell transplantation of hAFS cells to tissue engineered vascularized collagen scaffold. Our final goal, in this model now, is to implement the systemic cell delivery approach since it seems to be the more functional alternative to the invasive cardiac surgery in clinical settings.

In the second part of the *in vivo* work we analyzed the injection of hAFS cells in a rat model of acute cardiac ischemia by 30 minutes left ascending coronary ligation followed by 2 hours reperfusion. Since the application of freshly isolated rat bone marrow derived mononuclear cells in this model have showed very encouraging results in decreasing infarct size from 53.9 ± 2.3 % to 39.3 ± 0.2% of the ischemic area *(data not shown and published yet, by Lythgoe M and Cheung K, UCL, London)*, we tested hAFS cells injection as well.

For meseauring the infarct area we use a planimetry method previously shown for myocardial infarct size quantification [122].

At the beginning we employed gfp^+rAFS cells, injected i.v. via the cannulated external jugular vein as 10^7cells/animal dose, but all the treated rats died of pulmonary embolism because of the cell size and stickiness. We decreased the dosage to 10^6cells/animal and about 66% rats survived, but with no statistically significant infarct size reduction, compared to PBS injected control group.

We then analyzed hAFS cells, at first, with 10^7 cells/animal dosage, we experienced the same problems as before, with more than 50% of rats dying because of the big amount of cells injected i.v. So we tried half the dose, $5x10^6$ cells/animal, and 75% of the rats survived with an appreciable, statistically significant, decrease of the infarct size from 53,9±2,3%, obtained with PBS injection, to 40.0±3.0% of the ischemic region. This result was really surprisingly encouraging. Moreover, for these experiments we used *in vitro* expanded hAFS cells, previously cryopreserved: these data all together seem to support the idea that hAFS cells could be a very promising and useful cell source for clinical applications.

When we analyzed, soon after 2 hours reperfusion, heart, lungs, liver and spleen specimens to study the *in vivo* hAFS cells distribution, we found that most of the

injected cells were trapped in the lungs and spleen, as expected. What we did not expected was to found a reasonable amount of cells even in the myocardium, after such a short time. The most reasonable explanation could deal with the hAFS cells size and their propensity in being sequestred by the host tissue. Besides, most of the hAFS cells found in the heart were expressing von Willebrand factor and smooth muscle α actin, markers expressed also in standard condition by these cells [(94)]: the remarkable aspect is that these cells were found organized in circular "vessel-like" structure, alone or near/participating pre-existing capillaries.

On the whole, such a result about the reduction of the infarct size (about 14% smaller in the hAFS cels treated rats compared to the control ones) was quite surprisingly, considering that it has been obtained after only 2 hours from subministration. This result, achieved in such a little short time, could be only due to a stem cell-mediated paracrine effect, as already mentioned before.

As previously remarked, three different hypothesis have been suggested to explain *in vivo* improvement after stem cell injection, so far: creation of a milieu that enhances regeneration of endogenous cells by releasing paracrine factors, transdifferentiation, and perhaps cell fusion [(123)].

If in the past years the most acclaimed hypothesis were about engraftment and differentiation/fusion of stem cells with resident cells from the host cardiac tissue, recently the cardiac improvement, usually seen in the ischemic heart after *in vivo* delivery, has been more strongly suggested to be due to the secretion of angiogenic, anti-inflammatory and cardioprotective factors from the cells transplanted, via paracrine signalling,. Lately, indeed, it has become evident that the beneficial effect of cell transplantation on ventricular function and myocardial perfusion is in large part mediated through paracrine effects on the host myocardium: paracrine effects of the donor cells include but are not limited to angiogenesis, mobilization of both circulating and bone-marrow-derived stem cells, activation of cardiac-resident stem cells, and stabilization of the extracellular matrix. [(124)].

Furthermore, recent reports have also demonstrated both *in vitro* and *in vivo* stem cells-mediated paracrine effect on cardiac resident cells: Nakanishi et al.[(125)] showed in fact that mesenchymal stem cells-derived conditioned medium was able to exert protective effects on cardiac progenitor cells and enhanced their migration and differentiation,

inhibiting their apoptosis, induced by hypoxia and serum starvation, whereas Li and colleagues [126] analyzed the paracrine action of mesenchymal stem cells in a rat model of global heart failure, where cell transplantation significantly improved heart function, decreased collagen volume fraction and increased expression of adrenomedullin, an antifibrotic factor in myocardium.

More similar to our acute *in vivo* approach, Schwarting et al. [127] also reported that Lin(-)-HSCs, systemically applied to an acute mouse model of cerebral stroke, obtained by a 45-minute transient cerebral ischemia, and analyzed 24 hours after, reduced infarct volumes, cerebral postischemic inflammation, attenuate peripheral immune activation and mediate neuroprotection.

To validate the *in vivo* paracrine hypothesis on the basis of the results from this work, we further analyzed if hAFS cells were able to secrete thymosin β4 in the culture medium. As recently highlighted by Smart et al. [128] and Srivastava and colleagues [129], this protein is a potent stimulator of coronary vasculogenesis and angiogenesis, promoting cardiomyocyte and endothelial migration, survival and possibly sustaining neovascularization, following cardiac injury. More in details, Hinkel et al. [130] investigated the role of thymosin β4 as a mediator of *in vitro* and *in vivo* embryonic endothelial precursors cell-mediated cardioprotection, reporting that short-term effect from embryonic endothelial precursos cells, can be attributed, at least in part, to this protein.

The ELISA assay performed on the conditioned medium of both gfp^{+}rAFS and hAFS stem cells confirmed that thymosin β4 is actively secreted by these cells, in particular by the human ones, supporting the hypothesis of a cell-mediated paracrine action *in vivo* as possible explanation for the infarct size decrease we have seen.

Therefore, we speculated if hAFS cells could contain a subset of cardiac progenitors as amiotic fluid is well known to contain different progenitors, mainly with mesenchymal characteristics [88, 105].

As we have been previously demonstrated that hAFS cells are able to express mRNA for the early cardiac transcription factors Nkx 2.5 and Gata4 in control conditions [94], here we further performed RT-PCR to characterize more in details a possible subpopulation of early cardiac progenitors, identified by the molecular signature of Isl1 and Kdr, as reported before by Laugwitz et al. [131] and Yang et al. [132]. hAFS cells

indeed express all these markers, suggesting they can contain therefore cardiac progenitor cells able to exert paracrine effect *in vivo*.

3. Conclusions.

In conclusions, in this work it has been demonstrated the cardiomyogenic potential of the Amniotic Fluid Stem cells *in vitro* and *in vivo*. The results achieved are very encouraging and challenging, suggesting that these cells have a cardiovascular differentiation potential that has to be triggered under specific conditions.
Moreover, these cells showed to be able to acquire a functional "cardiac pacemaker-like" phenotype *in vitro* and could grow with a well defined organization on micro textured bidimensional scaffold, which can be employed as *in vivo* delivery system or as biocompatible scaffold for engineering tissues.
In vivo, AFS cells were demonstrated to be more prone to differentiate into vascular cells than into cardiac muscle as they were able to correlate with the pre-existing host vessels, enhancing angiogenesis and vasculogenesis by chimeric vessels formation in a cardiac cryoinjury model and exerted paracrine cardioprotective effects in an acute ischemia/reperfusion scenario.
According to these observations and considering also that amniotic fluid can represent an easily to collect, accessible advantageous autologous source of immature pluripotent stem cells, AFS cells have a promising great potential as stem source for the repair of paediatric congenital cardiovascular diseases. In paediatric cardiology, indeed, congenital heart malformations often require surgery soon after birth, so it would be very useful finding a suitable source of foetal progenitors to engineer autologous cardiovascular tissues *in vitro,* during pregnancy, using biocompatible scaffold, to be then transplanted when needed.

References.

1. Kaihara S, Vacanti JP. Tissue engineering: toward new solutions for transplantation and reconstructive surgery. Arch Surg. 1999;134:1184-8.

2. Atala A. Engineering tissues, organs and cells. J Tissue Eng Regen Med 2007; 1:83–96.

3. Wu KH, Mo XM, Liu YL, Zhang YS, Han ZC. Stem cells for tissue engineering of myocardial constructs. Ageing Res Rev. 2007;6:289-301.

4. Shinoka T, Ma PX, Shum-Tim D, et al. Tissue-engineered heart valves. Autologous valve leaflet replacement study in a lamb model. Circulation. 1996;94:II164-8.

5. Zimmermann WH, Fink C, Kralisch D, et al. Three-dimensional engineered heart tissue from neonatal rat cardiac myocytes. Biotechnol Bioeng. 2000;68:106-14.

6. Jawad H, Ali NN, Lyon AR, et al. Myocardial tissue engineering: a review. J Tissue Eng Regen Med. 2007;1:327-42.

7. Mirensky TL, Breuer CK. The development of tissue-engineered grafts for reconstructive cardiothoracic surgical applications. Pediatr Res. 2008;63:559-68.

8. Di Eusanio M, Schepens MA. Left atrial thrombus on a Teflon patch for ASD closure. Eur J Cardiothorac Surg. 2002; 21(3):542.

9. Zimmermann WH, Melnychenko I, Wasmeier G, et al. Engineered heart tissue grafts improve systolic and diastolic function in infarcted rat hearts. Nat Med. 2006;12:452-8.

10. Vandenburgh HH, Karlisch P, Farr L. Maintenance of highly contractile tissue-cultured avian skeletal myotubes in collagen gel. In Vitro Cell Dev Biol. 1988;24(3):166-74.

11. Eschenhagen T, Fink C, Remmers U, Scholz H, et al. Three-dimensional reconstitution of embryonic cardiomyocytes in a collagen matrix: a new heart muscle model system. FASEB J. 1997;11(8):683-94.

12. Li RK, Jia ZQ, Weisel RD, et al. Survival and function of bioengineered cardiac grafts.Circulation. 1999;100(19 Suppl):II63-9.

13. Zimmermann WH, Schneiderbanger K, Schubert P, et al. Tissue engineering of a differentiated cardiac muscle construct. Circ Res. 2002;90(2):223-30.

14. Shimizu T, Yamato M, Isoi Y, et al. Fabrication of pulsatile cardiac tissue grafts using a novel 3-dimensional cell sheet manipulation technique and temperature-responsive cell culture surfaces. Circ Res. 2002;90(3):e40.

15. Hobo K, Shimizu T, Sekine H, et al. Therapeutic angiogenesis using tissue engineered human smooth muscle cell sheets. Arterioscler Thromb Vasc Biol. 2008 Apr;28(4):637-43.

16. Radisic M, Park H, Shing H, et al. Functional assembly of engineered myocardium by electrical stimulation of cardiac myocytes cultured on scaffolds. Proc Natl Acad Sci U S A. 2004;101:18129-34.

17. Polak JM, Mantalaris S. Stem cells bioprocessing: an important milestone to move regenerative medicine research into the clinical arena. Pediatr Res. 2008;63:461-6.

18. Laflamme MA, Murry CE. Regenerating the heart. Nat Biotechnol. 2005;23:845-56.

19. Cebotari S, Lichtenberg A, Tudorache I, et al. Clinical application of tissue engineered human heart valves using autologous progenitor cells. Circulation. 2006;114(1 Suppl):I132-7.

20. Flanagan TC, Cornelissen C, Koch S, et al. The in vitro development of autologous fibrin-based tissue-engineered heart valves through optimised dynamic conditioning. Biomaterials. 2007;28(23):3388-97.

21. Hahn MS, McHale MK, Wang E, Schmedlen RH, West JL. Physiologic pulsatile flow bioreactor conditioning of poly(ethylene glycol)-based tissue engineered vascular grafts. Ann Biomed Eng. 2007;35(2):190-200.

22. Gonen-Wadmany M, Gepstein L, Seliktar D. Controlling the cellular organization of tissue-engineered cardiac constructs.N Y Acad Sci. 2004;1015:299-311.

23. Yang C, Sodian R, Fu P, et al. In vitro fabrication of a tissue engineered human cardiovascular patch for future use in cardiovascular surgery. Ann Thorac Surg. 2006;81(1):57-63.

24. Fromstein JD, Zandstra PW, Alperin C et al. Seeding bioreactor-produced embryonic stem cell-derived cardiomyocytes on different porous, degradable, polyurethane scaffolds reveals the effect of scaffold architecture on cell morphology. Tissue Eng Part A. 2008;14(3):369-78.

25. Zimmermann WH, Didié M, Döker S, et al. Heart muscle engineering: an update on cardiac muscle replacement therapy. Cardiovasc Res. 2006;71:419-29.

26. Shimizu T, Sekine H, Isoi Y, et al. Long-term survival and growth of pulsatile myocardial tissue grafts engineered by the layering of cardiomyocyte sheets. Tissue Eng. 2006;12:499-507.

27. Wu KH, Mo XM, Liu YL, Zhang YS, Han ZC. Stem cells for tissue engineering of myocardial constructs. Ageing Res Rev. 2007;6:289-301.

28. Pasumarthi KB, Field LJ. Cardiomyocyte cell cycle regulation. Circ Res. 2002;90:1044-54.

29. Harada M, Itoh H, Nakagawa O, et al. Significance of ventricular myocytes and nonmyocytes interaction during cardiocyte hypertrophy: evidence for endothelin-1 as a paracrine hypertrophic factor from cardiac nonmyocytes. Circulation. 1997;96:3737-44.

30. Verfaillie CM. Adult stem cells: assessing the case for pluripotency. Trends Cell Biol. 2002 Nov;12(11):502-8.

31. Segers VF, Lee RT. Stem-cell therapy for cardiac disease. Nature. 2008;451(7181):937-42.

32. Nakanishi C, Yamagishi M, Yamahara K, et al. Activation of cardiac progenitor cells through paracrine effects of mesenchymal stem cells. Biochem Biophys Res Commun. 2008; 374:11-6.

33. Beeres SL, Atsma DE, van Ramshorst J, Schalij MJ, Bax JJ. Cell therapy for ischaemic heart disease. Heart. 2008; 94(9):1214-26.

34. Martin GR. Isolation of a pluripotent cell line from early mouse embryos cultured in medium conditioned by teratocarcinoma stem cells. Proc Natl Acad Sci U S A. 1981;78:7634-8.

35. Mummery C, Ward D, van den Brink CE, Bird SD, Doevendans PA, Opthof T, Brutel de la Riviere A, Tertoolen L, van der Heyden M, Pera M. Cardiomyocyte differentiation of mouse and human embryonic stem cells. J Anat. 2002;200:233-42.

36. Kofidis T, de Bruin JL, Hoyt G, et al. Myocardial restoration with embryonic stem cell bioartificial tissue transplantation. J Heart Lung Transplant. 2005;24:737-44.

37. Caspi O, Lesman A, Basevitch Y, Gepstein A, Arbel G, Habib IH, Gepstein L, Levenberg S. Tissue engineering of vascularized cardiac muscle from human embryonic stem cells. Circ Res. 2007;100:263-72.

38. Gepstein L. Experimental molecular and stem cell therapies in cardiac electrophysiology. Ann N Y Acad Sci. 2008 Mar;1123:224-31.

39. De Coppi P, Pozzobon M, Piccoli M et al. Isolation of mesenchymal stem cells from human vermiform appendix. J Surg Res. 2006 Sep;135(1):85-91.

40. Mathur A., Martin JF. Stem Cell And Repair Of The Heart. Lancet. 364, 183, 2004.

41. Fukuda K. Use of adult marrow mesenchymal stem cells for regeneration of cardiomyocytes. Bone Marrow Transplant. 2003;32 Suppl 1:S25-7.

42. Rangappa S, Fen C, Lee EH, et al. Transformation of adult mesenchymal stem cells isolated from the fatty tissue into cardiomyocytes. Ann Thorac Surg. 2003;75(3):775-9.

43. Takahashi T, Lord B, Schulze PC, et al. Ascorbic acid enhances differentiation of embryonic stem cells into cardiac myocytes. Circulation. 2003; 107(14):1912-6.

44. Mummery C, Ward-van Oostwaard D, Doevendans P, et al. Differentiation of human embryonic stem cells to cardiomyocytes: role of coculture with visceral endoderm-like cells. Circulation. 2003;107(21):2733-40.

45. Condorelli G, Borello U, DeAngelis L, et al. Cardiomyocytes induce endothelial cells to trans-differentiate into cardiac muscle: implications for myocardium regeneration. Proc Natl Acad Sci USA. 2001; 98(19):10733-8.

46. Muller-Borer BJ, Cascio WE, Anderson PA et al. Adult-derived liver stem cells acquire a cardiomyocyte structural and functional phenotype ex vivo. Am J Pathol. 2004; 165(1):135-45.

47. Muller-Borer BJ, Cascio WE, Esch GL et al. Acquired Cell-to-Cell Coupling and "Cardiac-Like" Calcium Oscillations in Adult Stem Cells in a Cardiomyocyte Microenvironment. Conf Proc IEEE Eng Med Biol Soc. 2006; 1:576-9.

48. Nishiyama N, Miyoshi S, Hida N et al The significant cardiomyogenic potential of human umbilical cord blood-derived mesenchymal stem cells in vitro. Stem Cells. 2007; (8):2017-24.

49. Liao R, Pfister O, Jain M, Mouquet F. The bone marrow-cardiac axis of myocardial regeneration. Prog Cardiovasc Dis. 2007;50(1):18-30.

50. Knight RL, Booth C, Wilcox HE, Fisher J, Ingham E.J Tissue engineering of cardiac valves: re-seeding of acellular porcine aortic valve matrices with human mesenchymal progenitor cells.Heart Valve Dis. 2005;14:806-13.

51. Bin F, Yinglong L, Nin X, et al. Construction of tissue-engineered homograft bioprosthetic heart valves in vitro. ASAIO J. 2006;52:303-9.

52. Xiang Z, Liao R, Kelly MS, Spector M. Collagen-GAG scaffolds grafted onto myocardial infarcts in a rat model: a delivery vehicle for mesenchymal stem cells. Tissue Eng. 2006 ;12:2467-78.

53. Vincentelli A, Wautot F, Juthier F, et al. In vivo autologous recellularization of a tissue-engineered heart valve: are bone marrow mesenchymal stem cells the best candidates? J Thorac Cardiovasc Surg. 2007;134:424-32.

54. Ohnishi S, Yanagawa B, Tanaka K, et al. Transplantation of mesenchymal stem cells attenuates myocardial injury and dysfunction in a rat model of acute myocarditis. J Mol Cell Cardiol. 2007;42:88-97.

55. Dawn B, Tiwari S, Kucia MJ, et al. Transplantation of bone marrow-derived very small embryonic-like stem cells attenuates left ventricular dysfunction and remodeling after myocardial infarction. Stem Cells. 2008;26:1646-55.

56. Gong Z, Niklason LE. Small-diameter human vessel wall engineered from bone marrow-derived mesenchymal stem cells (hMSCs). FASEB J. 2008;22:1635-48.

57. Eisen HJ. Skeletal myoblast transplantation: no MAGIC bullet for ischemic cardiomyopathy. Nat Clin Pract Cardiovasc Med. 2008 . [Epub ahead of print]

58. Memon IA, Sawa Y, Fukushima N, Matsumiya G, et al. Repair of impaired myocardium by means of implantation of engineered autologous myoblast sheets. J Thorac Cardiovasc Surg. 2005;130:1333-41.

59. Siepe M, Giraud MN, Pavlovic M, et al. Myoblast-seeded biodegradable scaffolds to prevent post-myocardial infarction evolution toward heart failure. J Thorac Cardiovasc Surg. 2006;132:124-31.

60. Siepe M, Giraud MN, Liljensten E, et al. Construction of skeletal myoblast-based polyurethane scaffolds for myocardial repair. Artif Organs. 2007;31:425-33.

61. Ye L, Haider HK, Tan R, et al. Angiomyogenesis using liposome based vascular endothelial growth factor-165 transfection with skeletal myoblast for cardiac repair. Biomaterials. 2008;29:2125-37.

62. De Coppi P, Delo D, Farrugia L, et al. Angiogenic gene-modified muscle cells for enhancement of tissue formation. Tissue Eng. 2005 Jul-Aug;11(7-8):1034-44.

63. Bianco P, Riminucci M, Gronthos S, Robey PG. Bone marrow stromal stem cells: nature, biology, and potential applications. Stem Cells. 2001;19:180-92.

64. Pittenger MF, Mackay AM, Beck SC, et al. Multilineage potential of adult human mesenchymal stem cells. Science. 1999; 284(5411):143-7.

65. Guan K, Wagner S, Undold B, et al. Generation of Functional Cardiomyocytes From Adult Mouse Spermatogonial Stem Cells. Circ Res 2007; 100:1615-25.

66. Mardanpour P, Guan K, Nolte J, et al. Potency of germ cells and its relevance for regenerative medicine. J Anat. 2008;213(1):26-9.

67. Takahashi K, Okita K, Nakagawa M, Yamanaka S. Induction of pluripotent stem cells from fibroblast cultures. Nat Protoc. 2007;2:3081-9.

68. Okita K, Ichisaka T, Yamanaka S. Generation of germline-competent induced pluripotent stem cells. Nature. 2007;448:313-7.

69. Wernig M et al. *In Vitro* reprogramming of fibroblasts into pluripotent ES-cell-like state. Nature 2007; 448: 318-324.

70. Maherali N. et al. Directly reprogrammed fibroblasts show epigenetic remodelling and widespread tissue contribution. Cell Stem Cell 2007; 1: 55-70.

71. Lowry WE et al. Generation of human induced pluripotent stem cells from dermal fibroblasts. PNAS 2008; 105:2883-2888.

72. Narazaki G, Uosaki H, Teranishi M et al. Directed and Systematic Differentiation of Cardiovascular Cells From Mouse Induced Pluripotent Stem Cells. Circulation 2008; 118: 498-506.

73. Mauritz C, Schwanke K, Reppel M, et al. Generation of functional murine cardiac myocytes from induced pluripotent stem cells.Circulation. 2008;118:507-17.

74. Nishikawa S, Goldstein RA, Nierras CR. The promise of human induced pluripotent stem cells for research and therapy. Nat Rev Mol Cell Biol 2008. [Epub ahead of print]

75. Kadner A, Hoerstrup SP, Tracy J, et al. Human umbilical cord cells: a new cell source for cardiovascular tissue engineering. Ann Thorac Surg. 2002;74:S1422-8.

76. Schmidt D, Breymann C, Weber A, et al. Umbilical cord blood derived endothelial progenitor cells for tissue engineering of vascular grafts. Ann Thorac Surg. 2004;78(6):2094-8.

77. Yen BL, Huang HI, Chien CC, et al. Isolation of multipotent cells from human term placenta. Stem Cells. 2005;23:3-9.

78. Miao Z, Jin J, Chen L, Zhu J, et al. Isolation of mesenchymal stem cells from human placenta: comparison with human bone marrow mesenchymal stem cells. Cell Biol Int. 2006; 30: 681-7.

79. Chan J, Kennea NL, Fisk NM. Placental mesenchymal stem cells. Am J Obstet Gynecol. 2007;196(2):e18.

80. Moise KJ Jr. Umbilical cord stem cells. Obstet Gynecol. 2005;106:1393-407.

81. Kadner A, Hoerstrup SP, Tracy J, et al. Human umbilical cord cells: a new cell source for cardiovascular tissue engineering. Ann Thorac Surg. 2002;74:S1422-8.

82. Schmidt D, Breymann C, Weber A, et al. Umbilical cord blood derived endothelial progenitor cells for tissue engineering of vascular grafts. Ann Thorac Surg. 2004;78(6):2094-8.

83. Schmidt D, Mol A, Neuenschwander S, et al. Living patches engineered from human umbilical cord derived fibroblasts and endothelial progenitor cells. Eur J Cardiothorac Surg. 2005;27(5):795-800.

84. Fang NT, Xie SZ, Wang SM, et al. Construction of tissue-engineered heart valves by using decellularized scaffolds and endothelial progenitor cells. Chin Med J (Engl). 2007;120(8):696-702.

85. Ventura C, Cantoni S, Bianchi F, et al. Hyaluronan mixed esters of butyric and retinoic Acid drive cardiac and endothelial fate in term placenta human mesenchymal stem cells and enhance cardiac repair in infarcted rat hearts. J Biol Chem. 2007;282:14243-52.

86. Okamoto K, Miyoshi S, Toyoda M, et al. 'Working' cardiomyocytes exhibiting plateau action potentials from human placenta-derived extraembryonic mesodermal cells. Exp Cell Res. 2007; 313: 2550-62.

87. In 't Anker PS, Scherjon SA, Kleijburg-van der Keur C, et al. Amniotic fluid as a novel source of mesenchymal stem cells for therapeutic transplantation. Blood. 2003;102(4):1548-9.

88. Prusa AR, Marton E, Rosner M, Bernaschek G, Hengstschläger M. Oct-4-expressing cells in human amniotic fluid: a new source for stem cell research? Hum Reprod. 2003;18(7):1489-93.

89. Kaviani A, Perry TE, Dzakovic A, et al. The amniotic fluid as a source of cells for fetal tissue engineering. J Pediatr Surg. 2001;36(11):1662-5.

90. Kaviani A, Guleserian K, Perry TE,et al. Foetal tissue engineering from amniotic fluid. J Am Coll Surg. 2003;196:592-7.

91. De Coppi P, Callegari A, Chiavegato A, et al. Amniotic fluid and bone marrow derived mesenchymal stem cells can be converted to smooth muscle cells in the cryo-injured rat bladder and prevent compensatory hypertrophy of surviving smooth muscle cells. J Urol. 2007;177(1):369-76.

92. De Coppi P, Bartsch G Jr, Siddiqui MM, et al. Isolation of amniotic stem cell lines with potential for therapy. Nat Biotechnol. 2007;25(1):100-6.

93. Trounson A. A fluid means of stem cell generation. Nat Biotechnol. 2007; 25(1):62-3.

94. Chiavegato A, Bollini S, Pozzobon M, et al. Human amniotic fluid-derived stem cells are rejected after transplantation in the myocardium of normal, ischemic, immuno-suppressed or immuno-deficient rat. J Mol Cell Cardiol 2007;42(4):746-59.

95. Zhao P, Ise H, Hongo M, et al. Human amniotic mesenchymal cells have some characteristics of cardiomyocytes. Transplantation. 2005;79(5):528-35.

96. Schmidt D, Achermann J, Odermatt B, et al. Prenatally fabricated autologous human living heart valves based on amniotic fluid derived progenitor cells as single cell source. Circulation. 2007;116(11 Suppl):I64-70.

97. Shmelkov SV, Meeus S, Moussazadeh N, et al. Cytokine preconditioning promotes codifferentiation of human fetal liver CD133+ stem cells into angiomyogenic tissue. Circulation 2005; 111(9):1175-83.

98. Perin L, Sedrakyan S, Da Sacco S, De Filippo R. Characterization of human amniotic fluid stem cells and their pluripotential capability. Methods Cell Biol. 2008;86:85-99.

99. Perin L, Giuliani S, Sedrakyan S, DA Sacco S, De Filippo RE. Stem cell and regenerative science applications in the development of bioengineering of renal tissue. Pediatr Res. 2008 May;63(5):467-71.

100. Simantov R. Amniotic stem cell international. Reprod Biomed Online. 2008 Apr;16(4):597-8.

101. Delo D, Olson J, Baptista P, et al. Non-invasive longitudinal tracking of human amniotic fluid stem cells in the mouse heart. Stem Cells Dev. 2008. [Epub ahead of print]

102. Sessarego N, Parodi A, Podestà M, et al. Multipotent mesenchymal stromal cells from amniotic fluid: solid perspectives for clinical application. Haematologica. 2008;93:339-46.

103. Steigman SA, Armant M, Bayer-Zwirello L, et al .Preclinical regulatory validation of a 3-stage amniotic mesenchymal stem cell manufacturing protocol. J Pediatr Surg. 2008;43(6):1164-9.

104. Kunisaki SM, Armant M, Kao GS, et al. Tissue engineering from human mesenchymal amniocytes: a prelude to clinical trials. J Pediatr Surg. 2007;42(6):974-9.

105. Fauza D.O. Amniotic fluid and placental stem cells. Best Practice and Research Clinical Obstet and Gynaecol. 2004; 18(6): 877-891.

106. Kaushal S, Amiel GE, Guleserian KJ, et al. Functional small-diameter neovessels created using endothelial progenitor cells expanded ex vivo. Nat Med. 2001;7(9):1035-40.

107. Wilcox HE, Korossis SA, Booth C, et al Biocompatibility and recellularization potential of an acellular porcine heart valve matrix. J Heart Valve Dis. 2005;14(2):228-36.

108. Mol A, Rutten MC, Driessen NJ, et al. Autologous human tissue-engineered heart valves: prospects for systemic application. Circulation. 2006;114(1 Suppl):I152-8.

109. Ott HC, Matthiesen TS, Goh SK, et al. Perfusion-decellularized matrix: using nature's platform to engineer a bioartificial heart. Nat Med. 2008;14:213-21.

110. Landa N, Miller L, Feinberg MS, et al. Effect of injectable alginate implant on cardiac remodeling and function after recent and old infarcts in rat. Circulation. 2008;117:1388-96.

111. Fuchs JR, Nasseri BA, Vacanti JP, Fauza DO. Postnatal myocardial augmentation with skeletal myoblast-based fetal tissue engineering. Surgery. 2006 ;140:100-7.

112. Au P, Tam J, Fukumura D, Jain RK. Bone marrow-derived mesenchymal stem cells facilitate engineering of long-lasting functional vasculature. Blood. 2008 May 1;111(9):4551-8.

113. Callegari A, Bollini S, Iop L, et al. Neovascularization induced by porous collagen scaffold implanted on intact and cryoinjured rat hearts. Biomaterials. 2007;28:5449-6.

114. Cimetta E, Pizzato S, Bollini S, et al. Production of arrays of cardiac and skeletal muscle myofibers by micropatterning techniques on a soft substrate.
Biomed Microdevices. 2008. [Epub ahead of print]

115. Au HT, Cheng I, Chowdhury MF et al. Interactive effects of surface topography and pulsate electrical field stimulation on orientation and elongation of fibroblasts and cardiomyocytes. Biomaterials. 2007;28(29):4277-93.

116. Motlagh D, Hartman TJ, Desai TA, Russell B. Micro fabricated grooves recapitulate neonatal myocyte connexion 43 and N-cadherin expression and localization. J Biomed Mater Res A. 2003;67(1):148-57.

117. Motlagh D, Senyo SE, Desai TA, Russell B. Micro textured substrata alter gene expression, protein localization and the shape of cardiac myocytes. Biomaterials. 2003;24(14):2463-76.

118. Potapova IA., Doronin SV., Kelly DJ., Rosen AB., et al. Replacing damaged myocardium. J Electrocardiol. 2007;40(6 Suppl):S199-201.

119. Cohen IS, Rosen AB, Gaudette GR. A caveat emptor for myocardial regeneration: mechanical without electrical recovery will not suffice. J Mol Cell Cardiol. 2007;42(2):285-8.

120. Simpson D, Liu H, Fan TH, Nerem R, Dudley SC Jr. A tissue engineering approach to progenitor cell delivery results in significant cell engraftment and improved myocardial remodeling. Stem Cells. 2007;25(9):2350-7.

121. Suuronen EJ, Veinot JP, Wong S, et al. Tissue-engineered injectable collagen-based matrices for improved cell delivery and vascularization of ischemic tissue using CD133+ progenitors expanded from the peripheral blood. Circulation. 2006;114(1 Suppl):I138-44.

122. Fishbein MC, Meerbaum S, Rit J, et al. Early phase acute myocardial infarct size quantification: validation of the triphenyl tetrazolium chloride tissue enzyme staining technique. Am Heart J. 1981;101(5):593-600.

123. Prockop DJ. "Stemness" does not explain the repair of many tissues by mesenchymal stem/multipotent stromal cells (MSCs). Clin Pharmacol Ther. 2007;82(3):241-3.

124. Cheng AS, Yau TM. Paracrine effects of cell transplantation: strategies to augment the efficacy of cell therapies. Semin Thorac Cardiovasc Surg. 2008; 20(2):94-101.

125. Nakanishi C, Yamagishi M, Yamahara K, et al. Activation of cardiac progenitor cells through paracrine effects of mesenchymal stem cells. Biochem Biophys Res Commun. 2008 12;374(1):11-6.

126. Li L, Zhang S, Zhang Y, et al. Paracrine action mediate the antifibrotic effect of transplanted mesenchymal stem cells in a rat model of global heart failure. Mol Biol Rep. 2008.

127. Schwarting S, Litwak S, Hao W, et al. Hematopoietic stem cells reduce postischemic inflammation and ameliorate ischemic brain injury. Stroke. 2008;39(10):2867-75.

128. Smart N, Risebro CA, Melville AA, et al. Thymosin □4 induces adult epicardial progenitor mobilization and neovascularization. Nature 2007 11;445(7124):177-82.

129. Srivastava D, Saxena A, Michael Dimaio J and Bock-Marquette I. Thymosin beta4 is cardioprotective after myocardial infarction. Ann N Y Acad Sci. 2007;1112:161-70.

130. Hinkel R, El-Aouni C, Olson T, et al. Thymosin beta4 is an essential paracrine factor of embryonic endothelial progenitor cell-mediated cardioprotection. Circulation. 2008; 29;117(17):2232-40.

131. Laugwitz KL, Moretti A, Caron L, Nakano A, Chien KR. Islet1 cardiovascular progenitors: a single source for heart lineages? Development. 2008;135(2):193-205.

132. Yang L, Soonpaa MH, Adler ED, et al. Human cardiovascular progenitor cells develop from a KDR^{+} embryonic-stem-cell-derived population. Nature. 2008;453(7194):524-8.

Appendix: Publications and Abstracts.

1. Publications.

Cimetta E, Pizzato S, **Bollini S**, Serena E, De Coppi P, Nelvassore N.
Production of arrays of cardiac and skeletal muscle myofibers by micropatterning techniques on a soft substrate.
Biomed Microdevices. 2008 Nov 6. [Epub ahead of print], i.f 3.073.

Iop L, Chiavegato A, Callegari A, **Bollini S**, Piccoli M, Pozzobon M, Rossi CA, Calamelli S, Chiavegato D, Gerosa G, De Coppi P, Sartore S.
Different cardiovascular potential of adult- and fetal-type mesenchymal stem cells in a rat model of heart cryoinjury.
Cell Transplantation. 2008;17(6):679-94, i.f. 3.871.

Pozzobon M, Piccoli M, Ditadi A, **Bollini S**, Destro R, André-Schmutz I, Masiero L, Lenzini E, Zanesco L, Petrelli L, Cavazzana-Calvo M, Gazzola MV, De Coppi P.
Mesenchymal stromal cells can be derived from bone marrow CD133+ cells: implications for therapy.
Stem Cell and Development. 2008 Jul 3. [Epub ahead of print], i.f. 3.224.

Callegari A, **Bollini S,** Iop L, Chiavegato A, Torregrossa G, Pozzobon M, Gerosa G, De Coppi P, Elvassore N, Sartore S.
Neovascularization induced by porous collagen scaffold implanted on intact and cryoinjured rat hearts.
Biomaterials. 2007; 28(36):5449-61, i.f.: 6.262.

Chiavegato A, **Bollini S**, Pozzobon M, Callegari A, Gasparotto L, Taiani J, Piccoli M, Lenzini E, Gerosa G, Vendramin I, Cozzi E, Angelini A, Iop L, Zanon GF, Atala A, De Coppi P, Sartore S.
Human amniotic fluid-derived stem cells are rejected after transplantation in the myocardium of normal, ischemic, immuno-suppressed or immuno-deficient rat.
Journal of Molecular and Cell Cardiology. 2007; 42(4):746-59, i.f. 5.246.

2. Abstracts.

CHEUNG K, DONG X, **BOLLINI S**, YATES M, LEHTOLAINEN P, MATHUR A, MARTIN J, DE COPPI P, LYTHGOE M.
"Effect of Various Cell Types Administered During Early Reperfusion Following MI in the Rat".
Oral presentation by Bollini S. e Cheung K. at the "UK Cardiovascular Collaborative meeting on Stem Cell Repair" meeting. September 15th 2008, University College of London, London, UK.

BOLLINI S, POZZOBON M, CHEUNG K, DONG X, FIGALLO E, PICCOLI M, GIULIANI S,
CALLEGARI A, SARTORE S, LYTHGOE M, ELVASSORE N, DE COPPI P.
"Amniotic Fluid Stem Cells Potential for Cardiac Regeneration."
Poster presentation at the UCL Cardiovascular Science and Medicine Day meeting, June 12th 2008. Institute of Child Health University College of London, London, UK

PICCOLI M, GRISAFI D, POZZOBON M, **BOLLINI S**, ZARAMELLA P, ZANON GF, CHIANDETTI L, SCARPA M, DE COPPI P AND TOMANIN R.
"High transduction efficiency of human amniotic fluid stem cells mediated by adenovirus vectors."
Poster presentation at the 5th ISSCR Annual Meeting June 17th-20th 2007 Cairns, Queensland, Australia.

BOLLINI S, FIGALLO E, PIZZATO S, POZZOBON M, ZANON GF, GAMBA PG, ZANESCO L, ELVASSORE N, DE COPPI P.
"Cardiomyocyte Differentiation of Amniotic Fluid Stem Cell on Biocompatible Polymeric Scaffold."
Poster presentation at the Cardiovascular Science and Medicine Day meeting, May 16th 2007, Institute of Child Health University College of London, London, UK

POZZOBON M, **BOLLINI S**, CHIAVEGATO A, PICCOLI M, DESTRO R, ZANON GF, CARLI M, GAZZOLA MV, SARTORE S, DE COPPI P.
"In vitro human CD133+ cardiomyocyte differentiation."
Poster presentation at the AIEOP (Italian Association Paediatric Ematology and Oncology) meeting October 22nd-26th 2006, Abano Terme (Padova), Italy.

BOLLINI S, FIGALLO E, CIMETTA E, POZZOBON M, ZANON G.F, MESSINA C, ZANESCO L, ELVASSORE N, DE COPPI P.
"3D Tissue engineering approaches to improve in vitro cardiac differentiation of amniotic stem cells: role of topological stimulation."
Poster presentation at the Annual TERMIS-EU Meeting October 8th-11th 2006 Rotterdam (NL).

CIMETTA E, PIZZATO S, SERENA E, **BOLLINI S**, DE COPPI P, ELVASSORE N.
"Micropatterned functional cardiac organoids and skeletal muscle fibers for pharmacological screening."
Poster presentation at the Annual TERMIS-EU Meeting October 8th-11th 2006 Rotterdam (NL).

CIMETTA E, PIZZATO S, **BOLLINI S**, SERENA E, DE COPPI P, ELVASSORE N.
"Production of arrays of cardiac organoids and skeletal muscle fibers by micropatterning techniques."
Poster presentation at the SBE's 2nd International Conference on Bioengineering and Nanotechnology, ICBN, September 5th-7th 2006, SantaBarbara, USA.

BOLLINI S, BOLDRIN L, CALLEGARI A, CHIAVEGATO A, POZZOBON M, PICCOLI M, SLANZI E, ZANON GF, CARLI M, SARTORE S, ATALA A, GAMBA PG, DE COPPI P.
"Muscle differentiation of amniotic fluid stem cell. New hopes for the treatment of congenital malformations."
Poster presentation at the XXI SICP (Italian Society Paediatric Surgery) meeting, September 19th-23rd 2006 Chieti (AN), Italy.

BOLLINI S, FIGALLO E, CIMETTA E, POZZOBON M, ZANON GF, MESSINA C, ELVASSORE N, DE COPPI P.
"Amniotic Fluid Stem Cells Have the Potential to Give Rise to Cardiomyocytes in a Three-dimensional scaffold."
Poster presentation at the 4th ISSCR Annual Meeting, June 28th-July 1st 2006, Toronto, Ontario, Canada.

3. Training Period Abroad.

From 11th January 2008 until 17th December 2008 the PhD candidate worked full time as PhD Visiting Student in the Paediatric Surgery Unit, ICH-Institute of Child Healt, UCL-University College of London with the extra supervision of Dr. Paolo De Coppi, Senior Lecturer and Consultant and Prof. Agostino Pierro, in collaboration with Dr. Mark Lythgoe from the Biophysics Unit, with Dr. Muriel Nobles from the Cardiovascular Science Department and Prof. Andy Tinker from Metabolism and Experimental Therapeutics Department and with Dr. Paul Riley, Molecular Medicine Unit, UCL-University College of London.

...Acknowledgements!

I'd like to say THANK YOU to a lot of people that during these 3 years have always been so friendly , thoughtful and helpful to me!

I want to say *Thanks* to my Supervisor, Prof. Chiara Messina and to Prof. Luigi Zanesco, to Dr. Maria Vittoria Gazzola and Roberta Destro for being so helpful in these years.
A big Thank you to Prof. Saverio Sartore, Dr. Angela Chiavegato, Dr. Nicola Elvassore for all the help they gave me.

A big *Thank you* to my Lab Team, Paolo, Michela, Martina, Luisa, Carlo, Andrea, Piera: you guys have always been by my side in the right moment with the right suggestion!
In particular a huge thank to Michela, Martina and Luisa for all the moments we have shared beyond the work...and the bench!

I'd like to say *Thanks* to people of my other Lab Team...the English one for all these months we have shared: Mara, Cinzia, Giuseppe, Annalisa and Augusto.

I'd like to say a special *Thank you very very much* also to the people I've worked with in these months in London, who have always helped me through: Ken, Xuebin, Johannes and Nicola.

A huge *Thank you* then to Dr. Mark Lythgoe, to Dr. Muriel Nobles and Andy Tinker, to Dr. Waseem Qasim, Dr. Simon Eaton and to Dr. Paul Riley.

... Thanks so Much!